Selected Key Aspects of Climate Change in Stabilization Scenarios

DISSERTATION
zur Erlangung des akademischen Grades eines
Doktors der Naturwissenschaften
am Fachbereich Geowissenschaften
der Freien Universität Berlin

vorgelegt von
Janina Körper
aus Berlin

Berlin, 2014

Erstgutachter: Prof. Dr. Ulrich Cubasch
Zweitgutachter: Prof. Dr. Uwe Ulbrich
Tag der Disputation: 17.12.2014

Contents

Selbstständigskeitserklärung

Hiermit erkläre ich an Eides Statt, dass ich die vorliegende Arbeit selbstständig und ohne fremde Hilfe angefertigt, keine anderen als die angegebenen Quellen und Hilfsmittel benutzt und die den benutzten Quellen wörtlich oder inhaltlich entnommenen Stellen als solche kenntlich gemacht habe. Diese Arbeit hat in gleicher oder ähnlicher Form noch keiner Prüfungsbehörde vorgelegen.

Berlin, Juli 2014

(Janina Körper)

Abstract

This thesis aims at a deeper understanding of committed climate change and the climate response in mitigation scenarios. Focusing on selected key aspects of climate change climate models are employed to study global mean changes as well as regional changes of different subsystems.

Therefore, a fully-coupled ocean atmosphere general circulation model is employed simulating climate change under increasing greenhouse gas (GHG) concentrations and stabilization of GHG concentrations thereafter. Additionally, an ensemble of ocean-atmosphere general circulation models and Earth system models is analyzed under a mitigation scenario that is consistent with the target of limiting global mean temperature change to $2°C$ relative to the pre-industrial era. To identify the portion of climate change that can be avoided, simulations of the mitigation scenario are compared to a business-as-usual scenario.

This thesis shows that the $2°C$ target — commonly assumed for example by policy makers to be suitable to prevent dangerous anthropogenic interference with the climate system — alone will not be sufficient to avoid all adverse impacts of climate change. This applies to the global scale, with the effect of mitigation on the hydrological cycle being weaker than the effect on surface temperature. It also applies to the regional scale in very sensitive regions. While some adverse effects such as excessive melting of Arctic summer sea ice resulting in a nearly ice free Arctic can be avoided, other aspects such as a strong reduction in the extent of Taiga and Tundra may evolve even under strong mitigation efforts. Furthermore, climate commitment plays an important role for the temporal evolution during the 21^{st} century (e.g., temperature increases despite of decreasing GHG emissions) and beyond the scenario period (e.g., sea level rise).

Zusammenfassung

Ziel dieser Dissertation ist es, ein tieferes Verständnis für Klima-Commitment — d.h. eine in der Vergangenheit oder rezent verursachte Klimaänderung, die in der Zukunft eintreffen wird — und Klimaänderungungen in Mitigationsszenarien zu erlangen. Es werden Klimamodelle verwendet, um sowohl globale als auch regionale Änderungen in den verschiedenen Subsystemen zu untersuchen, wobei der Fokus auf ausgewählten Schlüsselaspekten liegt.
Ein vollgekoppeltes Ozean-Atmosphäre-Allgemeine-Zirkulations-Modell wird verwendet, um Klimaänderungen unter ansteigenden Treibhausgaskonzentrationen und anschließender Stabilisierung dieser Konzentration zu simulieren. Darüber hinaus wird ein Ensemble von gekoppelten Klimamodellen sowie Erdsystemmodellen in einem Szenario analysiert, das konsistent ist mit dem Ziel, eine Änderung der globalen Mitteltemperatur von nicht mehr als $2°C$ verglichen mit der vorindustriellen Periode zu erreichen. Um den Anteil der Klimaänderungen zu identifizieren, der vermieden werden kann, werden Simulationen des Mitigationsszenarios mit Simulationen eines "Weiter-so-wie-bisher" Szenarios verglichen. Diese Arbeit zeigt, dass das $2°C$-Ziel — gemeinhin insbesondere von politischen Entscheidungsträgern für geeignet erachtet, gefährliche anthropogene Eingriffe in das Klimasystem zu verhindern — allein nicht ausreichen wird, alle ungewollten Folgen des Klimawandels zu vermeiden. Dies betrifft die globale Skala, da der Einfluss von Mitigationsmaßnahmen auf den hydrologischen Zyklus geringer ist als auf die bodennahe Temperatur. Es betrifft aber auch die regionale Skala in besonders sensitiven Regionen. Einige ungewollte Effekte, wie das exzessive Schmelzen arktischen Meereises im Sommer und somit eine nahezu eisfreie Arktis, können vermieden werden. Andere Prozesse, wie der starke Rückgang der Fläche von Gebieten mit Taiga- und Tundravegetation, werden auch bei starken Mitigitationsmaßnahmen voranschreiten. Darüber hinaus spielt Klima-Commitment eine wichtige Rolle für den zeitlichen Verlauf von Klimaänderungen während des 21. Jahrhunderts (zum Beispiel steigt die Temperatur auch unter sinkenden Treibhausgasemissionen weiter an) und über diesen Zeitraum hinaus (zum Beispiel mit einem anhaltenden Meeresspiegelanstieg).

Chapter 1

Introduction

1.1 Motivation

Article 2 of the United Nations Framework Convention on Climate Change (UNFCCC) states that the ultimate objective is the stabilization of greenhouse gas (GHG) concentrations in the atmosphere at a level that 'would prevent dangerous anthropogenic interference with the climate system' (UNFCCC, 1992). While the definition of dangerous anthropogenic interference with the climate system is debated, the Intergovernmental Panel on Climate Change (IPCC) presented five reasons for concern, widely known as "burning embers diagram" (IPCC, 2001). These are: risks to unique and threatened systems, risks from extreme climate events, distribution of impacts, aggregate impacts and risks from future large-scale discontinuities. Based on these reasons for concern and their relationship to global mean near surface temperature rise, it is now widely accepted that global mean warming needs to be limited to $2°C$ or less compared to the pre-industrial era (as recognized in the Cancun Agreements and the Copenhagen Accord) to avoid dangerous anthropogenic interference with the climate system.

Observations reveal atmospheric and oceanic warming, an increase in atmospheric GHG concentrations, acidification of the world's oceans (Hartmann *et al.*, 2013; Rhein *et al.*, 2013), a decrease in the amounts of snow and ice (Vaughan *et al.*, 2013) and rising sea levels (Church *et al.*, 2013). The dominant cause of the observed warming since the mid-20^{th} century can be attributed to the human influence (Bindoff *et al.*, 2013).

Climate models provide an important tool for scientists to gain a better understanding of relevant key processes for past, current and future climate change and its variability. Since the 1960s models initially developed for weather forecasts are adapted as climate models and have become increasingly comprehensive in terms of processes that

are incorporated. State of the art climate models (some further developed to Earth system models) include stratospheric dynamics, atmospheric chemistry and the carbon cycle.

Model simulations show that increases of GHG concentrations lead to a positive radiative forcing of the climate system and thus to an increase of surface temperatures and rising sea levels (e.g., Collins *et al.*, 2013; Meehl *et al.*, 2007). Additionally, climate change commitment, a delayed response of the climate system that will be realized even if GHG concentrations are stabilized (e.g., Collins *et al.*, 2013; Hansen *et al.*, 2005; Meehl *et al.*, 2005, 2006; Wigley, 2005), needs to be taken into account, when providing guidance on future GHG emissions consistent with temperature targets such as the $2°C$ goal. Therefore, stabilization scenarios are designed that provide the means to gain a better understanding of both, fast adjustments to radiative forcing, e.g., surface warming and melting of sea ice, and the climate change commitment, e.g., warming of the deep ocean, adjustment of the oceanic circulation and sea level rise from thermal expansion.

1.2 State of Knowledge

1.2.1 Climate Change Commitment and Stabilization Scenarios

When the GHG concentrations increase, they induce a radiative forcing, i.e. a change in the net radiative flux at top of the atmosphere, and the climate system warms. However, due to the large thermal reservoir of the ocean and slow processes in the cryosphere and land surfaces, the full surface response is not realized during the time of the radiative forcing. Instead, warming also includes a portion that will be realized after the radiative forcing is stabilized, for example when GHG concentrations stabilize. Moreover, the different subsystems of the climate system involve different response times. With the atmosphere reacting to stabilization of GHG concentrations within a few years and the upper ocean adjusting on a time-scale of several decades, the deep ocean and ice-sheets involve longer response times up to millennia (e.g., Church *et al.*, 2013; Li *et al.*, 2013). The portion of unrealized warming as well as other unrealized adjustments in the climate system, for example in the hydrological cycle, is referred to as climate change commitment (Wigley, 2005).

Climate change commitment has been investigated since the early 1980s (Bryan *et al.*, 1982; Hansen *et al.*, 1984, 1985; Mitchell *et al.*, 2000; Schlesinger, 1986; Siegenthaler and Oeschger, 1984; Wetherald *et al.*, 2001). Since then, model studies with simple

climate models were conducted to assess the portion of committed warming compared to the portion of realized warming (e.g., Hansen *et al.*, 1984; Wigley and Raper, 1993). Although vegetation changes and melting of glaciers and ice sheets also continue after GHG concentrations have stabilized, the portion of the realized warming and the response time of the climate system depends mainly on the climate sensitivity, oceanic heat uptake and the strength of climate feedbacks.

The main tool to analyze climate commitment are climate model simulations under stabilization scenarios. In these scenarios the radiative forcing due to GHG concentrations first increases and is then assumed to stay constant. Several different GHG pathways have been employed before stabilization of the radiative forcing, which are used to analyze the relationship between climate commitment and the GHG concentration evolution before stabilization. For example, in idealized experiments a transient increase of the CO_2 concentrations of one percent per year is used until doubling or quadrupling of the concentrations before stabilization (e.g., Cubasch *et al.*, 2001; Manabe and Stouffer, 1994; Voss and Mikolajewicz, 2001; Wetherald *et al.*, 2001). In more realistic scenarios first GHG concentrations are employed according to socio-economic assumptions such as the scenarios of the Special Report on Emission Scenarios (SRES) of the IPCC (Nakicenovic *et al.*, 2000). To analyze climate commitment in these scenarios the concentrations are stabilized either in the year 2000 (e.g., Wigley, 2005), usually referred to as COMMIT experiment, or in the year 2100 to analyze climate commitment beyond the 21^{st} century (e.g., Meehl *et al.*, 2007, 2005, 2006). Most recently, representative concentration pathways (RCPs) (Taylor *et al.*, 2009; van Vuuren *et al.*, 2011) for the 21^{st} century have been employed, which assume an increase in the radiative forcing until a certain level such as 4.5 W/m^2 before stabilization and are then continued under stabilized forcing, referred to as extended concentration pathways (Meinshausen *et al.*, 2011).

Models with a higher climate sensitivity simulate a lower portion of realized change and a longer response time than models with a lower climate sensitivity (Knutti *et al.*, 2005; Raper *et al.*, 2002; Stouffer *et al.*, 2006). This is due to a relationship between a model's climate sensitivity and the efficiency of oceanic heat uptake. The oceanic heat uptake provides a negative feedback (Dufresne and Bony, 2008; Gregory and Forster, 2008; Raper *et al.*, 2002). While the climate sensitivity of the models is known from experiments, the nature of the oceanic heat uptake is less clear. The role of oceanic heat uptake has been assessed comparing results of a coupled atmosphere ocean model with a mixed layer ocean only to results using the same model but including a model of the full ocean (atmosphere ocean general circulation model (AOGCM)), i.e. including the deeper

layers (Wetherald *et al.*, 2001). The comparison shows that the AOGCM approaches the equilibrium less quickly than the mixed layer ocean model. Note that the portion of unrealized warming is not constant in time but varies with past and current radiative forcing.

In addition to committed near surface warming, sea level rise is an important aspect of committed climate change. Oceanic heat uptake leads to sea level rise due to thermal expansion. Thermal expansion, and thus global mean sea level change, does not only depend on the oceanic heat uptake itself but also on the expansion efficiency of heat (Russell *et al.*, 2000), i.e. how oceanic heat uptake is translated into the thermal expansion. Since the expansion efficiency of water increases with temperature, salinity and pressure, its global mean value also depends on the region and depth of the heat uptake in the ocean. Therefore, analyses of the spatial patterns of ocean heat uptake are needed to gain a better understanding of regional sea level change and consequently global mean sea level change.

Several studies have focused on the spatial patterns of sea level changes and some of them explore differences between different AOGCMs (e.g., Gregory, 2000; Gregory *et al.*, 2001; Landerer *et al.*, 2007; Meehl *et al.*, 2007; Pardaens *et al.*, 2011). Common features of the spatial structures of 21^{st} century sea level rise are enhanced sea level rise in the Arctic due to enhanced freshwater input and weaker sea level rise in the Southern Ocean. Still, there are significant differences among the models that are insufficiently understood.

To explain the differences of the steric sea level rise anomalies at the surface, one has to understand the vertical structure of the density anomalies that sum up to the anomalies at the surface. Landerer *et al.* (2007) present differences in the vertical structure of thermosteric and halosteric contributions for different ocean areas for the A1B scenario. Likewise, Pardaens *et al.* (2011) have shown the zonal mean profiles of these contributions for the Atlantic basin and find significant differences between the climate models in the depth of the expanding layer. These differences are found to be related to differences in the overturning circulation.

Another key aspect of climate change commitment is the change in the oceanic circulation, since the heat transport by the ocean is an important factor for spatial patterns of surface temperature and affects the atmospheric circulation and regional sea level change. Ongoing oceanic density changes affect the oceanic circulation, for example the Atlantic Meridional Overturning Circulation (AMOC), which in turn influences density structures and steric sea level expansion. Landerer *et al.* (2007) and Yin *et al.* (2009) have shown

that regional sea level change in the North Atlantic is connected to changes in the oceanic circulation. While simulations of scenarios for the 21^{st} century with increasing GHG concentrations indicate a weakening of the AMOC, after stabilization of GHG concentrations the AMOC starts to recover (Collins *et al.*, 2013; Meehl *et al.*, 2007). However, some models reveal a stabilization below the pre-industrial level.

In summary, there have been a number of studies focusing on climate commitment in terms of the global mean temperature rise, global mean sea level rise and the relationship of committed warming to the climate sensitivity. By contrast regional sea level rise and the vertical structure of oceanic density changes are less well understood. Neither the temporal development of the vertical structures of density changes that sum up to sea level rise, nor their relation to different GHG concentration pathways, nor how these patterns would change under stabilized GHG concentrations have been investigated. Further understanding of the two components of steric expansion, i.e. thermosteric and halosteric effects, are not only important for a better understanding of sea level rise itself but also of circulation changes. Therefore, the decomposition of the two effects provides means to explore the reasons for the different evolutions of the AMOC after stabilization simulated by climate models.

1.2.2 Climate Response to Mitigation

While the IPCC 4^{th} Assessment Report (AR4) gave a comprehensive overview of the understanding of climate change under a wide range of future scenarios, none of the SRES scenarios included particular mitigation options that would limit warming to this target. Moreover, due to climate commitment, scenarios need to be designed and analyzed, which take into account that some portion of climate change will be realized after the radiative forcing has stabilized. For this purpose Integrated Assessment Models (e.g., Clarke *et al.*, 2010; Edenhofer *et al.*, 2010) and Earth System Models of Intermediate Complexity (e.g., Plattner *et al.*, 2008; van Vuuren *et al.*, 2007, 2008) have been used to explore various mitigation scenarios. Based on these models that include a rather simple and less comprehensive representation of the climate system compared to state of the art climate models and Earth system models some initial guidance can be provided. However, for a deeper understanding of key aspects of climate change, climatic feedbacks, climate variability and the related uncertainty, simulations employing more complex climate models need to be analyzed.

While there is a strong focus on global mean temperature change, the global hydrological cycle will change as well. Moreover, the warming is not spatially homogeneous and thus, in terms of regional adaptation strategies, the regional response and local feedback processes and climate variability in mitigation scenarios compared to "business-as-usual' scenarios need to be understood. Thereby, not only temperature changes but for example changes in the hydrological cycle and shifts of vegetation zones as well as sea ice changes in the polar regions are of importance for adaptation strategies. Moreover, due to the long response time of the deep ocean and the large portion of committed sea level rise, the effect of mitigation on sea level rise is expected to be weaker than for other climate parameters such as surface air temperature (e.g., Lowe *et al.*, 2006; Meehl *et al.*, 2012).

Simulations with the ECHAM5-MPIOM model have been performed in an idealized experimental setup by prescribing well-mixed GHG concentrations of the year 2020 according to the SRES A1B scenario onwards and rapidly relaxing the stratospheric ozone concentrations and sulfate aerosol loading towards their year 2100 values according to the SRES A1B scenario over the period 2020-2036 (May, 2008). In these simulations global mean warming does not exceed $2°C$ compared to the pre-industrial era. The future climate changes associated with this stabilization resemble the typical features of other climate scenarios, including the amplified Northern Hemisphere high latitude warming accompanied by a marked reduction of the sea-ice cover, which appears remarkably strong with regard to the magnitude of global mean warming (May, 2008).

Employing the GISS ModelE Hansen *et al.* (2007) analyzed two scenarios: (1) the "alternative" scenario proposed by Hansen and Sato (2004), that is designed to prevent temperature rise above 1 K with respect to the temperatures of the year 2000 by keeping the added forcing at about 1 W/m^2 in 2000-2050 and 0.5 W/m^2 in 2050-2100; (2) a "2°" scenario with an CO_2 peak at 560 ppm in 2100 and other GHGs following the SRES A1B scenario. In their regional analysis of the Artic they find a clear distinction between a "business-as-usual" scenario such as the SRES A1B scenario and the "alternative" scenario. They conclude, that positive feedbacks between the sea ice area and the surface albedo may be minimized, if the forcing is kept small.

In a study employing the Community Climate System Model Washington *et al.* (2009) analyze warming, sea level rise and Arctic sea ice changes in a mitigation scenario (Clarke *et al.*, 2007). They find significant reductions in global mean near surface temperature increases, sea level rise and Arctic sea ice decreases compared to a scenario without mitigation.

In summary, a number of studies comparing "business-as-usual" scenarios with mitigation scenarios have focused on global mean temperature change, global mean sea level rise and Arctic sea ice changes. However, since most of these studies rely on simulations with a single climate model, uncertainties in the projected effect of mitigation measures and the understanding of the underlying processes related to these uncertainties are less well explored. Moreover, other important aspects, such as the hydrological cycle and vegetation shifts, will affect regional adaptation to climate change, but are less well studied than temperature changes and sea level rise.

1.3 Thesis Objective

Building up on the work presented in the previous sections, this thesis aims at a deeper understanding of committed climate change and the climate response in mitigation scenarios. For this purpose, the thesis focuses on selected key aspects of climate change that represent both, climatic feedbacks, relevant for the response time of the climate system, and regional changes that are important in terms of adaptation strategies.

To gain a deeper understanding of key aspects of committed climate change, the EGMAM model (Huebener *et al.*, 2007) is employed to study oceanic heat uptake and consequently sea level change in terms of its temporal evolution and response to stabilization as well as its horizontal and vertical distribution. Therefore, the SRES scenarios (Nakicenovic *et al.*, 2000) are used with an extension under stabilized GHG concentrations at their 2100 level. As regional sea level changes are related to oceanic circulation changes, building up on the work of Landerer *et al.* (2007) and Yin *et al.* (2009), the patterns of North Atlantic sea level changes and their connection to the response of the AMOC to stabilized GHG concentrations are analyzed.

To study key aspects of climate change in mitigation scenarios the E1 scenario developed within the European Commission's 6^{th} Framework Program project ENSEMBLES (Hewitt and Griggs, 2004) is analyzed. In contrast to the SRES scenarios and stabilization afterwards, the E1 scenario includes an overshoot, i.e. GHG levels peak at 530 ppmv CO_2-equivalents in 2049 and then gradually decrease to stabilize at 450 ppmv CO_2-equivalents in the 22^{nd} century. Thereby, the scenario takes into account that even under agressive mitigation strategies GHG concentrations may increase to a level that, especially due to climate change commitment, is not consistent with the $2°C$ target. Therefore, the con-

centrations need to decrease afterwards to a level that is consistent with such a target. In addition to the EGMAM+ model results from a number of climate models and Earth system models participating in an intermodel comparison as part of the ENSEMBLES project are employed. Note that EGMAM+ is based on the EGMAM model, but also includes an interactive aerosole transport model, changing land use and a time varying 3d ozone field. The ENSEMBLES multimodel ensemble allows for a deeper understanding of the processes involved in response to mitigation and stabilizing GHG concentrations. Moreover, the multimodel ensemble represents an estimate of uncertainty — in terms of the uncertainty of the processes that are included in these models — of climate change consistent with the $2°C$ target.

In an effort to give a comprehensive insight into climate change under mitigation the analyses focus on selected aspects of several components of the climate system:

- representative of atmospheric processes global and regional temperature patterns as well as the response of the hydrological cycle are investigated;
- representative of oceanic processes sea level rise is analyzed;
- representative of cryospheric processes sea ice changes are investigated and a brief discussion of the surface mass balance the Greenland Ice Sheet is given;
- representative of processes in the biosphere shifts in potential vegetation zones are analyzed.

1.4 Thesis Outline

The major findings are described in the following five chapters. Each chapter is prepared as an article for publication in a scientific journal. The abstracts of these articles are presented in the chapters and the full articles are found in the Appendix of this thesis. Four have already been published; one is currently in revision. Thus, each article can be read independently. Each of them contains an introduction and an overview of the experimental set-up and the data employed for the analysis.

The contents of the papers are grouped into two research themes that differ from each other in the climate change scenarios analyzed and in the models employed for the analysis. The first research theme deals with the response of the climate system to stabilization of GHG concentrations following a continuous increase of GHG concentrations during the

21^{st} century. For this purpose the AOGCM EGMAM is employed. In the following two chapters findings on this research theme are presented.

- The near surface temperature change and steric sea level rise under increasing and stabilized greenhouse gas concentrations is presented in Chapter 2. This chapter is currently in revision[1].

- Chapter 3 focuses on the evolution of the AMOC beyond stabilization of GHG concentrations by decomposing the North Atlantic steric sea level rise into its thermal and haline contributions. This chapter has been published in *Geophysical Research Letters*[2].

In the second research theme simulations of the E1 scenario are compared to the SRES A1B scenario in terms of some key aspects of the climate system; these are temperature and precipitation changes, sea ice changes, sea level rise and shifts of vegetation zones. The results on the second research theme are presented in Chapter 4 to Chapter 6.

- Chapter 4 gives a first overview on the results of the response of the climate system to the E1 scenario compared to the SRES A1B scenario focusing on global temperature and precipitation changes. This chapter has been published in *Climate Dynamics*[3]. Although I am not the lead author of this article I provided substantial contributions to it. I conducted all but one of the model simulations performed with EGMAM+ that are presented. Furthermore, I wrote parts of the temperature, precipitation and concluding discussion section.

- As two further key parts of the climate system in Chapter 5 sea level rise and sea ice changes in the E1 scenario compared to the SRES A1B scenario are analyzed. This paper has been published in *Climate Dynamics*[4].

[1]Körper J, Spangehl T, Cubasch U, Huebener H (2014) Surface warming and sea level rise under increasing and stabilized greenhouse gas concentrations simulated in EGMAM.

[2]Körper J, Spangehl T, Cubasch U, Huebener H (2009) Decomposition of Projected Regional Sea Level Rise in the North Atlantic and its Relation to the AMOC, *Geophy. Res. Lett*, **36**, L19714, doi:10.1029/2009GL039757

[3]Johns TC, Royer J-F, Höschel I, Huebener H, Roeckner E, Manzini E, May W, Dufresne J-L, Otterå OH, van Vuuren DP, Salas y Melia D, Giorgetta MA, Denvil S, Yang S, Fogli PG, Körper J, Tjiputra JF, Stehfest E, Hewitt CD (2011) Climate change under aggressive mitigation: The ENSEMBLES multi-model experiment, *Clim. Dyn.*,**37**, doi:10.1007/s00382-11-1005-5

[4]Körper J, Höschel I, Lowe JA, Hewitt CD, Salas y Melia D, Roeckner E, Huebener H, Royer J-F, Dufresne J-L, Pardaens A, Giorgetta MA, Sanderson MG, Otterå OH, Tjiputra JF, Denvil S (2013) The effects of aggressive mitigation on steric sea level rise and sea ice changes, *Clim. Dyn.*, **40**, doi:10.1007/s00382-012-1612-9

- The terrestrial biosphere is especially vulnerable to climatic changes. Therefore, simulated potential vegetation in the SRES A1B scenario and the E1 scenario are compared in Chapter 6. This chapter has been published in *Journal of Environmental Protection*[5]. Although I am not the lead author of this article I provided substantial contributions to it. In addition to the conduction of the experiments with EGMAM+ (see above), I analyzed the multi-model output with regard to impacts on the potential vegetation and wrote substantial parts of the paper.

Finally, in Chapter 7 the main results and conclusions are summarized. A brief discussion is given as well as an outlook on research that may be focused on in future work.

[5]Huebener H, Körper J (2013) Changes in Regional Potential Vegetation in Response to an Ambitious Mitigation Scenario, *Journal of Environmental Protection*, **4**, doi:10.4236/jep.2013.48A2003

Chapter 2

Climate Change under Increasing and Stabilized Greenhouse Gas Concentrations Simulated with a Coupled Ocean-Troposphere-Stratosphere Model

Abstract A fully-coupled ocean-troposphere-stratosphere general circulation model is employed to investigate the committed climate change, once the greenhouse gas (GHG) concentrations have stabilized after an increase following different emission pathways. In a first numerical experiment the GHG concentrations are fixed at year 2000 values at the end of a transient simulation of the 20^{th} century. This model experiment is then continued for 100 years. In two additional experiments the Intergovernmental Panel on Climate Change (IPCC) scenarios (A1B, B1) are prescribed up to the end of the 21^{st} century. Afterwards the greenhouse gas concentrations have been held constant at their respective year 2100 values for the next 100 years.

Most of the temperature increase is realized during the 21^{st} century, while the GHG concentrations increase. The rate of global mean surface temperature rise decreases once the GHG concentrations become constant. The steric sea level continues to rise, however, with decreasing rates when the GHG concentrations are stabilized. The large scale spatial distribution of steric sea level rise at the sea surface during the stabilization period resembles the patterns during the GHG concentration increase except for a less pronounced

maximum sea level rise Northern Hemisphere high latitudes. The vertical patterns during the stabilization display a shift of the layers of maximum expansion from near surface to deeper oceanic depth. This shift develops earlier B1 scenario compared to the A1B scenario, illustrating that once the increase of GHG concentrations weakens as for the second half of the 21^{st} century in the B1 scenario or the concentrations stabilize the heat uptake penetrates into the deeper ocean layers with time.

Chapter 3

Decomposition of Projected Regional Sea Level Rise in the North Atlantic and its Relation to the AMOC

Abstract While it is well understood that thermal expansion dominates global mean steric sea level rise, climate models show large differences in spatial patterns. This study aims to decompose regional steric sea level rise in the North Atlantic into thermal and saline effects in a fully coupled model. In contrast to other studies we focus on the differences between two climate change scenarios and establish a link between the sea level changes and the differences in the response of the overturning circulation. While overturning is reduced in the phase of the greenhouse gas increase, differences between the scenarios are not significant until the stabilization in the 22$^{\text{nd}}$ century. The influence from thermosteric and halosteric contributions on the meridional density gradient is of the same size during the increase of greenhouse gas concentrations. The haline effect becomes prominent afterwards, reducing the meridional density gradient and preventing the overturning from recovery.

Chapter 4

Climate Change under Aggressive Mitigation: the ENSEMBLES Multi-Model Experiment

Abstract We present results from multiple comprehensive models used to simulate an aggressive mitigation scenario based on detailed results of an Integrated Assessment Model. The experiment employs ten global climate and Earth System models (GCMs and ESMs) and pioneers elements of the long-term experimental design for the forthcoming 5^{th} Intergovernmental Panel on Climate Change assessment. Atmospheric carbon-dioxide concentrations pathways rather than carbon emissions are specified in all models, including five ESMs that contain interactive carbon cycles. Specified forcings also include minor greenhouse gas concentration pathways, ozone concentration, aerosols (via concentrations or precursor emissions) and land use change (in five models). The new aggressive mitigation scenario (E1), constructed using an integrated assessment model (IMAGE 2.4) with reduced fossil fuel use for energy production aimed at stabilizing global warming below 2 K, is studied alongside the medium-high non-mitigation scenario SRES A1B. Resulting twenty-first century global mean warming and precipitation changes for A1B are broadly consistent with previous studies. In E1 twenty-first century global warming remains below 2 K in most models, but global mean precipitation changes are higher than in A1B up to 2065 and consistently higher per degree of warming. The spread in global temperature and precipitation responses is partly attributable to inter-model variations in aerosol loading and representations of aerosol-related radiative forcing effects. Our study illustrates that the benefits of mitigation will not be realised in temperature terms until several decades after emissions reductions begin, and may vary considerably between regions. A subset of the models containing integrated carbon cycles agree that land and ocean sinks remove roughly half of present day anthropogenic carbon emissions from the

atmosphere, and that anthropogenic carbon emissions must decrease by at least 50% by 2050 relative to 1990, with further large reductions needed beyond that to achieve the E1 concentrations pathway. Negative allowable anthropogenic carbon emissions at and beyond 2100 cannot be ruled out for the E1 scenario. There is selfconsistency between the multi-model ensemble of allowable anthropogenic carbon emissions and the E1 scenario emissions from IMAGE 2.4.

Chapter 5

The Effect of Aggressive Mitigation on Sea Level Rise and Sea Ice Changes

Abstract With an increasing political focus on limiting global warming to less than $2°C$ above pre-industrial levels it is vital to understand the consequences of these targets on key parts of the climate system. Here, we focus on changes in sea level and sea ice, comparing twenty-first century projections with increased greenhouse gas concentrations (using the mid-range IPCC A1B emissions scenario) with those under a mitigation scenario with large reductions in emissions (the E1 scenario). At the end of the twenty-first century, the global mean steric sea level rise is reduced by about a third in the mitigation scenario compared with the A1B scenario. Changes in surface air temperature are found to be poorly correlated with steric sea level changes. While the projected decreases in sea ice extent during the first half of the twenty-first century are independent of the season or scenario, especially in the Arctic, the seasonal cycle of sea ice extent is amplified. By the end of the century the Arctic becomes sea ice free in September in the A1B scenario in most models. In the mitigation scenario the ice does not disappear in the majority of models, but is reduced by 42% of the present September extent. Results for Antarctic sea ice changes reveal large initial biases in the models and a significant correlation between projected changes and the initial extent. This latter result highlights the necessity for further refinements in Antarctic sea ice modelling for more reliable projections of future sea ice.

Chapter 6

Changes in Regional Potential Vegetation in Response to an Ambitious Mitigation Scenario

Abstract Climate change impacts on the potential vegetation (biomes) are compared for an ambitious emissions-reduction scenario (E1) and a medium-high emissions scenario with no mitigation policy (A1B). The E1 scenario aims at limiting global mean warming to $2°C$ or less above pre-industrial temperatures and is closely related to the RCP2.6 in the CMIP5. A multi-model ensemble of ten state-of-the-art coupled atmosphere-ocean general circulation models (GCMs) is analyzed. A simple biome model is used to assess the response of potential vegetation to the different forcing in the two scenarios. Changes in biomes in response to the simulated climate change are less pronounced in E1 than in the A1B scenario. Most biomes shift polewards, with biomes adapted to colder climates being replaced by biomes adapted to warmer climates. In some regions cold biomes (e.g. Tundra, Taiga) nearly disappear in the A1B scenario but are also significantly reduced under the E1 scenario.

Chapter 7

Conclusions and Discussion

7.1 Conclusions

The studies presented in this thesis focus on selected key aspects of climate change in stabilization scenarios with respect to climate commitment and the climate response to mitigation scenarios. In two research themes research gaps identified in Section 1.2.1 and Section 1.2.2 are addressed.

7.1.1 Climate Change Commitment and Stabilization Scenarios

In Chapter 2 to 3 and in the full publications given in Appendix A.1 and Appendix A.2 climate commitment is analyzed. The response of global mean temperature and global mean sea level rise in EGMAM compared to the range of other climate models is briefly introduced. A focus is laid on patterns of sea level rise in terms of their horizontal and vertical features (Chapter 2) and their relation to the oceanic circulation changes in the North Atlantic (Chapter 3). The temporal development from a period with increasing GHG concentrations to a period under stabilized GHG concentrations following two different GHG concentration pathways reveals that long term climate change — in addition to the well-studied dependency on climate sensitivity and oceanic heat uptake efficiency — depends on the rate of increase of GHG concentrations before stabilization.

While global mean sea level rise in the SRES B1 scenario is of about the same value during the scenario period with increasing GHG concentrations and during the stabilization period afterwards, in the stabilization period following the SRES A1B scenario it is even larger than during the scenario period. This is due to a significant increase in the rates of sea level rise during the 21^{st} century in the SRES A1B scenario and thus higher

rates during the 22^{nd} century. These rates but not the sea level itself, however, decrease during the stabilization period.

The main characteristics of the large scale patterns of regional sea level rise do not change from the scenario period to the stabilization period, except for a less pronounced maximum of Arctic expansion. The vertical profiles reveal a shift of the layer with maximum expansion rates to deeper depth. This shift to deeper oceanic layers indicates a penetration of oceanic heat uptake into the deeper ocean layers with time. This leads to a larger volume of ocean water that expands. In the SRES B1 scenario this shift is already evident at the end of the 21^{st} century with decreasing rates of the GHG concentrations increase.

In EGMAM the decreasing strength of the AMOC during the scenario period of the SRES A1B and the SRES B1 scenarios do not significantly differ. However, the evolution in the stabilization period in the two scenarios differs significantly. Committed AMOC changes, are explained by a density pattern that develops already during the scenario period. Employing decomposition of thermosteric and halosteric effects in North Atlantic steric sea level changes it is shown that the saline contribution dominates the meridional density gradient, once the AMOC has weakened. Since this halosteric effect favors further weakening of the AMOC, while the thermosteric increase of the meridional density gradient favors a recovery of the AMOC, the dominance of the saline contribution explains, why the AMOC does not recover after stabilization. These results indicate that decomposition holds potential for further understanding of model differences of committed AMOC change.

7.1.2 Climate Response to Mitigation

In Chapter 4 to 6 and in the full publications given in Appendix A.3, Appendix A.4 and Appendix A.5 key aspects of the response of an ensemble of climate models to an aggressive mitigation scenario compared to a business-as-usual scenario are presented. Previous studies have focused on global mean temperature change, global mean sea level rise and Arctic sea ice changes based on simulations by a single model. In contrast to these studies, the multi-model ensemble is used to explore the uncertainties in the projected effect of mitigation measures and the understanding of the underlying processes related to these uncertainties. Furthermore, for a more comprehensive insight into climate change under mitigation, analyses on selected aspects of several components of the climate sys-

tem ranging from atmospheric processes and the carbon cycle (Chapter 4) over oceanic and cryospheric processes (Chapter 5) to processes in the biosphere (Chapter 6) are shown.

According to most models of the multi-model ensemble warming in the 21^{st} century remains below $2°C$ in the mitigation scenario E1. The subset of models that includes a carbon cycle indicates that, in order to achieve the GHG concentrations consistent with the E1 scenario, anthropogenic carbon emissions must decrease by at least 50% by 2050 relative to 1990 and further reductions afterwards. Moreover, a need for negative anthropogenic carbon emissions, i.e. carbon removal from the atmosphere, at the end of the 21^{st} century and thereafter cannot be ruled out employing this ensemble of models. Indicative of a significant impact of the committed response to past emissions, although GHG concentration pathways of the E1 scenario and the SRES A1B scenario diverge around 2010, this does not have a strong impact on the temperature response in the first half of the century. The hydrological response, illustrated by change in global precipitation per degree warming, is consistently stronger in the E1 scenario, which is mainly explained by differences in the aerosol loading of the two scenarios. Given the same total radiative forcing, aerosol-induced forcing tends to exhibit a stronger hydrological response than GHG-induced forcing (Feichter *et al.*, 2004). For both, temperature and precipitation changes, the ensemble spread is partly attributable to inter-model variations in the aerosol-loading and response to the radiative effects of aerosols.

Although 21^{st} century sea level rise is reduced by about a third in the E1 scenario, compared to the SRES A1B scenario, a large ensemble spread leads to an overlap of the projections at the end of the century, with the model with least sea level rise in the SRES A1B scenario projecting less sea level rise than the model with most sea level rise in the E1 scenario. This is explained by a combination of differences in oceanic heat uptake, i.e. the portion of heat that is transferred to the oceanic component of the climate system, and variations in expansion efficiency, i.e. the efficiency of how the heat uptake is translated into expansion. In the mitigation scenario E1, a shift in the locations of heat uptake leads to a decreasing expansion efficiency, which is consistent with a shift towards deeper colder waters. Moreover, a significant difference in the rates of sea level rise at the end of the 21^{st} century of the E1 scenario compared to the SRES A1B scenario indicates that mitigation efforts can reduce the committed sea level rise beyond the 21^{st} century.

With an amplification of the seasonal cycle of Arctic sea ice, in the majority of the models of the ensemble analyzed in Chapter 5 by the end of the 21^{st} century the Arctic becomes almost ice free at the end of the melting season in the SRES A1B scenario, which

can be mitigated following the E1 scenario in the majority of the models. The uncertainty, indicated by the ensemble spread of Artic sea ice extent, is attributed to a combination of the spread in global mean temperature response and a robust relationship between the initial sea ice area and sea ice reduction. The analysis of the possible effect of mitigation on Antarctic sea ice changes is particularly hampered by large biases in present day sea ice extent and a strong correlation of the projected changes and the initial ice extent.

Potential vegetation changes, represented by biomes, are shown to be less pronounced in E1 than in the SRES A1B scenario, with particularly strong differences in half of the 26 regions defined by Giorgi and Bi (2005). In both scenarios, the E1 and the SRES A1B scenario, a polewardshift of biomes is simulated, with biomes adapted to colder climates being replaced by biomes adapted to warmer climates. While in some regions, cold biomes such as Tundra and Taiga nearly disappear, in the E1 scenario they are still found at the end of the 21^{st} century, however, with a strongly reduced extent. This shows that some regions, such as Tibet, Alaska and Greenland are particularly sensitive to climate change, even when the $2°C$ target is achieved.

7.2 Discussion and Outlook

After the publication of most of the studies of this thesis the CMIP5 simulations have now become available using state-of-the-art climate models assuming representative concentration pathways (RCPs), which share some features with the scenarios used in this thesis. The main characteristics of these simulations are presented in the most recent IPCC report (IPCC, 2013a). This thesis complements the ongoing research. In each of the publications of this thesis the results are discussed in terms of the specific focus of the respective publication. By contrast, in this section the main conclusions given in Section 7.1 are discussed in comparison to the most recently published research for example based on the CMIP5 ensemble. Moreover, this section points to further research that is needed to gain a comprehensive understanding of climate change under mitigation and beyond the 21^{st} century.

Scenarios

The E1 scenario presented in Chapter 4 to Chapter 6 implies a radiative forcing very similar to the one of the RCP2.6 (see Figure 2 in Johns *et al.*, 2011), which has been used in the CMIP5 ensemble presented in Collins *et al.* (2013). The temperature response at the

end of the 21^{st} century of the ensemble used in this thesis for the E1 scenario is similar to the one of the CMIP5 ensemble for the RCP2.6, however, with a slightly smaller ensemble spread. Additionally, the RCP2.6 is extended to 2300 with decreasing radiative forcing (Meinshausen *et al.*, 2011). Therefore, in contrast to the results from the stabilization scenarios used in Chapter 2 and Chapter 3 with constant GHG concentrations, the global mean temperatures in the extension of the RCP2.6 drop below their 2100 values (Collins *et al.*, 2013). Note that the extension implies continued negative emissions, i.e. net carbon uptake, throughout the extended period, which demonstrates the need for further strong mitigation efforts.

By contrast to stabilization scenarios assuming constant composition of GHGs, in the extension of the RCP6.0 concentrations increase beyond the 21^{st} century to a level slightly higher than in the SRES A1B stabilization scenario. Therefore, the reported increase of global mean temperatures in the 22^{nd} scenario (Collins *et al.*, 2013) is explained by both, climate commitment and an increase in the radiative forcing in the first half of the 22^{nd} century. Consequently, the projected increases of global mean temperature and sea level rise cannot be directly compared to the climate commitment based on the constant composition scenarios presented in Chapter 2 and 3. Despite a different pathway of GHG increases during the 21^{st} century, the stabilization of CO_2-equivalent GHG concentration of RCP4.5 is at the same level as in the SRES B1 stabilization case. Likewise, the committed global mean temperature rise in the 22^{nd} century reported in Appendix A.1 and in Meehl *et al.* (2007) is in the range of the CMIP5 projections for the extension of RCP4.5.

Commitment

In order to reduce the uncertainty of estimates of climate commitment, further research is needed focusing on constraining the range of estimates of the equilibrium climate sensitivity and gaining further understanding of oceanic heat uptake. Since the climate sensitivity is an important factor for climate commitment, reducing the uncertainty of this variable is essential for better estimates of climate commitment. Still, the range of equilibrium climate sensitivity of the CMIP5 ensemble is very similar to the one of the CMIP3 ensemble with a nearly identical ensemble mean and with an only very slightly larger spread (Flato *et al.*, 2013). Based on observations and climate models the equilibrium climate sensitivity is likely in the range of $1.5°C$ and $4.5°C$ (IPCC, 2013b).

Based on multi-century simulations beyond stabilizations Li *et al.* (2013) show con-

tinued oceanic expansion with a growing contribution from deeper layers. In addition, Chapter 2 reveals a heterogeneous meridional distribution of the shift of heat uptake towards deeper oceanic layers. The expansion efficiency depends on the temperature and salinity of the water. Thus, in addition to the global mean uptake, the specific locations of the oceanic warming are important for global mean sea level rise (e.g., Russell *et al.*, 2000). Consequently, two models that show the same global oceanic heat uptake may display a different global mean sea level rise due to differences in the spatial patterns of heat uptake (Körper *et al.*, 2013). Therefore, future studies need to take into account not only the global mean sea level rise but also the horizontal and vertical patterns of oceanic heat uptake and connected changes in the oceanic circulation in order to constrain estimates of climate commitment.

Finally, for a full understanding of climate commitment in addition to climate commitment in the physical sense, such as the constant composition commitment discussed here or zero-emission commitment assuming no further GHG emissions (e.g., Zickfeld *et al.*, 2013), the inertia in a political, economic, technological and societal form and the resulting commitment from these aspects need to be explored. These aspects are beyond the scope of climate science, but will affect the probability of limiting warming below $2°C$.

Climate Models and Modelling Approaches

The studies presented in this thesis are either based on simulations using a single AOGCM (Chapter 2 and Chapter 3) or on an ensemble of AOGCMs and Earth system models (Chapter 4 to Chapter 6) representing the current generation of climate models. While models have become increasingly comprehensive (for an overview of models development from the 1970s, see Cubasch *et al.*, 2013) and computational capacities are increasing, harmonized multi-model comparisons such CMIP5 provide the means to study several aspects of the climate systems. Still, especially for a better understanding of long-term effects of climate change and complex interactions on regional to local scales model improvements and complementary approaches are necessary.

In Körper *et al.* (2013) and Collins *et al.* (2013) it has been shown that an ice-free Arctic in September may be mitigated in a scenario limiting global mean temperature increases below $2°C$ with respect to preindustrial. A large model spread of Arctic sea ice change is partly explained by different sensitivities of the Arctic sea ice response relative to the global mean temperature change and partly the initial sea ice extent, i.e. biases. Therefore, a number of studies constrain Arctic sea ice projections by either using only the models that reproduce observed Arctic sea ice features (e.g., Stroeve *et al.*, 2012; Wang

and Overland, 2012) or its relationship to surface temperature change (Zhang, 2010) or a combination of both (Massonnet *et al.*, 2012). The disadvantage of these approaches are the in some cases strong reduction of the ensemble size and thereby a loss of information from other contributions to uncertainty. By contrast, Mahlstein and Knutti (2012) recalibrate Arctic sea ice projections based on the observed relationship between September Arctic sea ice extent and global mean temperature change. This provides the means to reduce the uncertainty of the sea ice projections but does not lead to a physically consistent view of the climate system. The Antarctic sea ice response is even less understood due to large model biases (Körper *et al.*, 2013) and the inability of models to reproduce the mean seasonal cycle, interannual variability and observed increase in sea ice extent in the last few decades (Flato *et al.*, 2013). The reasons for the poor simulation of Antarctic sea ice coverage vary, including shortcomings that are not directly related to the sea ice models employed, such as problems in the simulation of the radiative budget and the oceanic ventilation (Körper *et al.*, 2013). This points to the need for model improvements of the complex atmosphere-ocean interaction related to sea ice.

Although the melting ice sheets will provide a large contribution to future sea level rise, they are not routinely modelled in global coupled climate models. Therefore, process based models using the output of AOGCMs are applied, which require high spatial resolutions to account for grounding line migration of the Antarctic ice sheet or topographic adjustments of the Greenland ice sheet (Church *et al.*, 2013). These uncoupled model simulations and statistical techniques are employed to explore relationships between global mean temperature change and melting of the ice sheets. Derived thresholds for a global temperature increase, above which the Greenland ice sheet would eventually melt, range from less than $1°C$ to more than $5°C$ (Gregory and Huybrechts, 2006; Robinson *et al.*, 2012). Especially improvements of process based modelling are needed to reduce the uncertainty of the ice sheet contribution, since statistical relationships between observed temperature change and ice sheet melting may not persists when specific thresholds are reached.

Current state-of-the-art Earth system models of the CMIP5 ensemble include the carbon cycle and a subset of them dynamic vegetation. By contrast to offline approaches, as used in Chapter 6, these models provide the means to simulate not only vegetation dynamics but also feedbacks of these vegetation changes with other subsystems. Computationally less costly offline models such as the BIOME model and further added features and refinements (Kaplan *et al.*, 2003; Prentice *et al.*, 1992) or climate zones such as the Köppen-Geiger classification (e.g., Hanf *et al.*, 2012), can be employed to study the im-

pact of warming on vegetation. One advantage of these less complex models is their calculation of the equilibrium response (Cramer, 2002) in contrast to the instant response of dynamic vegetation models. Thus, they include committed changes in vegetation — once temperature and precipitation characteristica stabilize. Still, a combination of both approaches is necessary to study the robustness of the results.

Summary

This thesis provides insights into important key aspects of climate commitment and mitigation of climate change in terms of atmospheric processes, such as the relationship between the temperature and the hydrological response, oceanic processes, such as the relationship between oceanic heat uptake, the oceanic circulation and sea level rise, cryospheric processes, such as the melting of Arctic and Antarctic sea ice, and land processes, such as shifts of biomes. The analyses reveal the complex interplay between the different subsystems of the climate systems. Using different analysis methods, ranging from a single-model study and a multi-model ensemble to offline-calculations with a more simple model, the thesis provides a comprehensive view of key processes, key uncertainties as well as very sensitive regions. The discussion in the individual publications as well as the discussion in the previous section points to further research, identifying the processes that explain the remaining uncertainty. As for example shown for sea ice changes, further model improvements need to focus not only on the individual subsystems but also on their interactions.

Bibliography

Bindoff, N., P. Stott, K. AchutaRao, M. Allen, N. Gillett, D. Gutzler, K. Hansingo, G. Hegerl, Y. Hu, S. Jain, I. Mokhov, J. Overland, J. Perlwitz, R. Sebbari and X. Zhang (2013): Detection and attribution of climate change: from global to regional. In *Climate Change 2013: The Physical Science Basis. Contribution of Working Group I to the Fifth Assessment Report of the Intergovernmental Panel on Climate Change*, ed. by T. Stocker, D. Qin, G.-K. Plattner, M. Tignor, S. Allen, J. Boschung, A. Nauels, Y. Xia, V. Bex and P. Midgley, Cambridge University Press.

Bryan, K., F. Komro, S. Manabe and M. Spelman (1982): Transient climate response to increasing atmospheric carbon-dioxide. *Science*, **215**, 56–58.

Church, J., P. Clark, A. Cazenave, J. Gregory, S. Jevrejeva, A. Levermann, M. Merrifield, G. Milne, R. Nerem, P. Nunn, A. Payne, W. Pfeffer, D. Stammer and A. Unnikrishnan (2013): Sea level change. In *Climate Change 2013: The Physical Science Basis. Contribution of Working Group I to the Fifth Assessment Report of the Intergovernmental Panel on Climate Change*, ed. by T. Stocker, D. Qin, G.-K. Plattner, M. Tignor, S. Allen, J. Boschung, A. Nauels, Y. Xia, V. Bex and P. Midgley, Cambridge University Press.

Clarke, L., J. Edmonds, H. Jacoby, H. Pitcher, J. Reilly and R. Richels (2007): Scenarios of greenhouse gas emissions and atmospheric concentrations. *Syn. Assess. Prod.*, **2.1a**, 154 pp, Department of Energy, Washington, DC, Available at http://www.climatescience.gov/Library/sap/sap2-1/default.php.

Clarke, L., J. Edmonds, V. Krey, R. R. Richels, S. Rose and M. Tavoni (2010): International climate policy architectures: overview of the emf 22 international scenarios. *Energy Econ*, **31**, 64–81.

Collins, M., R. Knutti, J. Arblaster, J.-L. Dufresne, T. Fichefet, P. Friedlingstein, X. Gao, W. Gutowski, T. Johns, G. Krinner, M. Shongwe, C. Tebaldi, A. Weaver and M. Wehner (2013): Long-term climate change: Projections, commitments and irreversibility. In *Climate Change 2013: The Physical Science Basis. Contribution of Working Group I to the Fifth Assessment Report of the Intergovernmental Panel on Climate Change*, Cambridge University Press.

Cramer, W. (2002): Biome models. In *The Earth system: biological and ecological dimensions of global environmental change. Encyclopedia of Global Environmental Change*, Vol. 2, ed. by H. Mooney and J. G. Canadell, pp. 166,171, John Wiley &, Ltd.

Cubasch, U., G. Meehl, G. Boer, R. Stouffer, M. Dix, A. Noda, C. Senior, S. Raper and K. Yap (2001): Projections of future climate. In *Climate Change 2001: The Scientific Basis. Contribution of Working Group I to the Third Assessment Report of the Intergovernmental Panel on Climate Change*, ed. by

Y. Houghton, J. T.and Ding, D. Griggs, M. Noguer, X. van der Linden, P.and Dai, K. Maskell and C. Johnson, Cambridge University Press.

Cubasch, U., D. Wuebbles, D. Chen, M. C. Facchini, D. Frame, N. Mahowald and J.-G. Winther (2013): Introduction. In *Climate Change 2013: The Physical Science Basis. Contribution of Working Group I to the Fifth Assessment Report of the Intergovernmental Panel on Climate Change*, ed. by T. Stocker, D. Qin, G.-K. Plattner, M. Tignor, S. Allen, J. Boschung, A. Nauels, Y. Xia, V. Bex and P. Midgley, Cambridge University Press.

Dufresne, J. and S. Bony (2008): An assessment of the primary sources of spread of global warming estimates from coupled atmosphere-ocean models. *J. Clim.*, **21**, 5135–5144.

Edenhofer, O., B. Knopf, T. Barker, L. Baumstark, E. Bellevrat, B. Chateau, P. Criqui, M. Isaac, A. Kitous, S. Kypreos, M. Leimbach, K. Lessmann, B. MagneÂ´, S. Scrieciu, H. Turton and D. van Vuuren (2010): The economics of low stabilization: model comparison of mitigation strategies and costs. *Energy J*, **31**, 11–48.

Feichter, J., E. Roeckner, U. Lohmann and B. Liepert (2004): Nonlinear aspects of the climate response to greenhouse gas and aerosol forcing. *J Clim*, **17**, 2384–2398.

Flato, G., J. Marotzke, B. Abiodun, P. Braconnot, S. C. Chou, W. Collins, P. Cox, F. Driouech, S. Emori, V. Eyring, C. Forest, P. Gleckler, E. Guilyardi, C. Jakob, V. Kattsov, C. Reason and M. Rummukainen (2013): Evaluation of climate models. In *Climate Change 2013: The Physical Science Basis. Contribution of Working Group I to the Fifth Assessment Report of the Intergovernmental Panel on Climate Change*, ed. by T. Stocker, D. Qin, G.-K. Plattner, M. Tignor, S. Allen, J. Boschung, A. Nauels, Y. Xia, V. Bex and P. Midgley, Cambridge University Press.

Giorgi, F. and X. Bi (2005): Updated regional precipitation and temperature changes for the 21st century from ensembles of recent aogcm simulations. *Geophysical Research Letters*, **32**, L21715, doi:10.1029/2005GL024288.

Gregory, J. (2000): Vertical heat transports in the ocean and their effect on time-dpendent climate change. *Climate Dynamics*, **16**, 501–515.

Gregory, J., J. Church, G. Boer, K. Dixon, G. Flato, D. Jackett, J. Lowe, S. O'Farrell, E. Roeckner, G. Rusell, R. Stouffer and M. Winton (2001): Comparison of results from several aogcms for global and regional sea-level change 1900-2100. *Clim. Dyn.*, **18**, 225–240, doi:10.1007/s003820100180.

Gregory, J. and P. Forster (2008): Transient climate response estimated from radiative forcing and observed temperature change. *J. Geophys. Res.*, **113**, D23105.

Gregory, J. M. and P. Huybrechts (2006): Ice-sheet contributions to future sea-level change. *Philosophical Transactions of the Royal Society A*, **364**, 1709–1732.

Hanf, F., J. Körper, T. Spangehl and U. Cubasch (2012): Shifts of climate zones in multi-model climate change experiments using the köppen climate classification. *Meteorologische Zeitschrift*, **21**, doi:10.1127/0941-2948/2012/0344.

Hansen, J., A. Lacis, D. Rind, G. Russell, P. Stone, I. Fung, R. Ruedy and J. Lerner (1984): Climate sensitivity: Analysis of feedback mechanisms. In *Climate Processes and Climate Sensitivity*, *Geophys. Monogr. Ser.*, Vol. 29, ed. by J. Hansen and T. Takahashi, pp. 130–163, AGU.

Hansen, J., S. M., R. R., P. Kharecha, A. Lacis, R. Miller, L. Nazarenko, K. Lo, G. Schmidt, G. Russell, I. Aleinov, S. Bauer, E. Baum, B. Cairns, V. Canuto, M. Chandler, Y. Cheng, A. Cohen, A. Del Genio, G. Faluvegi, E. Fleming, A. Friend, T. Hall, C. Jackman, J. Jonas, M. Kelley, N. Kiang, D. Koch, G. Labow, J. Lerner, S. Menon, T. Novakov, V. Oinas, J. Perlwitz, J. Perlwitz, D. Rind, A. Romanou, R. Schmunk, D. Shindell, P. Stone, S. Sun, D. Streets, N. Tausnev, D. Thresher, N. Unger, M. Yao and S. Zhang (2007): Dangerous human-made interference with climate: a GISS model study. *Atmos. Chem. Phys.*, **7**, 2287–2312.

Hansen, J., L. Nazarenko, R. Ruedy, M. Sato, J. Willis, A. Del Genio, D. Koch, A. Lacis, K. Lo, S. Menon, T. Novakov, J. Perlwitz, G. Russell, G. Schmidt and N. Tausnev (2005): Earth's energy imbalance: Confirmation and implications. *Science*, **308**, 1431, doi:10.1126/science.1110252.

Hansen, J., G. Russell, A. Lacis, I. Fung, D. Rind and P. Stone (1985): Climate response times - dependence on climate sensitivity and ocean mixing. *Science*, **229**, 857–859.

Hansen, J. and M. Sato (2004): Greenhouse gas growth rates. *Proc. Natl. Acad. Sci.*, **101**, 16109–16114.

Hartmann, D., A. Klein Tank, M. Rusticucci, L. Alexander, S. Broennimann, Y.-R. Charabi, F. Dentener, E. Dlugokencky, D. Easterling, A. Kaplan, B. Soden, P. Thorne, M. Wild and P. Zhai (2013): Observations: Atmosphere and surface. In *Climate Change 2013: The Physical Science Basis. Contribution of Working Group I to the Fifth Assessment Report of the Intergovernmental Panel on Climate Change*, ed. by T. Stocker, D. Qin, G.-K. Plattner, M. Tignor, S. Allen, J. Boschung, A. Nauels, Y. Xia, V. Bex and P. Midgley, Cambridge University Press.

Hewitt, C. and D. Griggs (2004): Ensembles-based predictions of climate change and their impacts (ENSEMBLES). *EOS Trans AGU*, **85**, 566.

Huebener, H., U. Cubasch, U. Langematz, T. Spangehl, F. Niehörster, I. Fast and K. M (2007): Ensemble climate simulations using a fully coupled ocean-troposphere-stratosphere gcm. *Philos. Trans. R. Soc., Ser. A*, **365**, 2089–2101, doi:10.1098/rsta.2007.2078.

IPCC (2001): Summary for policymakers. In *Climate Change 2001: Impacts, Adaptation and Vulnerability. Contribution of Working Group II to the Third Assessment Report of the Intergovernmental Panel on Climate Change*, ed. by J. McCarthy, O. Canziani, N. Leary, D. Dokken and K. White, Cambridge University Press.

IPCC (2013a): *Climate Change 2013: The Physical Science Basis. Contribution of Working Group I to the Fifth Assessment Report of the Intergovernmental Panel on Climate Change*. Cambridge University Press, 1535 pp.

IPCC (2013b): Summary for policymakers. In *Climate Change 2013: The Physical Science Basis. Contribution of Working Group I to the Fifth Assessment Report of the Intergovernmental Panel on Climate Change*, ed. by T. Stocker, D. Qin, G.-K. Plattner, M. Tignor, S. Allen, J. Boschung, A. Nauels, Y. Xia, V. Bex and P. Midgley, Cambridge University Press.

Johns, T. C., J.-F. Royer, I. Höschel, H. Huebener, E. Roeckner, E. Manzini, W. May, J.-L. Dufresne, O. H. Otterå, D. Van Vuuren, D. Salas y Melia, M. A. Giorgetta, S. Denvil, S. Yang, P. G. Fogli, J. Körper, J. F. Tjiputra, E. Stehfest and C. D. Hewitt (2011): Climate change under agressive mitigation: The ENSEMBLES multi-model experiment. *Climate Dynamics*, **37**, doi: 10.1007/s00382-011-1005-5.

Kaplan, J. O., N. H. Bigelow, I. C. Prentice, S. P. Harrison, P. J. Bartlein, T. R. Christensen, W. Cramer, N. V. Matveyeva, A. D. McGuire, D. F. Murray, V. Y. Razzhivin, B. Smith, D. A. Walker, P. M. Anderson, A. A. Andreev, L. B. Brubaker, M. E. Edwards and A. V. Lozhkin (2003): Climate change and arctic ecosystems ii: Modeling, paleodata-model comparisons, and future projections. *Journal of Geophysical Research*, **108**, 8171, doi:10.1029/2002JD002559.

Knutti, R., F. Joos, S. Mueller, G. Plattner and T. Stocker (2005): Probabilistic climate change projections for co_2 stabilization profiles. *Geophys. Res. Lett.*, **32**, L20707.

Körper, J., I. Höschel, J. A. Lowe, C. D. Hewitt, D. Salas y Melia, E. Roeckner, H. Huebener, J.-F. Royer, J.-L. Dufresne, A. Pardaens, M. A. Giorgetta, M. G. Sanderson, O. H. Otterå, J. Tjiputra and S. Denvil (2013): The effects of aggressive mitigation on steric sea level rise and sea ice changes. *Climate Dynamics*, **40**, 531–550, doi:10.1007/s00382-012-1612-9.

Landerer, F., J. Jungclaus and J. Marotzke (2007): Regional dynamic and steric sea level change in response to the IPCC-A1B scenario. *J. Phys. Oceanogr.*, **37**, 296–312, doi:10.1175/JPO3013.1.

Li, C., J.-S. von Storch and J. Marotzke (2013): Deep-ocean heat uptake and equilibrium climate response. *Clim. Dyn.*, **40**, 1071–1086.

Lowe, J., J. Gregory, J. Ridley, P. Huybrechts, R. Nicholls and M. Collins (2006): The role of sea-level rise and the greenland ice sheet in dangerous climate change: implications for the stabilisation of climate. In *Avoiding dangerous climate change*, ed. by H. Schnellnhuber, W. Cramer, N. Nakicenovic, T. Wigley and G. Yohe, pp. 29–36, Cambridge University Press.

Mahlstein, I. and R. Knutti (2012): September arctic sea ice predicted to disappear near 2°c global warming above present. *Journal of Geophysical Research*, **117**, D06104.

Manabe, S. and R. Stouffer (1994): Multiple-century response of a couples ocean-atmosphere model to an increase of atmospheric carbon dioxide. *Journal of Climate*, **7**, 5–23.

Massonnet, F., T. Fichefet, H. Goosse, C. M. Bitz, G. Philippon-Berthier, M. Holland and P. Y. Barriat (2012): Constraining projections of summer arctic sea ice. *Cryosphere*, **6**, 1383–1394.

May, W. (2008): Climatic changes associated with a global "2° stabilization" scenario simulated by the ECHAM5/MPI-OM coupled climate model. *Clim Dyn*, **31**, 283–313.

Meehl, G., A. Hu, C. Tebaldi, J. Arblaster, W. Washington, H. Teng, B. Sanderson, T. Ault, W. Strand and J. White (2012): Relative outcomes of climate change mitigation related to global temperature versus sea-level rise. *Nat. Clim. Chang.*, **2**, 576–580.

Meehl, G., T. Stocker, W. Collins, P. Friedlingstein, A. Gaye, J. Gregory, A. Kitoh, R. Knutti, J. Murphy, A. Noda, S. Raper, I. Watterson, A. Weaver and Z.-C. Zhao (2007): Global climate projections. In *Climate Change 2007: The Physical Science Basis: Contribution of Working Group I to the Fourth Assessment Report on the Intergovernmental Panel on Climate Change*, ed. by S. Solomon, D. Qin, M. Manning, Z. Chen, M. Marquis, K. Averyt, M. Tignor and H. Miller, Cambridge University Press.

Meehl, G., W. Washington, W. Collins, J. Arblaster, A. Hu, L. Buja, W. Strand and H. Teng (2005): How much more global warming and sea level rise? *Science*, **307**, 1769–1772, doi:10.1126/science.1106663.

Meehl, G., W. Washington, B. Santer, W. Collins, J. Arblaster, A. Hu, D. Lawrence, H. Teng, L. Buja and W. Strand (2006): Climate change projections for the 21st century and climate change commitment in the CCSM3. *J. Clim.*, **19**, 2597–2616.

Meinshausen, M., S. Smith, K. Calvin, J. Daniel, M. Kainuma, J.-F. Lamarque, K. Matsumoto, S. Montzka, S. Raper, K. Riahi, A. Thomson, G. Velders and D. van Vuuren (2011): The RCP greenhouse gas concentrations and their extensions from 1765 to 2300. *Climatic Change*, **109**, 213–241.

Mitchell, J., T. Johns, W. Ingram and J. Lowe (2000): The effect of stabilising atmospheric carbon dioxide concentrations on global and regional climate change. *Geophys. Res. Lett.*, **27**, 2977–2980.

Nakicenovic, N., J. Alcamo, G. Davis, B. de Vries, J. Fenhann, S. Gaffin, K. Gregory, A. Grübler, T. Jung, T. Kram, E. La Rovere, L. Michaelis, S. Mori, T. Morita, W. Pepper, H. Pitcher, L. Price, K. Riahi, A. Roehrl, H.-H. Rogner, A. Sankovski, M. Schlesinger, P. Shukla, S. Smith, R. Swart, S. van Rooijen, N. Victor and Z. Dadi (2000): *Special Report on Emissions Scenarios: A Special Report of Working Group III of the Intergovernmental Panel on Climate Change.* Tech. rep.

Pardaens, A., L. J.A., S. Brown, R. Nicholls and D. de Gusmaõ (2011): Sea-level rise and impacts projections under a future scenario with large greenhouse gas reductions. *Geophys. Res. Lett.*, **38**, L12604, doi:doi:10.1029/2011GL047678.

Plattner, G., R. Knutti, F. Joos, T. Stocker, W. von Bloh, V. Brovkin, D. Cameron, E. Driesschaert, S. Dutkiewicz, M. Eby, N. Edwards, T. Fichefet, J. Hargreaves, C. Jones, M. Loutre, H. Matthews, A. Mouchet, S. Müller, S. Nawrath, A. Price, A. Sokolov, K. Strassmann and A. Weaver (2008): Long-term climate commitments projected with climate-carbon cycle models. *J Clim*, **21**, 2721–2751.

Prentice, I. C., W. Cramer, S. P. Harrison, R. Leemans, R. A. Monserud and A. M. Solomon (1992): A global biome model based on plant physiology and dominance, soil properties and climate. *Journal of Biogeographie*, **19**, 117–134.

Raper, S., J. Gregory and R. Stouffer (2002): The role of climate sensitivity and ocean heat uptake on AOGCM transient temperature response. *Journal of Climate*, **15**, 124–130.

Rhein, M., S. Rintoul, S. Aoki, E. Campos, D. Chambers, R. Feely, S. Gulev, G. Johnson, S. Josey, A. Kostianoy, C. Mauritzen, D. Roemmich, L. Talley and F. Wang (2013): Observations: Ocean. In *Climate Change 2013: The Physical Science Basis. Contribution of Working Group I to the Fifth Assessment Report of the Intergovernmental Panel on Climate Change*, ed. by T. Stocker, D. Qin, G.-K. Plattner, M. Tignor, S. Allen, J. Boschung, A. Nauels, Y. Xia, V. Bex and P. Midgley, Cambridge University Press.

Robinson, A., R. Calov and A. Ganopolski (2012): Multistability and critical thresholds of the greenland ice sheet. *Nature Climate Change*, **2**, 429,432.

Russell, G., V. Gornitz and J. Miller (2000): Regional sea level changes projected by the NASA/GISS atmosphere ocean model. *Clim. Dyn.*, **16**, 789–797.

Schlesinger, M. (1986): Equilibrium and transient climatic warming induced by increased atmospheric CO_2. *Clim. Dyn.*, **1**, 35–51.

Siegenthaler, U. and H. Oeschger (1984): Transient temperature changes due to increasing CO_2 using simple models. *Ann. Glaciol.*, **5**, 153–159.

Stouffer, R., J. Yon, J. Gregory, K. Dixon, M. Spelman, W. Hurlin, A. Weaver, M. Eby, G. Flato, H. Hasumi, A. Hu, J. Jungclaus, I. Kamenkovich, A. Levermann, M. Montoya, S. Murakami, S. Nawrath, A. Oka, W. Peltier, D. Robitaille, A. Sokolov, G. Vettoretti and S. Weber (2006): Investigating causes of the response of the thermohaline circulation to past and future climate changes. *Journal of Climate*, **19**, 1365–1387.

Stroeve, J. C., V. Kattsov, A. Barrett, M. Serreze, T. Pavlova, M. Holland and W. N. Meier (2012): Trends in arctic sea ice extent from cmip5, cmip3 and observations. *Geophysical Research Letters*, **39**, L16502, doi:10.1029/2012GL052676.

Taylor, K., R. Stouffer and G. Meehl (2009): A summary of the CMIP5 experiment design. URL `http://cmip-pcmdi.llnl.gov/cmip5/`.

UNFCCC, 1992 (1992): United nations framework convention on climate change, fccc/informal/84 ge.05-62220 (e) 200705. UNFCCC 1992.

van Vuuren, D., M. den Elzen, P. Lucas, B. Eickhout, B. Strengers, B. van Ruijven, S. Wonink and R. van Houdt (2007): Stabilizing greenhouse gas concentrations at low levels: an assessment of reduction strategies and costs. *Clim. Change.*, **81**, 119–159, doi:10.1007/s/10584-006-9172-9.

van Vuuren, D., M. Meinshausen, G.-K. Plattner, F. Joos, K. Strassmann, S. Smith, T. Wigley, S. Raper, K. Riahi, F. de la Chesnaye, M. den Elzen, J. Fujino, K. Jiang, N. Nakicenovic, S. Paltsev and J. Reilly (2008): Temperature increase of 21st century mitigation scenarios. *Proc Natl Acad Sci*, **105 (40)**, 15258–15262, doi:10.1073/pnas.0711129105.

van Vuuren, D. P., J. Edmonds, M. Kainuma, K. Riahi, A. Thomson, T. Matsui, G. Hurtt, J.-F. Lamarque, M. Meinshausen, S. Smith, C. Grainer, S. Rose, K. Hibbard, N. Nakicenovic, V. Krey and T. Kram (2011): Representative concentration pathways: An overview. *Climatic Change*, **109**, 5–31, doi:10.1007/s10584-011-0148-z.

Vaughan, D., J. Comiso, I. Allison, J. Carrasco, G. Kaser, R. Kwok, P. Mote, T. Murray, F. Paul, J. Ren, E. Rignot, O. Solomina, K. Steffen and T. Zhang (2013): Observations: Cryosphere. In *Climate Change 2013: The Physical Science Basis. Contribution of Working Group I to the Fifth Assessment Report of the Intergovernmental Panel on Climate Change*, ed. by T. Stocker, D. Qin, G.-K. Plattner, M. Tignor, S. Allen, J. Boschung, A. Nauels, Y. Xia, V. Bex and P. Midgley, Cambridge University Press.

Voss, R. and U. Mikolajewicz (2001): Long-term climate changes due to increased CO_2 concentration in the coupled atmosphere-ocean general circulation model ECHAM3/LSG. *Climate Dynamics*, **17**, 45–60.

Wang, M. and J. E. Overland (2012): A sea ice free summer arctic within 30 years–an update from cmip5 models. *Geophysical Research Letters*, **39**, L18501, doi:10.1029/2012GL052868.

Washington, W., R. Knutti, G. Meehl, H. Teng, C. Tebaldi, D. Lawrence, B. Lawrence and W. Strand (2009): How much climate change can be avoided by mitigation? *Geophys. Res. Lett.*, **36**, L08703, doi:10.1029/2008GL037074.

Wetherald, R., R. Stouffer and K. Dixon (2001): Committed warming and its implications for climate change. *Geophys. Res. Lett.*, **28**, 1535–1538.

Wigley, T. (2005): The climate change committment. *Science*, **307**, 1766–1769.

Wigley, T. and S. Raper (1993): Future changes in global mean temperature and sea level. In *Climate and Sea Level Change: Observations, Projections, and Implications*, ed. by B.-E. Warrick, R.A. and T. Wigley, pp. 111–113, Cambridge Univ. Press.

Yin, J., M. Schlesinger and S. R.J. (2009): Model projections of rapid sea-level rise on the northeast coast of the united states. *Nat. Geosci.*, **2**, 262–266, doi:10.1038/ngeo462.

Zhang, X. (2010): Sensitivity of arctic summer sea ice coverage to global warming forcing: towards reducing uncertainty in arctic climate change projections. *Tellus A*, **62**, 220–227.

Zickfeld, K., M. Eby, A. J. Weaver, K. Alexander, E. Crespin, N. R. Edwards, A. V. Eliseev, G. Feulner, T. Fichefet, C. E. Forest, P. Friedlingstein, H. Goosse, P. B. Holden, F. Joos, M. Kawamiya, D. Kicklighter, H. Kienert, K. Matsumoto, I. I. Mokhov, E. Monier, S. M. Olsen, J. O. P. Pedersen, M. Perrette, G. Philippon-Berthier, A. Ridgwell, A. Schlosser, T. Schneider Von Deimling, G. Shaffer, A. Sokolov, R. Spahni, M. Steinacher, K. Tachiiri, K. S. Tokos, M. Yoshimori, N. Zeng and F. Zhaos (2013): Long-term climate change commitment and reversibility: An EMIC intercomparison. *Journal of Climate*, **26**, 5782–5809, doi:10.1175/JCLI-D-12-00584.1.

Appendix A

Appendix

In this Appendix the full publications are shown that are commulatively submitted as the thesis. Körper et al. (2014) is currently in revision. The publications that have been already published are printed as published in the journals (including the journal formatting).

A.1 Körper et al. (2014)

Surface warming and sea level rise under increasing and stabilized greenhouse gas concentrations simulated in EGMAM

Janina Körper[1] (janina.koerper@met.fu-berlin.de), Thomas Spangehl[2] (spangehl@met.fu-berlin.de), Ulrich Cubasch[1](cubasch@zedat.fu-berlin.de), Heike Huebener[3] (Heike.Huebener@hlug.hessen.de)

1) Institute for Meteorology, Freie Universität Berlin, Carl-Heinrich-Becker-Weg 6.10, 12165 Berlin, Germany

2) German Meteorological Service, Offenbach, Germany

3) *Hessian Agency for Environment and Geology, Rheingaustr. 186, 65203 Wiesbaden, Germany*

Corresponding author: Janina Körper, Institute for Meteorology, Freie Universität Berlin, Carl-Heinrich-Becker-Weg 6-10, 12165 Berlin, Germany, Email: janina.koerper@met.fu-berlin.de)

Abstract

A fully-coupled ocean-troposphere-stratosphere general circulation model is employed to investigate the committed climate change, once the greenhouse gas (GHG) concentrations have stabilized after an increase following different emission pathways. In a first numerical experiment the GHG concentrations are fixed at year 2000 values at the end of a transient simulation of the 20th century. This model experiment is then continued for 100 years. In two additional experiments the Intergovernmental Panel on Climate Change (IPCC) scenarios (A1B, B1) are prescribed up to the end of the 21st century. Afterwards the greenhouse gas concentrations have been held constant at their respective year 2100 values for the next 100 years.

Most of the temperature increase is realized during the 21st century, while the GHG concentrations increase. The rate of global mean surface temperature rise decreases once the GHG concentrations become constant. The steric sea level continues to rise, however, with decreasing rates when the GHG concentrations are stabilized. The large scale spatial distribution of steric sea level rise at the sea surface during the stabilization period resembles the patterns during the GHG concentration increase except for a less pronounced maximum sea level rise Northern Hemisphere high latitudes. The vertical patterns during the stabilization display a shift of the layers of maximum expansion from near surface to deeper oceanic depth. This shift develops earlier B1 scenario compared to the A1B scenario, illustrating that once the increase of GHG concentrations weakens as for the second half of the 21st century in the B1 scenario or the concentrations stabilize the heat uptake penetrates into the deeper ocean layers with time.

Keywords: Stabilization – Climate Change – Sea Level Rise – Heat Uptake

German

Ein gekoppeltes Ozean-Troposphären-Stratosphären-Modell wird genutzt, um den langfristigen Klimawandel zu untersuchen, der auch dann eintritt, wenn die Treibhausgaskonzentrationen im Anschluss an verschiedene Verläufe des Treibhausgasanstiegs konstant gehalten werden. Im ersten numerischen Experiment werden im Anschluss an eine transiente Simulation des 20. Jahrhunderts die Treibhausgaskonzentrationen des Jahres 2000 festgehalten. Dieses Experiment wird für 100 Jahre fortgesetzt. In zwei weiteren Experimenten wird das Klima in zwei IPCC Szenarien

(A1B, B1) für das 21. Jahrhundert simuliert. Danach werden die Simulationen unter den jeweiligen Treibhausgaskonzentrationen des Jahres 2100 für die folgenden 100 Jahre fortgesetzt.

Der Großteil des Temperaturanstiegs wird bereits im 21. Jahrhundert realisiert, während die Konzentrationen ansteigen. Unter konstanten Treibhausgaskonzentrationen sinkt die Erwärmungsrate. Der Meeresspiegelanstieg setzt sich auch unter konstanten Treibhausgaskonzentrationen fort, wenn auch mit einer sinkenden Rate. Die großskalige horizontale Verteilung des Meeresspiegelanstiegs an der Oberfläche entspricht in der Stabilisierungsperiode mit Ausnahme eines geringeren Anstiegs in den hohen Breiten der Nordhemisphäre der Verteilung in der Periode des Treibhausgasanstiegs. Die vertikalen Muster der sterischen Expansion zeigen eine Verschiebung der Schicht mit der größten Expansion in tiefere ozeanische Schichten. Diese Verschiebung beginnt im B1 Szenario früher als im A1B Szenario. Dies verdeutlicht, dass die Wärme mit der Zeit in tiefere Schichten eindringt, wenn sich der Anstieg der Treibhausgaskonzentrationen verringert, wie in der zweiten Hälfte des 21. Jahrhunderts im B1 Szenario der Fall, oder sich die Konzentrationen stabilisieren.

1) Introduction

Increases of greenhouse gas (GHG) concentrations lead to a positive radiative forcing of the climate system and thus to an increase of surface temperatures and rising sea level (MEEHL et al., 2007). In addition to contributions from melting of glaciers and ice sheets, the sea level will rise from thermal expansion (e.g., MANABE and STOUFFER, 1994; MEEHL et al., 2007; CHURCH et al., 2013). Due to the thermal inertia of the climate system, particularly of the deep ocean, a delayed response will be realized even if GHG concentrations are stabilized and is called "committed warming" (e.g. WIGLEY 2005; MEEHL et al., 2006).

Starting in the 1980s model studies with simple climate models were conducted to assess the portion of committed warming (e.g. HANSEN et al., 1984; WIGLEY and RAPER 1993). For any given forcing the portion of the realized warming compared to the committed warming depends mainly on the climate sensitivity, which is model dependent, and oceanic heat uptake (WETHERALD et al., 2001).

While the atmosphere reacts to stabilization of GHG-concentrations within a few years, the upper ocean adjusts on a time-scale of several decades. The deep ocean attains equilibrium after a stabilization of the GHG-concentrations only after millennia (e.g., LI et al., 2012; CHURCH et al., 2013). To assess the role of oceanic heat uptake WETHERALD et al. (2001) compared the climate response of an atmosphere ocean general circulation model (AOGCM), i.e. a climate model coupled to a realistic ocean model, with the response of a model using the same atmospheric component and an ocean, which consisted of the mixed layer of 50 m depth only. Due to the longer timescale involved with the deep ocean, the AOGCM approaches the equilibrium less quickly than the mixed layer ocean model. Prescribing an idealized 1% CO_2 increase per year, they found the committed warming to increase from about 1 K for present day to almost 2 K in the year 2060, i.e. the climate is now closer to an equilibrium state and with increasing GHG concentrations it will depart farther from an equilibrium state. The realized warming was 0.6 K for the year 2000 and 3 K by 2060 in those experiments. In additional studies AOGCMs were forced with a 1% increase of CO_2 concentrations prescribed until doubling of CO_2 (VOSS and MIKOLAJEWICZ, 2001) and quadrupling (MANABE and STOUFFER, 1994) showing similar results.

Experiments, where AOGCMs have been forced according to the Special Report on Emission Scenarios (SRES) scenarios (NAKICENOVIC et al., 2000) and the Representative Concentration Pathways (MOSS et al., 2010) including stabilization after the 21st century confirm these findings and show that the global mean near surface temperature as well as the global steric

sea level will continue to rise even if GHG-concentrations are stabilized (STOUFFER et al., 2006; MEEHL et al., 2005, 2006, 2007, 2012; COLLINS et al., 2013).

While the climate sensitivity of the models is known from experiments, the nature of the ocean heat uptake is less clear. RAPER et al. (2002) analyzed an apparent relationship between a model's climate sensitivity and the efficiency of oceanic heat uptake as earlier suggested by HANSEN et al. (1984). They show that models with higher climate sensitivity simulate a lower portion of realized change compared to the ones with a lower climate sensitivity. STOUFFER et al. (2006) show in two different model versions of an AOGCM that the transient climate response in the model version with the larger equilibrium climate sensitivity is even smaller than in the version with the lower climate sensitivity. They attribute this to a larger oceanic heat uptake in the Southern Ocean related to a more realistic location of the tropospheric jet in the Southern Hemisphere in the model version with the lower climate sensitivity. Likewise, RUSSELL et al. (2006) have shown that the location of Southern Hemisphere westerlies is especially important for the oceanic heat and carbon storage in a warming climate.

Thermal expansion, and thus global mean sea level change, does not only depend on the oceanic heat uptake itself but also on the "expansion efficiency of heat" (RUSSELL et al., 2000), i.e. how oceanic heat uptake is translated into the thermal expansion. Since the expansion efficiency of heat increases with temperature, salinity and pressure, its global mean value also depends on the regions and depth of the heat uptake in the ocean.

Several studies have focused on the spatial patterns of sea level changes and some of them explore differences between different AOGCMs (e.g. GREGORY et al. 2001; GREGORY and LOWE 2000; LANDERER et al. 2007; MEEHL et al., 2007; PARDAENS et al., 2011). While there are some common features of the spatial structures of 21st century sea level rise, for example enhanced sea level rise in the Arctic due to enhanced freshwater input and weaker sea level rise in the Southern Ocean, there are significant differences among the models that are inadequately understood.

To explain the differences of the steric sea level rise anomalies at the surface, one has to understand the vertical structure of the density anomalies that sum up to the anomalies at the surface. LANDERER et al. (2007) present differences in the vertical structure of thermosteric and halosteric contributions for different ocean areas for the A1B scenario. Likewise, PARDAENS et al. (2011) have shown the zonal mean profiles of these contributions for the Atlantic basin and find significant differences between the AR4 models in the depth of the expanding layer. These differences are found to be related to differences in the overturning circulation. However, neither the temporal development of these vertical structures, nor the

relation to different GHG concentration pathways, nor how these patterns would change under stabilized GHG concentrations have been investigated.

Most of the AR4 models did not include a fully resolved stratosphere. However, based on comparisons of EGMAM, ECHO-G and other GCMs in the 20th century climate and the IPCC A2 scenario HUEBENER et al. (2007) have shown that the coupling of the three subsystems ocean, the troposphere and the stratosphere is important for long-term transient simulations. For example, while the climate-change signal in the ECHO-G storm track does not agree well with the other AR4 models, the inclusion of the stratosphere leads to a convergence to the IPCC model-mean signal. Furthermore, the inclusion of the stratosphere results in a shift of the extratropical circulation compared to simulations without explicitly resolved stratosphere, which alters the regional rainfall pattern (SCAIFE et al, 2011). The circulation change is caused by an increased warming in the Arctic stratosphere, thereby altering the Arctic Oscillation (SCHIMANKE, 2012). SCAIFE et al. (2011) conclude that extending models upwards may represent a first-order correction to climate projections for the mid-latitudes.

In this paper we use the fully coupled ocean-troposphere-stratosphere-GCM EGMAM (HUEBENER et al., 2007) to explore the response of the near surface temperature (section 3) during increasing GHG concentrations and after stabilization. Then the steric sea level rise is analyzed (section 4). Analysis is presented for global mean changes, both in terms of absolute changes and in terms of decadal rates of steric sea level rise (section 4.1), and for the horizontal and vertical structure of steric anomalies (section 4.2). Additionally we analyze the oceanic heat uptake as well as the expansion efficiency of heat in the stabilization experiments (section 5). Results are summarized and discussed in section 6.

2) Model Description and Experimental Design

The experiments presented in this study were performed with the fully coupled ocean-troposphere-stratosphere-GCM **E**CHO-**G** (LEGUTKE and VOSS, 1999) with **M**iddle **A**tmosphere **M**odel (EGMAM) (HUEBENER et al., 2007). The atmosphere model is an extended version of the ECHAM4 model (ROECKNER et al., 1996). The ocean model is the HOPE-G (LEGUTKE and VOSS, 1999). In order to prevent the coupled model to drift flux correction for heat and freshwater fluxes is applied which is constant in time and has vanishing global mean values. ECHO-G was employed in a number of climate studies (HUEBENER et al., 2007; KASPAR et al., 2007; MIN et al., 2006, 2005; ZORITA et al., 2004). It has been included in the multi model ensembles of the IPCC-AR4 (MEEHL et al., 2007). The atmospheric part of the EGMAM model resolves the atmosphere in the vertical with 39 levels

Name	Period	Realizations	GHG Forcing
20C3M	1860-1999	3	Observed
A1B	2000-2100	3	SRES A1B
B1	2000-2100	2	SRES B1
COMMIT	2000	2	Const. composition of year 2000
B1stab	2100-2199	2	Const. composition of SRES B1 of year 2100
A1Bstab	2100-2199	3	Const. composition of SRES A1B of year 2100
A1Bstabextr	2200-2299	1	Const. composition of SRES A1B of year 2100

Table 1) Overview of experiment names, time periods and GHG forcing.

up to the mesosphere (0.01hPa). A gravity wave drag parameterization by MANZINI and MCFARLANE (1998) is included. The EGMAM model has an equilibrium climate sensitivity of 2.1K and a transient climate response of 1.5 K (KÖRPER et al., 2009).

Simulations driven by historical forcings of the last 400 years show that EGMAM simulates a Northern Hemisphere mean near surface temperature evolution which is similar to simulations with the ECHO-G model, i.e. the model without highly resolved stratosphere. In terms of the regional climate response, simulations of the last 400 years with the EGMAM model are more realistic than simulations with the ECHO-G model (SPANGEHL et al., 2010). Moreover, climate change signals for example for the Northern Hemisphere storm track (SCAIFE et al. 2011; HUEBENER et al., 2007) and upper tropospheric and lower stratospheric circulation changes (SCHIMANKE et al., 2012) are significantly altered by a extending the model to the stratosphere, proving the benefits of an explicitly resolved stratosphere.

In this study we focus on an analysis of the climate commitment. The simulations for the analysis are summarized in Table 1. Natural forcing (e.g. solar variability or volcanoes) as well as the anthropogenic effect on aerosols and ozone are not included in any of the experiments. Three 20^{th} century simulations starting from different initial conditions from a 600 year pre-industrial control simulation are performed, forced by time-evolving changes of GHGs, i.e. CO_2, CH_4, N_2O and CFCs, of the 20^{th} century (20C3M). For the 21^{st} century, all three experiments are continued with the forcing of the IPCC SRES scenarios A1B and two of them are additionally continued using the B1 scenario forcing (NAKICENOVIC et al., 2000).

Time Period	**A1B / A1Bstab**	**B1 / B1stab**	**COMMIT**
2080-2099 – 1980-1999 Scenario period	2.2K /0.23m/ 227 10^{22} J	1.4K /0.19m/ 181 10^{22} J	0.4K / 0.11m/ 104 10^{22} J
2180-2099 – 2080-2099 Stabilization period	0.4K /0.27m/ 240 10^{22} J	0.3K /0.19m/ 169 10^{22} J	---

Table 2) Simulated and global mean temperature increase (first value [K]), steric sea level rise (second value [m]) and oceanic heat uptake (third value [J]).

Based on these simulations, three stabilization experiments of 100 years each have been run: one simulation is run with GHG held constant at year 2000 concentrations (COMMIT), and two simulations are run with concentrations held constant at the values reached in the year 2100 under the B1 scenario (B1stab) and another 3 runs with concentrations held constant at the values reached in the year 2100 under the A1B scenario (A1Bstab) (see Figure 1 for CO_2 concentrations). One of the A1Bstab runs is extended for another 100 years to year 2300 under constant concentrations (A1Bstabextr) to estimate the longer term behavior of the climate system.

3) Temperature response

The long term temporal development of the global mean near surface temperature reflects the radiative forcing by increasing GHGs in the 20th and 21st century (Figure 1). The simulated warming in the 20th century with around 0.9 K (1980-1999 relative to 1880-1899) (HUEBENER et al., 2007) is within one standard deviation (0.2 K) of the observed value of 0.7 K (TRENBERTH et al., 2007). The slight overestimation of 20th century warming may be related to the cooling effect of anthropogenic aerosols, which is not included in our simulations. Moreover, the preindustrial control simulation is colder than observed leading to a global mean temperature bias of less than 0.01K compared to ERA40 reanalysis for the end of the 20th century (1980-1999). At the end of the 21st century, in line with the comparably low climate sensitivity, simulated global mean warming in the A1B and the B1 scenario (Table 2) is in the lower range compared to other GCMs (MEEHL et al., 2007). MEEHL et al. (2007) give ranges of the multimodel mean surface air temperature warming and associated uncertainty ranges for the time period of 2090 to 2099 relative to 1980 to 1999 +2.8°C (1.7°C to 4.4°C) for the A1B scenario and +1.8°C (1.1°C to 2.9°C) for the B1 scenario. However, comparison of our results with the AR4 models is complicated due to the aerosol forcing of the AR4

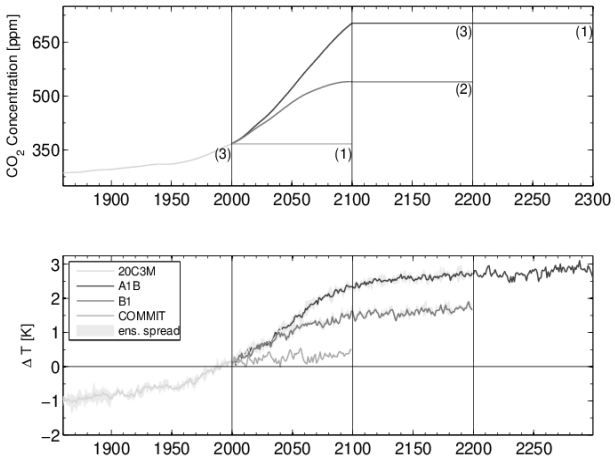

Figure 1) Top: Time series of CO2 concentrations of the SRES scenarios; number of realizations given in brackets Bottom: Time series of temperature; ensemble mean is depicted as well as the ensemble spread where applicable.

model results in contrast to the sole GHG forcing of the simulations presented in this study. After the stabilization of the GHG-concentrations the warming rate decreases quickly (Figure 1, Table 2) similar as described by MEEHL et al. (2006).

The simulated large scale spatial patterns in A1B (2080-2099 relative to 1980-1999, Figure 2) are very similar to those of B1 for this period (not shown) and in agreement with MEEHL et al. (2007). They resemble the well known large spatial distribution with an amplification of the warming in the Arctic Region and an increased land-sea contrast, which is also evident in simulations assuming the representative concentration pathways employed in CMIP5 (TAYLOR et al., 2012; COLLINS et al., 2013). The land-sea contrast vanishes during the stabilization period, indicating that it is caused by the delayed ocean warming due to the large heat capacity of water. The warming in the stabilization phase is strongest in the polar regions of the Northern Hemisphere, related to decreasing sea ice area, and in the Southern Ocean, related to a shift of the circulation.

4) Steric Sea Level Rise

4.1) Global Mean Sea Level Rise

The global mean steric sea level rise (Figure 3) reflects the heat-content change in the entire ocean and can be interpreted as a measure of oceanic inertia (GREGORY et al., 2001). In EGMAM the simulated global mean steric sea level rise is 4cm during the 20th century (1980-1999 relative to 1880-1899), close to the value of 4.7cm determined from CCSM3 (MEEHL et al., 2006). For the A1B-/ B1-scenario the steric sea level rises by about 23cm /19 cm until 2099. The sea level rise continues in the same rate during the stabilization period due

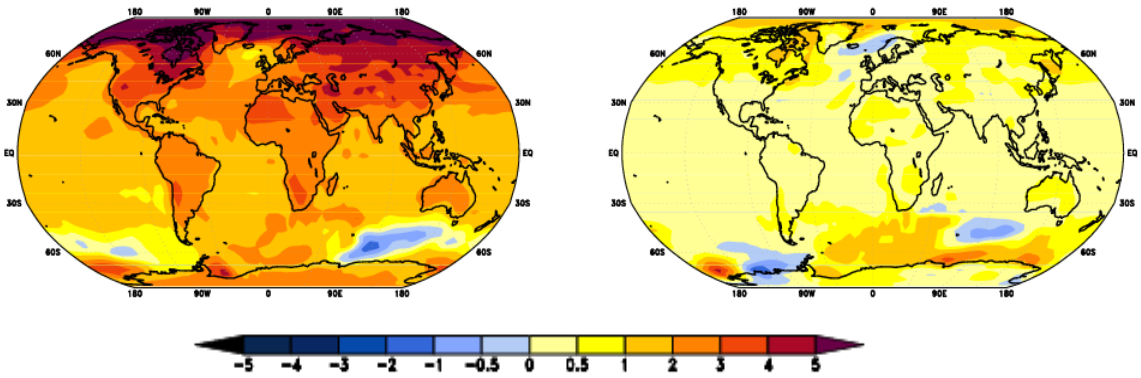

Figure 2) Ensemble mean annual mean surface air temperature change [K] for the A1B scenario (left, 2080-2099 relative to 1980-1999) and A1B stab (right, 2180-2199 relative to 2080-2099).

to the large inertia of the ocean (e.g. CHURCH et al., 2013). The steric sea level rise simulated in EGMAM for the A1B-scenario is even higher for the stabilization period compared to the scenario period (Table 2) and about the same size in both periods for the B1-scenario (Table 2) (cf. KÖRPER et al., 2009). The steric sea level rises during the 21st century in the COMMIT experiment by 11cm (Table 2), which is more than twice the already realized amount of 4 cm. This shows that about half of the 21st century rise of the A1B and B1 scenarios is due to sea level rise that was already committed in year 2000.

Furthermore, the steric sea level rise is assessed by means of trend analysis. The moving 11-year trends, i.e. time series of the slope of a linear fit of global mean sea level in 11-year windows (without overlap), of sea level rise stays positive after 1950. The eleven year window was chosen to reduce the variability on shorter timescales, e.g. interannual timescale. On the other hand, the use of longer windows, e.g. 20 or 30 year windows would decrease the amount of independent data, which would complicate the statistical validity of our results.

The rates of steric sea level rise for the latter half of the 20th century are considerably lower than the observed rates of sea level rise. Most of this difference is explained by the restriction of sea level rise to its steric component in this study and thus, the omission of contributions from glaciers and ice sheets. Moreover, the steric rates in our model of about 0.7-1 mm/y for the last decade of the 20th century are similar to the uncertainty range given by the observations of thermal expansion for the period 1971-2010 of 0.8 [0.5-1.1] mm/y and 1.1 [0.8-1.4] mm/y for the period 1993-2010 (RHEIN et al., 2013).

The rate of global mean steric sea level change increases in the A1B and the B1 scenario during the 21st century. This increase in the trend, illustrated by linear fits in Figure 3, is significant above the 95. percentile according to the t-distribution for each of the realizations of the A1B scenario. By contrast, for the B1 scenario for both realizations the positive trend is statistically not distinguishable from zero due to the limited amount of independent data

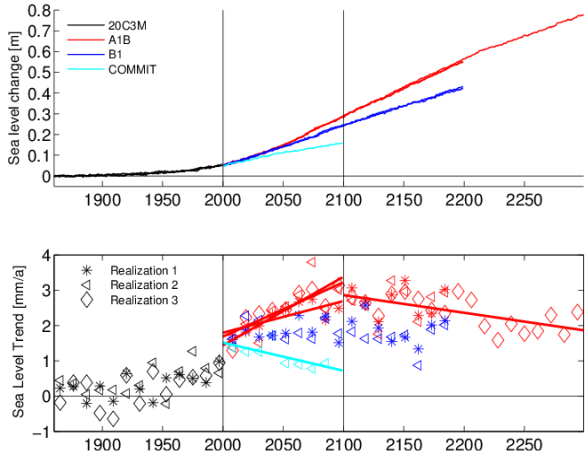

Figure 3) Top: Time series of steric sea level anomaly relative to pre-industrial control simulation for each realization of the historical period and the scenarios; Bottom: 11 –year trend (no overlap) of sea level rise and linear fits for those realizations, where the trend is significantly (above 95 % uncertainty range) different from zero.

points given the interdecadal variability of the rate of sea level rise. However, the rates are higher than for the 20th century leading to more sea level rise than during the 20th century.

The rates of sea level rise decrease once the GHG concentrations have stabilized (Figure 3) in the COMMIT scenario during the 21st century and in the A1Bstab and B1stab. Again, due to the limited amount of data these negative trends are not significant. However, taking into account the 200 year stabilization period in A1Bstabextr, we find a significant negative trend, i.e. the sea level rise is decelerating. Note that the rates of this realization are within the variability of the other two realization of A1Bstab for the 22nd century (Figure 3).

In summary, we find an acceleration of steric sea level rise, while the GHG concentrations are increasing. For stabilized GHG concentrations there is a deceleration of sea level rise. However, there is variability on decadal and multi-decadal timescales in our model, for example due to multi-decadal variability of the oceanic heat uptake in the North Atlantic (e.g. SCHIMANKE et al. 2011), and thus, longer simulations or larger ensembles are needed to draw statistically robust conclusions.

4.2) Horizontal and Vertical Patterns of Steric Sea Level Rise

Spatially heterogeneous density changes cause changes in the regional distribution of sea level compared to the global mean. Although the regional sea level projections of the IPCC-AR4 and IPCC-AR5 multi-model ensembles share some common features, there is considerable spread in the projected patterns (CHURCH et al., 2013; PARDAENS et al. 2011; LANDERER et al., 2007; MEEHL et al., 2007; GREGORY et al 2001). The local amplitudes of

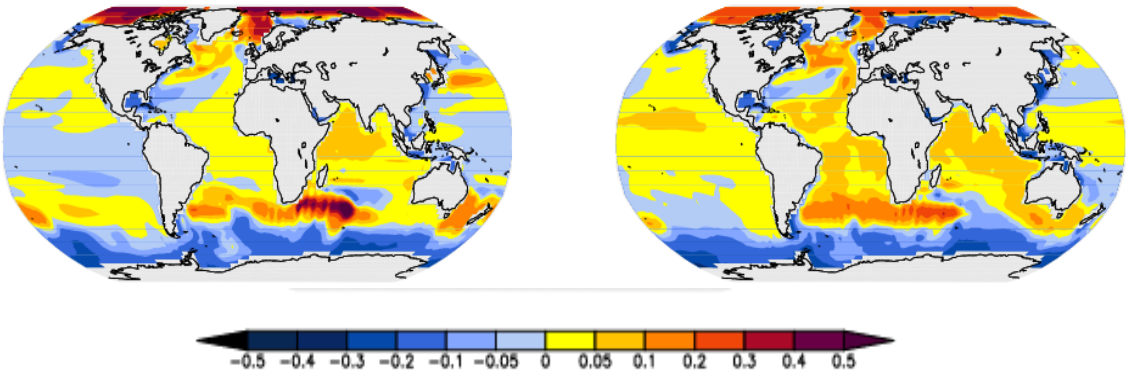

Figure 4) Ensemble mean regional sea level change [m] minus global mean change for the A1B scenario (left, 2080-2099 relative to 1980-1999) and A1B stab (right, 2180-2199 relative to 2080-2099)

regional sea level change compared to global mean range from -0.51 to +0.77 m in the A1B scenario (2080-2099 relative to 1980-1999), a somewhat larger range than found by LANDERER et al. (2007) for the ECHAM5-MPI-OM model for 2090-2099 in the A1B scenario compared to their preindustrial control run, and -0.49 to°+0.66°m in the B1 scenario (2080-2099 relative to

1980-1999). In the stabilization period the range decreases to -0.35 to +0.31 m in A1Bstab and -0.2 to°+0.27 m in B1stab, mainly due to less pronounced sea level amplitudes in the Arctic (see below). We will exemplarily discuss results of the A1B scenario and A1Bstab, because at least concerning the spatial distribution at the surface the features of regional sea level change for the A1B scenario and the B1 scenario are very similar. This has also been shown for the IPCC AR4 models (MEEHL et al., 2007). In EGMAM the simulated spatial patterns of steric sea level rise of the A1B-scenario share most of the large scale features of the multi-model ensemble in the IPCC-AR4 (compare Figure 4 of this study with Fig.1 in PARDAENS et al., 2011). For example, steric sea level change is especially strong in the Arctic, which is related to freshening. Resulting from a southwards shift of the Antarctic Circumpolar Current one finds a band of enhanced sea level rise extending from the South Atlantic towards the Indian Ocean forming a dipole with less than global mean sea level rise in the Southern Ocean south of about 60°S. In the latter region low thermal expansivity leads to less expansion for a given input of heat. The pattern of sea level rise in the North Atlantic is connected to change in the meridional overturning circulation (KÖRPER et al., 2009).

During the stabilization period (Figure 4 right) the large scale spatial distribution of steric sea level rise is similar to the one during the scenario period (Figure 4 left), suggesting that the mechanisms for changes in the regional distribution do not change. However, the difference

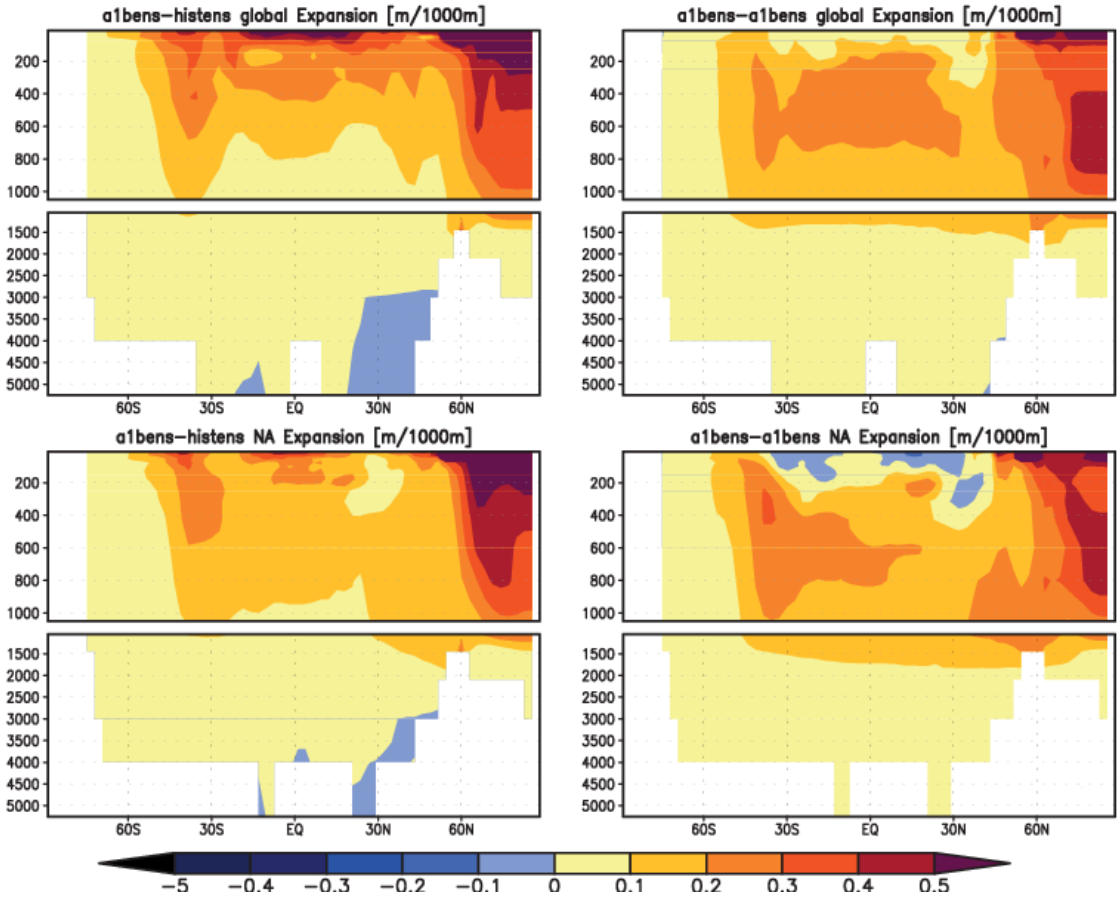

Figure 5) Ensemble mean zonal mean oceanic expansion over the A1B scenario (2080-2099 relative to 1980-1999) (left column) and A1Bstab (2180-2199 relative to 2080-2099); units are meters expansion per 1000 m); for the global ocean (upper row) and the Atlantic and adjoining Southern Ocean section (lower row); note the different scaling for the upper 1000 meters and for deeper layers.

of Arctic expansion compared to global mean expansion is less pronounced. The projected sea level rise in the Atlantic Ocean and the Indian Ocean is larger than the global mean.

Steric sea level change results from subsurface temperature and salinity changes. The vertical profile of zonal mean expansion in the A1B scenario (Figure 5, top left) displays stronger expansion in the upper 700 meters of the ocean in most latitudes and less expansion in the deep ocean. Compared to the profiles of PARDAENS et al. (2011) in their Fig.8 EGMAM would be considered a model with an intermediate depth of expansion rates greater than 0.1 meters per 1000 m in the Atlantic. In A1Bstab the maximum of the expansion is shifted to deeper depth (Figure 5 top right). In the tropical and subtropical Atlantic even a slight contraction reaching from the surface until roughly 300 meter depth (Figure 5 lower row), which is related to increasing salinity. In KÖRPER et al. (2009) more details on the contributions of thermosteric and halosteric effects in the North Atlantic are presented.

Hofmoeller diagrams (Figure 6) illustrate how the layer with maximum expansion rates penetrates into the deeper ocean with time. In the A1B scenario and A1Bstab, the penetration

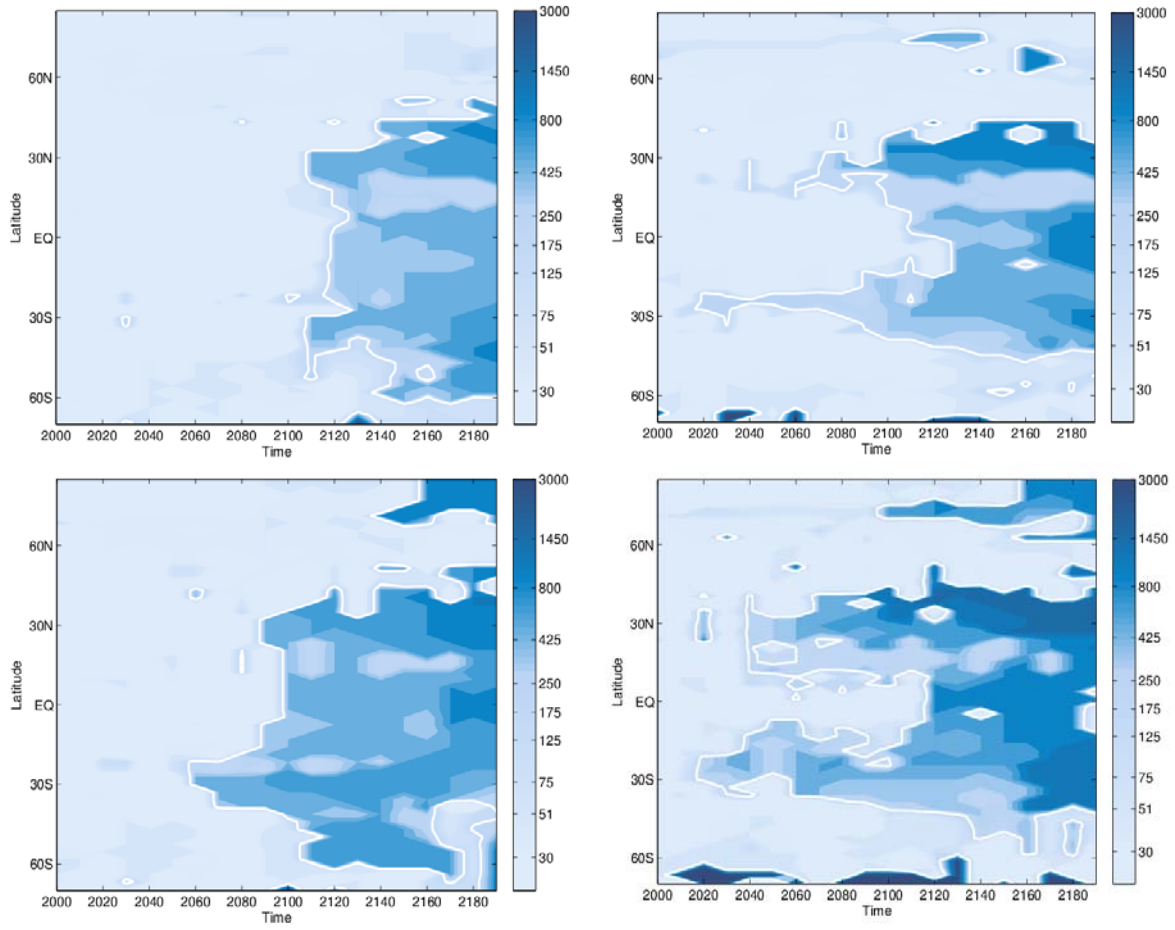

Figure 6) Hofmoeller diagrams of depth with maximum ensemble mean expansion rate [m below sea level] for the A1B scenario, A1B stab (top) and for the B1 scenario and B1stab (bottom) for the global ocean (left), the Atlantic Ocean (right); maximum expansion rates below 175 meters are indicated by a white contour line; calculation is based on expansion rates of the previous 50 years; for example values at year 2000 reflects expansion rates from 1950 to 2000.

into deeper oceanic depth is delayed compared to the B1 scenario and B1stab, which may be explained by the weaker GHG concentration increase in the second half of the 20th century. The shift to deeper oceanic layers is most pronounced south of 45°N. In the Arctic Ocean this feature is not displayed by the Hofmoeller diagrams, because two layers with enhanced expansion rates develop (Figure 5). Consistent with the decomposition of Arctic steric sea level change into halosteric and thermosteric effects by LANDERER (2007) there is a shallow but strong maximum of expansion rates in the surface layer, which can be explained by the halosteric effect of sea ice melting. In addition, there is a broader maximum between 500 and 1000 meter depth (Figure 5) due to thermosteric expansion. In the subtropics of the Atlantic Ocean (Figure 6 right column) and the Indian Ocean (not shown) the penetration into deeper ocean starts somewhat earlier than for example in tropical latitudes. As the lowest expansion rates are found in the Southern Ocean (Figure 5) especially deep layers with maximum

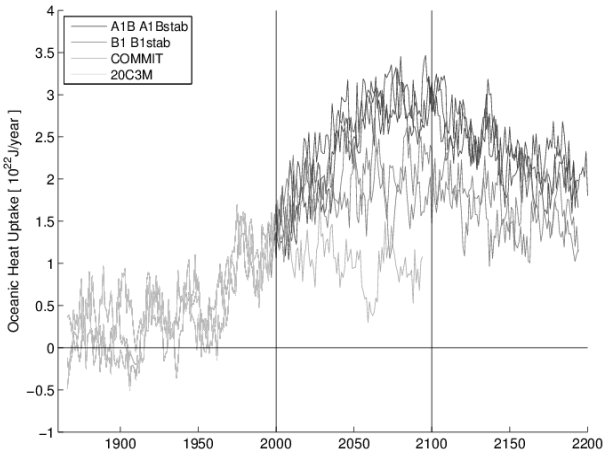

Figure 7) 11-year running mean of oceanic heat uptake [10^{22} J/year] ; all realizations are shown; normalized by subtracting the mean heat flux of pre-industrial control simulation; grey shades as in Figure 1.

expansion rates can be found in several periods throughout the 21st and 22nd century, but are not related to a penetration of heat from the surface into the deep ocean.

5) Oceanic Heat Uptake and Expansion Efficiency

Since the integral ocean bottom heat flux is defined to be zero in the model, the surface flux corresponds to the absolute heat uptake by the ocean. The oceanic heat uptake is 227/181 10^{22} J for the A1B/B1 scenarios (Table 2). In B1stab the heat uptake slightly decreases, while it increases for A1Bstab (Table 2). Since the total heat uptake is the temporal integral of the yearly uptake rates, the time-series of yearly uptake rates (Figure 7) are employed to explain the differences between the scenarios. The yearly rates of oceanic heat uptake of the A1B and the B1 scenario overlap during the first half of the 21st century, in the second half of the century they only occasionally overlap (Figure 7). By the end of the 21st century the yearly heat uptake in the A1B scenario is about 1 10^{22} J larger than in the B1 scenario. From year 2100 onwards in both scenarios, A1Bstab and B1stab, the yearly heat uptake decreases with similar trend. Thus, the larger value of the total heat uptake in the 22nd century in A1Bstab compared to B1stab results from the higher yearly heat uptake in the A1B-scenario throughout the stabilization period.

The steric sea level rise depends not only on the oceanic heat uptake but also on how this heat uptake is translated into expansion. Although the heat uptake for all scenarios is larger in EGMAM than in the CCSM3 reported by MEEHL et al. (2006) the steric sea level rise in the 21st century is comparable. This is related to the low expansion efficiency in EGMAM. The expansion efficiency is about 0.9-1.0 (m^3/kWyear), which is only two thirds of the expansion efficiency of the NASA/GISS model (RUSSELL et al., 2000) and slightly lower than in the

version of the GFDL model of BRYAN et al. (1996) (see RUSSELL et al., 2000 for more details). The comparably low expansion efficiency has also been found in a newer version of EGMAM, EGMAM+ (KÖRPER et al., 2012).

Since the expansion efficiency increases with temperature and salinity, a low expansion efficiency suggests that the heat penetrates into colder waters than in a model with a higher expansion efficiency. This may be partly related to the present day climatology of the model. Although the simulated global mean oceanic temperatures from 1950 to 2000 are slightly overestimated compared to the World Ocean Atlas 2009 climatology (LOCARNINI et al., 2010), simulated temperatures of the entire Arctic Ocean and the upper 200 m of the tropical Pacific are less than observed. In both of these regions the heat uptake is larger than global mean (without figure).

A different geographical distribution of heat uptake than observed may also explain a low global mean expansion efficiency. For example, LOWE and GREGORY (2006) show that the relative minimum of steric sea level rise in the Southern Ocean is related to the low expansion efficiency in this region. The spatial patterns of the net heat flux into the ocean in EGMAM, however, agree with the observed distribution described by STAMMER et al. (2004), indicating that the geographical distribution is not the dominant reason for the low expansion efficiency.

6) Discussion and Conclusions

The ocean-troposphere-stratosphere-GCM EGMAM is employed to simulate climate under increasing GHG-concentrations following historical and scenario story lines and stabilization of concentrations thereafter. These long stabilization simulations with AOGCMs are necessary to study the climate commitment to compliment the mitigation scenarios (e.g. VAN VUUREN et al., 2007) and representative concentration pathways (TAYLOR et al., 2012). On the global scale, the patterns of change simulated with EGMAM are comparable to other GCMs (COLLINS et al., 2013; MEEHL et al., 2007, 2006). As a consequence of stratospheric effects on the strength and the position of storm tracks, they differ, however, considerably in the extratropical precipitation distribution (SCAIFE et al, 2011). Consistent with RAPER et al. (2002) due to the low climate sensitivity of EGMAM the temperature increase is in the lower range compared to other GCMs.

In addition to the dependency of climate commitment on the climate sensitivity of the GCM (RAPER et al., 2002) and the oceanic heat uptake (WETHERALD et al., 2001), our results show that the long term climate change also depends on the rate of increase of GHG concentrations before stabilization. While the atmosphere reacts comparably fast to the stabilization of GHG

concentrations, the ocean responds more slowly. In the A1B scenario, which has the largest increase in GHG concentrations in this study, the oceanic heat uptake and consistently the steric sea level rise are higher in the 22nd century than in the 21st century. However, a trend analysis shows a weakening of the positive trend during the stabilization period.

In addition to the steric component of sea level rise, during the next millennium the melting of land ice will further contribute to sea level rise (e.g., CHURCH et al., 2013). The upper limit for the contribution of glaciers and ice caps outside Greenland and Antarctica can be given by the total ice volume available for melt. It is estimated to be less than 0.4 m sea level equivalent (e.g. STEFFEN et al. 2010 and references therein) and thus, in the longer term its contribution to sea-level rise will diminish. More importantly, if the Antarctic and Greenland Ice Sheets would be melted, the resulting sea level rise would be 7m. According to two studies at least for the Greenland Ice Sheet an estimate of the threshold for an ongoing decay over millennia is given at a global mean near surface warming of 1.9-5.1 °C (95% confidence interval) with a best estimate of 3.1 °C (GREGORY and HUYBRECHTS 2006) and 1.6 [0.9–2.8] °C (5–95% confidence interval) (ROBINSON et al., 2012) compared to the preindustrial climate. According to the simulations presented in this study, global mean surface warming is within the estimated range of the threshold in the A1B and the B1 scenario. If these temperatures would be prevailed over millennia there would be a virtual elimination of the Greenland Ice Sheet. For shorter periods above this threshold a new equilibrium may be possible (e.g. RIDLEY et al. 2010). However, for a detailed quantitative assessment of ice sheet contributions to sea level rise, studies using high-resolved AOGCMS coupled to an ice-model are needed and still not suitable for simulations covering millennia due to high computational cost.

While the large scale spatial patterns of steric sea level rise do not differ substantially between the scenario period and the stabilization period, there is a shift of the layers with maximum expansion rates from near surface towards greater depth after GHG concentrations have stabilized.

Acknowledgements

We gratefully acknowledge the ENSEMBLES project, funded by the European Commission's 6th Framework Programme (FP6) through contract GOCE-CT-2003-505539. We thank Henning Rust for comments on the statistical fitting methods and two anonymous for their very helpful comments on an earlier version of this paper.

References

BRYAN, K., 1996: The steric component of sea level rise associated with enhanced greenhouse warming: a model study. -- Clim. Dyn. **12**, 545—555

CHURCH, J.A., P.U. CLARK, A. CAZENAVE, J.M. GREGORY, S. JEVREJEVA, A. LEVERMANN, M.A. MERRIFIELD, G.A. MILNE, R.S. NEREM, P.D. NUNN, A.J. PAYNE, W.T. PFEFFER, D. STAMMER, A.S. UNNIKRISHNAN, 2013: Sea Level Change. – In: Climate Change 2013: The Physical Science Basis. Working Group I Contribution to the IPCC 5th Assessment Report (in press)

COLLINS, M., R. KNUTTI, J.M. ARBLASTER, J.-L. DUFERESNE, T. FICHEFET, P. FRIEDLINGSTEIN, X. GAO, W.J. GUTOWSKI JR., T. JOHNS, G. KRINNER, M. SHONGWE, C. TEBALDI, A.J. WEAVER, M. WEHNER, 2013 : Long-term Climate Change : Projections, Commitments and Irreversibility. – In: Climate Change 2013: The Physical Science Basis. Working Group I Contribution to the IPCC 5th Assessment Report (in press)

GREGORY, J.M., P. HUYBRECHTS, 2006: Ice-sheet contributions to future sea-level change. -- Phil. Trans. R. Soc. A **364**, 1709--1732, doi: 10.1098/rsta.2006.1796 GREGORY, J.M., J.A. CHURCH, G.J. BOER, K.W. DIXON, G.M. FLATO, D.R. JACKETT, J.A. LOWE, S.P. O'FARRELL, E. ROECKNER, G.L. RUSSELL, R.J. STOUFFER, M. WINTON, 2001: Comparison of results from several AOGCMs for global and regional sea-level change 1900-2100. -- Clim. Dyn. **18**, 225--240

GREGORY, J.M., J.A. LOWE, 2000: Predictions of global and regional sea level rise using AOGCMs with and without flux adjustment. -- Geophys. Res. Lett. **27**, 3069--3072
HANSEN, J., A. LACIS, D. RIND, G. RUSSELL, P. STONE, 1984: Climate sensitivity: Analysis of feedback mechanisms. -- In: J.E. HANSEN, T. TAKAHASHI (Eds.): Climate processes and climate sensitivity, AGU Geophysical Monograph 29, Maurice Ewing Vol. **5**, American Geophysical Union, 130--163.

HUEBENER, H., U. CUBASCH, U. LANGEMATZ, T. SPANGEHL, F. NIEHÖRSTER, I. FAST, M. KUNZE, 2007: Ensemble climate simulations using a fully coupled ocean-troposphere-stratosphere GCM. -- Phil. Trans. Roy. Soc. Series A **365**, 2089--2101.

KASPAR, F., T. SPANGEHL, U. CUBASCH, 2007: Northern hemisphere winter storm tracks of the Eemian interglacial and the last glacial inception. -- Climate of the Past **3**, 181--192.

KÖRPER, J., I. HÖSCHEL, J.A. LOWE, C.D. HEWITT, D. SALAS Y MELIA, E. ROECKNER, H. HUEBENER, J.-F. ROYER, J.-L. DUFRESNE, A. PARDAENS, M.A. GIORGETTA, M.G. SANDERSON, O.H. OTTERÅ, J. TJIPUTRA, S. DENVIL, 2012: The Effects of Aggressive Mitigation on Steric Sea Level Rise and Sea Ice Changes. -- Submitted to Clim. Dyn.

KÖRPER J., T. SPANGEHL, U. CUBASCH, H. HUEBENER, 2009: Decomposition of Projected Regional Sea Level Rise in the North Atlantic and its Relation to the AMOC. -- Geophys. Res. Lett. **36**, L19714, doi:10.1029/2009GL039757

LANDERER, F.W., J.H. JUNGCLAUS, J. MAROTZKE, 2007: Regional Dynamic and Steric Sea Level Change in Response to the IPCC-A1B Scenario. -- Journal of Physical Oceanography **37**, 296-312

LI, C., J-S. von Storch, J. MAROTZKE, 2012: Deep-ocean heat uptake and equilibrium climate response. -- Clim. Dyn., doi: 10.1007/s00382-012-1350-z

LOWE, J.A., J.M. GREGORY, 2006: Understanding projections of sea level rise in the Hadley Centre coupled climate model. -- J. Geophys. Res. **111**, C11014

LOCARNINI, R.A. , A.V. MISHONOV, J.I. ANTONOV, T.P. BOYER, H.E. GARCIA, O.K. BARANOVA, M.M. ZWENG, D.R. JOHNSON, 2010: World Ocean Atlas 2009, Volume I: Temperature. -- In: Levitus, S. (Ed.): NOAA Atlas NESDIS 68, U.S. Government Printing Office, Washington, D.C., 184 pp.

LEGUTKE, S., R. VOSS, 1999: The Hamburg Atmosphere-Ocean Coupled Circulation Model ECHO-G -- Technical Report **18**, DKRZ-Hamburg, Germany

MANZINI, E., N.A. MCFARLANE, 1998: The effect of varying the source spectrum of a gravity wave parameterization in a middle atmosphere general circulation model. -- J. Geophys. Res. **103**, 31523--31539

MANABE, S., R.J. STOUFFER, 1994: Century-scale effects of increased atmospheric CO_2 on the ocean-atmosphere system. -- Nature **364**, 215--218

MEEHL, G.A., A. HU, C. TEBALDI, J.M. ARBLASTER, W.M. WASHINGTON, H. TENG, B.M. SANDERSON, T. AULT, W.G. STRAND, J.B. WHITE, 2012: Relative outcomes of climate change

mitigation related to global temperature versus sea-level rise. -- Nature Climate Change **2**, 576--580

MEEHL, G.A., T.F. STOCKER, W.D. COLLINS, P. FRIEDLINGSTEIN, A.T. GAYE, J.M. GREGORY, A. KITOH, R. KNUTTI, J.M. MURPHY, A. NODA, S.C.B. RAPER, I.G. WATTERSON, A.J. WEAVER, Z.-C. ZHAO, 2007: Global Climate Projections. -- In: SOLOMON, S., D. QIN, M. MANNING, Z. CHEN, M. MARQUIS, K.B. AVERYT, M. TIGNOR, H.L. MILLER (Eds.): Climate Change 2007: The Physical Science Basis. Contribution of Working Group I to the Fourth Assessment Report of the Intergovernmental Panel on Climate Change -- Cambridge University Press, Cambridge, United Kingdom and New York, NY, USA

MEEHL, G.A., W.M. WASHINGTON, B.D. SANTER, W.D. COLLINS, J.M. ARBLASTER, A. HU, D.M. LAWRENCE, H. TENG, L.E. BUJA, W.G. STRAND, 2006: Climate change projections for the 21st century and climate change commitment in the CCSM3. -- J. Climate CCSM3 special issue

MEEHL, G.A., W.M. WASHINGTON, W.D. COLLINS, J.M. ARBLASTER, A. HU, L.E. BUJA, W.G. STRAND, H. TENG, 2005: How Much More Global Warming and Sea Level Rise? -- Science **307**, 1769--1772

MIN, S-K., S. LEGUTKE, A. HENSE, U. CUBASCH, W-T. KWON, J-H. OH, U. SCHLESE, 2006, East Asian Climate Change in the 21st Century as Simulated by the Coupled Climate Model ECHO-G under IPCC SRES Scenarios. -- J. Meteorol. Soc. Jpn. **84**, 1--26

MIN, S-K., S. LEGUTKE, A. HENSE, W-T. KWON, 2005: Internal variability in a 1000-yr control simulation with the coupled climate model ECHO-G - I. Near-surface temperature, precipitation and mean sea level pressure. -- Tellus A **57**, 605--621

MOSS, R.H., J.A. EDMONDS, K.A. HIBBARD, M.R. MANNING, S.K. ROSE, D.P. VAN VUUREN, T.R. CARTER, S. EMORI, M. KAINUMA, T. KRAM, G.A. MEEHL, J.F.B. MITCHELL, N. NAKICENOVIC, K. RIAHI, S.J. SMITH, R.J. STOUFFER, A.M. THOMSON, J.P. WEYANT, T.J. WILBANKS, 2010: The next generation of scenarios for climate change research and assessment. -- Nature **463**, 747--756

NAKICENOVIC, N., and coauthors, 2000: Special Report on Emissions Scenarios: A Special Report of Working Group III of the Intergovernmental Panel on Climate Change -- Cambridge University Press, 599 pp

PARDAENS, A.K., J.M. GREGORY, J.A. LOWE, 2011: A model study of factors influencing the projected changes in regional sea level over the twenty-first century. -- Clim. Dyn. **36**, 2015--2033

RAPER, S.C.B., J.M. GREGORY, R.J. STOUFFER, 2002: The Role of Climate Sensitivity and Ocean Heat Uptake on AOGCM Transient Temperature Response. -- J. Climate **15**, 124--211

RHEIN, M., S. R. RINTOUL, S. AOKI, E. CAMPOS, D. CHAMBERS, R. A. FEELY (USA), S. GULEV, G. C. JOHNSON, S. A. JOSEY, A. KOSTIANOY, C. MAURITZEN, D. ROEMMICH, L. TALLEY, F. WANG, 2013:Observations: Ocean . – In: Climate Change 2013: The Physical Science Basis. Working Group I Contribution to the IPCC 5th Assessment Report (in press)

RIDLEY, J., J.M. GREGORY, P. HUYBRECHTS, J. LOWE, 2010: Thresholds for irreversible decline of the Greenland ice sheet. -- Clim Dyn. **35**, 1049-- 1057, doi: 10.1007/s00382-009-0646-0

ROBINSON, A., R. CALOV, A. GANOPOLSKI, 2012: Multistability and critical thresholds of the Greenland ice sheet. Nature Climate Change, **2**, 429-432.

ROECKNER, E. , K. ARPE, L. BENGTSSON, M. CHRISTOPH, M. CLAUSSEN, L. DÜMENIL, M. ESCH, M. GIORGETTA, U. SCHLESE, U. SCHULZWEIDA, 1996: The atmospheric general circulation model ECHAM-4: Model description and simulation of present-day climate. -- Technical Report, Max Planck Institute for Meteorology, 218

RUSSELL, J.L., K.W. DIXON, A. GNANADESIKAN, R.J. STOUFFER, J.R. TOGGWEILER, 2006: The Southern Hemisphere Westerlies in a Warming World: Propping Open the Door to the Deep Ocean. -- J. Climate **19**, 6382--6390

RUSSELL, G.L., V. GORNITZ, J.R. MILLER, 2000: Regional sea-level changes projected by the NASA/GISS atmosphere-ocean model. -- Clim. Dyn. **16**, 789--797

SCAIFE, A.A., T. SPANGEHL, D.R. FEREDAY, U. CUBASCH, U. LANGEMATZ, H. AKIYOSHI, S. BEKKI, P. BRAESICKE, N. BUTCHART, M.P. CHIPPERFIELD, A. GETTELMANN, S.C. HARDIMAN, M. MICHOU, E. ROZANOV, T.G. SHEPHERD, 2011: Climate Change Projections and Stratosphere-Troposphere Interaction. -- Clim. Dyn., doi: 10.1007/s00382-011-1080-7

SCHIMANKE, S., T. SPANGEHL, H. HUEBENER, U. CUBASCH, 2012: Variability and trends of major stratospheric warmings in simulations under constant and increasing GHG concentrations. -- Clim. Dyn., doi: 10.1007/s00382-012-1530-x

SCHIMANKE, S., J. KÖRPER, T. SPANGEHL, U. CUBASCH, 2011: Multi-decadal variability of sudden stratospheric warmings in an AOGCM. -- Geophys. Res. Lett. **38**, L01801, doi: 10.1029/2010GL045756

SPANGEHL, T. , U. CUBASCH, C.C. RAIBLE, S. SCHIMANKE, J. KÖRPER, D. HOFER, 2010: Transient climate simulations from the Maunder Minimum to present day: the role of the stratosphere. -- J. Geophys. Res. **115**, doi:10.1029/2009JD012358

STAMMER D., K. UEYOSHI, A. KÖHL, W.G. LARGE, S.A. JOSEY, C. WUNSCH, 2004: Estimating air-sea fluxes of heat, freshwater, and momentum through global ocean data assimilation. -- J. Geophys. Res. **109**, C05023, doi:10.1029/2003JC002082

STEFFEN, K., R.H. THOMAS, E. RIGNOT, J.G. COGLEY, M.B. DYURGEROV, S.C.B. RAPER, P. HUYBRECHTS, E. HANNA, 2010: Cryospheric contributions to sea-level rise and variability. -- In: J.A. CHURCH, P.L. WOODWORTH, T. AARUP, W.S. WILSON (Eds.): Understanding sea-level rise and variability -- Oxford, UK: Wiley Publishing. doi: 10.1002/9781444323276.ch7.
STOUFFER, R.J., J.L. RUSSELL, M.J. SPELMAN, 2006: Importance of oceanic heat uptake in transient climate change. -- Geophys. Res. Lett. **33** (17), L17704

TAYLOR K.E., R.J. STOUFFER, G.A. MEEHL, 2012: An overview of CMIP5 and the Experiment Design. Bulletin of the American Meteorological Society, **93**, 485–498.
TRENBERTH, K.E., P.D. JONES, P. AMBENJE, R. BOJARIU, D. EASTERLING, A. KLEIN TANK, D. PARKER, F. RAHIMZADEH, J.A. RENWICK, M. RUSTICUCCI, B. SODEN, P. ZHAI, 2007: Observations: Surface and Atmospheric Climate Change. -- In: SOLOMON, S., D. QIN, M. MANNING, Z. CHEN, M. MARQUIS, K.B. AVERYT, M. TIGNOR, H.L. MILLER (Eds.): Climate Change 2007: The Physical Science Basis. Contribution of Working Group I to the Fourth Assessment Report of the Intergovernmental Panel on Climate Change -- Cambridge University Press, Cambridge, United Kingdom and New York, NY, USA

VAN VUUREN D.P., M.G.J. DEN ELZEN, B. EICKHOUT, 2007, Stabilizing greenhouse gas concentrations at low levels: an assessment of reduction strategies and costs. -- Climatic Change **81**(2), 119--159

VOSS, R., U. MIKOLAJEWICZ, 2001: Long-term climate changes due to increased CO_2 concentration in the coupled atmosphere-ocean general circulation model ECHAM3/LSG. -- Clim. Dyn. **17**, 45--60

WETHERALD R.T., R.J. STOUFFER, K.W. DIXON, 2001: Committed warming and its implications for climate change. -- Geophys. Res. Lett. **28**, 1535--1538

WIGLEY, T.M.L., 2005: The Climate Change Commitment. -- Science **307**, 1766-1769

WIGLEY, T.M.L.., S.C.B. RAPER, 1993: Future changes in global mean temperature and sea level. -- In: WARRICK, R.A., E.M. BARROW, T.M.L. WIGLEY (Eds.): Climate and Sea Level Change: Observations, Projections, and Implications. -- Cambridge Univ. Press, Cambridge,U.K., pp 111--113.

ZORITA, E., H. VON STORCH, F. GONZÁLEZ-ROUCO, U. CUBASCH, J. LUTERBACHER, S. LEGUTKE, I. FISCHER-BRUNS, U. SCHLESE, 2004: Climate evolution in the last five centuries simulated by an atmosphere- ocean model: global temperatures, the North Atlantic Oscillation and the Late Maunder Minimum. -- Meteorol. Z **13**, 271--289

A.2 Körper et al. (2009)

GEOPHYSICAL RESEARCH LETTERS, VOL. 36, L19714, doi:10.1029/2009GL039757, 2009

Decomposition of projected regional sea level rise in the North Atlantic and its relation to the AMOC

J. Körper,[1] T. Spangehl,[1] U. Cubasch,[1] and H. Huebener[2]

Received 24 June 2009; revised 11 August 2009; accepted 11 September 2009; published 14 October 2009.

[1] While it is well understood that thermal expansion dominates global mean steric sea level rise, climate models show large differences in spatial patterns. This study aims to decompose regional steric sea level rise in the North Atlantic into thermal and saline effects in a fully coupled model. In contrast to other studies we focus on the differences between two climate change scenarios and establish a link between the sea level changes and the differences in the response of the overturning circulation. While overturning is reduced in the phase of the greenhouse gas increase, differences between the scenarios are not significant until the stabilization in the 22nd century. The influence from thermosteric and halosteric contributions on the meridional density gradient is of the same size during the increase of greenhouse gas concentrations. The haline effect becomes prominent afterwards, reducing the meridional density gradient and preventing the overturning from recovery. **Citation:** Körper, J., T. Spangehl, U. Cubasch, and H. Huebener (2009), Decomposition of projected regional sea level rise in the North Atlantic and its relation to the AMOC, *Geophys. Res. Lett.*, *36*, L19714, doi:10.1029/2009GL039757.

1. Introduction

[2] Steric sea level changes reflect changes in the specific volume of the ocean due to temperature and salinity variations. In addition, variations of oceanic density influence pressure gradients, which are balanced by geostrophic velocity anomalies. These result in a redistribution of the water masses [*Landerer et al.*, 2007; *Levermann et al.*, 2005]. Therefore, the spatial patterns of sea level rise represent changes of the circulation.

[3] Due to the formation of dense North Atlantic Deep Water, sea level in the North Atlantic is low compared to the North Pacific [e.g., *Rio and Hernandez*, 2004]. In a future climate with increasing greenhouse gas (GHG) concentrations and a weaker Atlantic Meridional Overturning Circulation (AMOC) sea level rise in the North Atlantic may be stronger than in the North Pacific [*Levermann et al.*, 2005; *Yin et al.*, 2009].

[4] To estimate 21st century climate change the SRES scenarios (e.g., A1B and B1) [*Nakicenovic et al.*, 2000] are employed. Although atmosphere ocean general circulation models (AOGCMs) reveal large uncertainty in the response of the AMOC to the GHG increase, most models predict a weakening of the AMOC in the A1B scenario [*Schmittner et al.*, 2005]. In line with uncertainties of AMOC prediction, AOGCMs show large differences in North Atlantic spatial sea level rise [*Gregory et al.*, 2001; *Yin et al.*, 2009].

[5] The decomposition of spatial sea level rise into thermosteric and halosteric contributions gives further insights on the mechanisms involved. *Wang et al.* [2009] analyse observed changes in potential density in the upper 700m and link them to recent AMOC change. However, due to the sparseness of observations their analysis is limited to the upper ocean for a few decades. In an AOGCM *Landerer et al.* [2007] analyse the response in the A1B stabilization experiment and show a close link between steric sea level changes and the North Atlantic gyre circulation. Since their analysis is limited to the A1B scenario, the spatial sea level change representing only a single scenario for AMOC response is assessed. *Yin et al.* [2009] analyze dynamic and steric sea level rise in the A2, A1B and B1 scenario and a water hosing run focusing on the AOGCM GFDL CM2.1. They find dynamic sea level rise to be relatively scenario independent in the 21st century. Nevertheless, their analysis is limited to the 21st century thereby excluding effects of longer delay.

[6] In this paper we use the AOGCM EGMAM [*Huebener et al.*, 2007] to analyse North Atlantic spatial sea level rise and its connection to the AMOC. In contrast to previous studies we focus on the comparison of response in the A1B and B1 scenario. Furthermore, analysis is extended to the 22nd century assuming stabilization of GHG concentration in 2100.

2. Model Description and Experimental Design

[7] The experiments presented in this study were performed with the fully coupled ocean-troposphere-stratosphere-GCM **E**CHO-**G** [*Legutke and Voss*, 1999] with **M**iddle **A**tmosphere **M**odel (EGMAM) [*Huebener et al.*, 2007]. ECHO-G was applied in a number of climate studies [*Huebener et al.*, 2007; *Min et al.*, 2006, 2005]. It is included in the multi-model-ensembles of the IPCC-AR4 [*Meehl et al.*, 2007]. The atmospheric part of EGMAM contains 39 vertical levels reaching up into the mesosphere (0.01hPa). Gravity wave drag parameterization by *Manzini and McFarlane* [1998] is employed. The ocean model is the HOPE-G [*Legutke and Voss*, 1999]. EGMAM has an equilibrium climate sensitivity of 2.1K and a transient climate response of 1.5K.

[8] Three 20th century simulations starting from different initial conditions from a 600 year preindustrial control simulation are performed, forced by time-evolving changes of GHGs of the 20th century and the IPCC SRES scenarios A1B and B1 [*Nakicenovic et al.*, 2000] from 2000 to 2100. Natural forcing (e.g., solar variability or volcanoes) as well as aerosols and ozone are unchanged. Three stabilization

[1]Institute for Meteorology, Freie Universität Berlin, Berlin, Germany.
[2]Hessian Agency for Environment and Geology, Wiesbaden, Germany.

0094-8276/09/2009GL039757$05.00

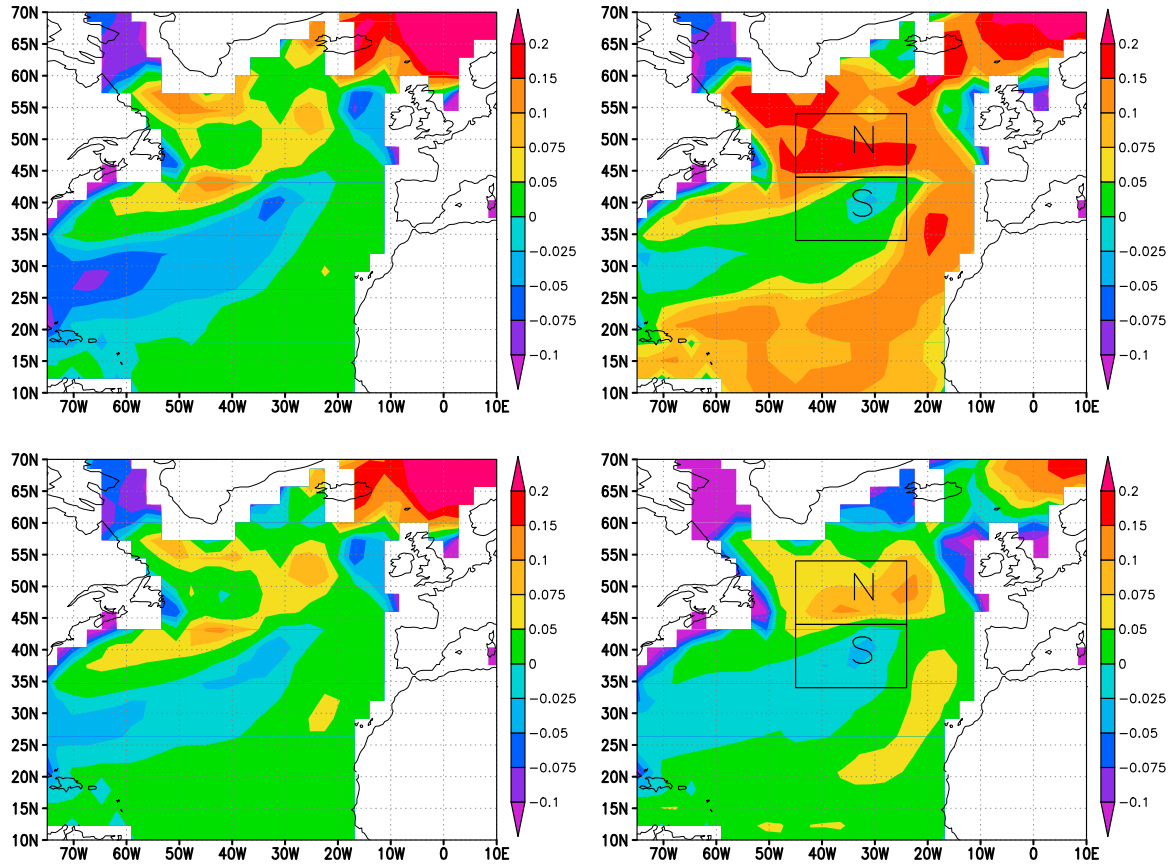

Figure 1. Steric sea level change minus global mean [m] and boxes used for density gradient. (top) A1B (left, 2080–2099 minus 1980–1999, global mean change 23 cm; right, 2180-2199-2080-2099, global mean change 27 cm). (bottom) Same as Figure 1 (top) but for B1 (left, global mean change 19 cm; right, global mean change 19 cm).

experiments of 100 years each are performed: one with GHG-concentrations held constant at year 2000 following the 20th century simulation (COMMIT) and two SRES (A1B and B1) scenarios with concentrations held constant at year 2100 values. These stabilization experiments are used to analyze the delayed response of the climate system [*Meehl et al.*, 2005, 2006, 2007]. To study the role of the initial state three/two realizations of the A1B/B1 stabilization experiment have been calculated.

3. Results

[9] During the scenario period as well as during stabilization mean sea level rise in the North Atlantic is above global mean in the A1B scenario and below it in the B1 scenario (Figure 1). Since the AMOC remains stronger during the B1 scenario (see below), this difference is in line with the concept that sea level rise in the North Atlantic will be stronger due to a slow down of the AMOC [*Levermann et al.*, 2005]. In agreement with *Yin et al.* [2009] the patterns for both scenarios reveal a tongue of reduced sea level rise extending from the Gulf of Mexico north-easterly towards about 20° W (Figure 1). As another indication for a stronger circulation change, the difference in sea level rise between this tongue and the surrounding is higher in the A1B than in the B1 scenario. However, for both periods the patterns for A1B and B1 generally agree in terms of regional characteristics. The differences in these characteristics are stronger between the scenario and stabilization period than between scenarios indicating a very similar pattern of circulation change. Furthermore, the differences between A1B and B1 for the scenario period (Figure 1) reflect the differences in AMOC response, which are only realized in the 20 years considered here (see below, Figure 3). Therefore, decomposition of steric sea level rise in thermosteric and halosteric contributions will focus on the A1B scenario.

[10] To separate the signal into a thermosteric and halosteric part, the steric sea level rise is calculated using either constant salinity or constant potential temperature (present-day climatology). In this approach the equation of state is linearized, because deviations are about two orders smaller than the effects themselves [cf. *Landerer et al.*, 2007].

[11] The North Atlantic zonally averaged thermosteric effect (Figure 2) in the northern hemisphere is positive for all latitudes. While the rate of thermosteric change is almost steady in the subtropics, temporal as well as meridional characteristics are heterogeneous in the subpolar and polar regions. North of about 45° N freshening leads to a positive halosteric contribution to sea level change (Figure 2) that is enhanced in the Arctic due to melting of sea ice. In the subtropics the halosteric contribution is negative reflecting a circulation change as well as the enhanced hydrological cycle. The rate of reduction in this region increases with

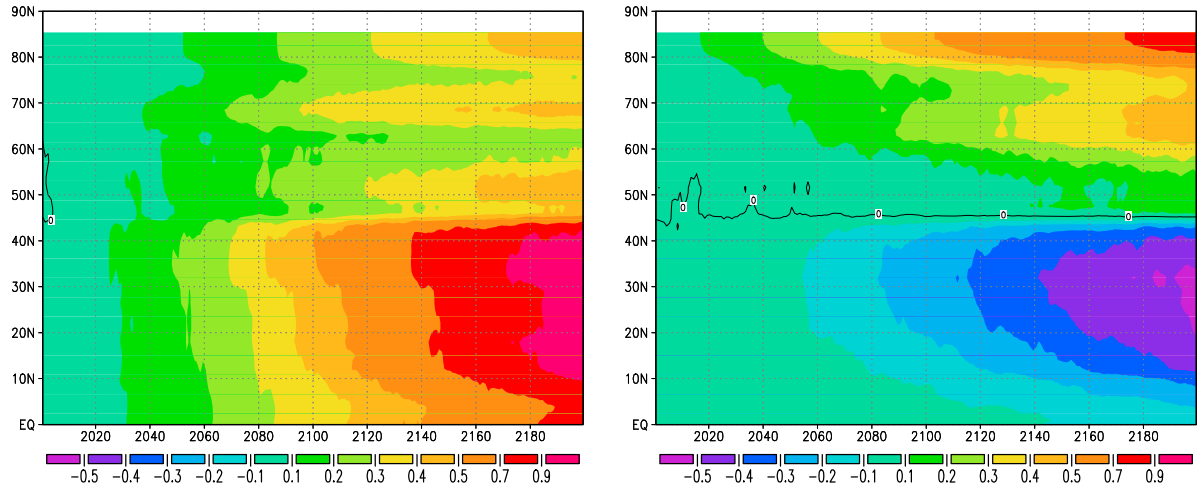

Figure 2. Time evolution of North Atlantic zonal mean (left) thermosteric and (right) halosteric contributions to sea level rise relative to 1980–1999 [m]. Black contour line indicates zero-change.

time indicating a delayed response. In summary, the tongue of lower sea level rise can be explained by a counteracting of thermosteric and halosteric effects south of about 45° N.

[12] The maximum AMOC is 10.9 Sv for present-day (1980–1999) (Figure 3), which is slightly lower than the range of observations 18 (±3–5) [*Talley et al.*, 2003] but in the range of other models [*Meehl et al.*, 2007]. The spread between the realizations is about 2 Sv. Note that the small negative trend in the AMOC during the 20th century is GHG induced as indicated by no trend in the control simulation for the respective periods (not shown). AMOC is reduced by 29%/24% at the end of the 21st century (2080–2099) according to the A1B/B1scenario. This reduction in the A1B scenario is slightly stronger than multi-model estimates [*Schmittner et al.*, 2005]. This small difference between A1B and B1 response is realized in the last 20 years of the 21st century. It is, however, less than two standard deviations. In contrast to *Meehl et al.* [2006] AMOC does not show a recovery in the first century after stabilization of GHG concentrations. At the end of the 22nd century (2180–2199) it is further reduced by 32%/13% to 5.2Sv/7.1Sv after the A1B/B1 scenario. At this time the AMOC differs significantly between the A1B and B1 stabilization as indicated by the spatial sea level change. Further development of the AMOC cannot be assessed due to the relatively short stabilization period simulated. However, in line with results from idealized experiments [*Manabe and Stouffer*, 1993] the temporal development of the 20th century stabilization experiment (COMMIT) indicates that AMOC will stabilize or recover, when stabilizing on comparably low level of GHG concentrations.

[13] As in the work by *Wang et al.* [2009] we subtract two regional means to analyse the meridional density gradient. Herein, the density gradient is defined as the difference of the regional means of the density weighted ocean layer from 112.5 m to 1200 m depth in the regions 24° W to 45° W and 44° N to 54° N and 24° W to 45° W and 34° N to 44° N (see Figure 1). In contrast to *Wang et al.* [2009] the analysis is not limited to the upper ocean. Therefore, the layer between 112.5 and 1200 m is chosen, because it reflects the relevant density gradients for the AMOC in the model. Note, that ocean layers above the top layer would introduce more noise to the time series without containing relevant trends. Ocean layers below this box rather reflect changes in the circulation of Antarctic Bottom Water and are one order smaller than changes in the medium layer. By choosing the central North Atlantic for regional means, the meridional density gradient represents best the spatial characteristics shown in Figure 1. As in the work by *Wang et al.* [2009] the density gradient is calculated under three different assumptions: varying salinity and temperature; varying temperature but constant salinity; varying salinity but constant temperature (Figure 4). Until 2000 the density gradient and the individual effects do not show a significant trend. In the 21st century the thermal effect will increase the density gradient and therefore strengthen the AMOC. On the other hand, the saline contribution decreases the meridional density gradient and therefore weakens the AMOC. Since both contributions are of the same size

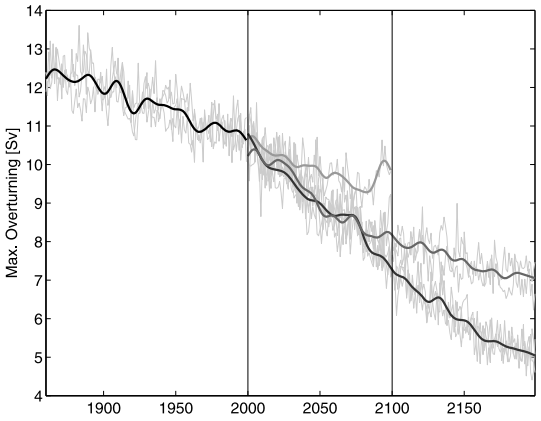

Figure 3. Maximum North Atlantic Overturning; thin lines individual realization; black ensemble mean of 3 historic simulations; light grey COMMIT; medium grey ensemble mean of 2 B1 simulations; dark grey ensembles mean of 3 A1B simulations; COMMIT and ensemble means lowpass filtered.

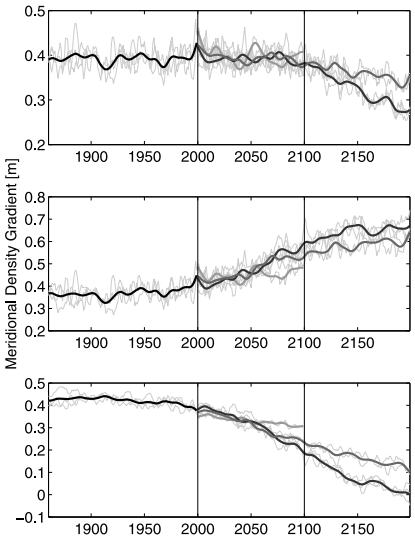

Figure 4. Meridional density gradient. (top) Temperature and salinity effects; (middle) temperature effect; (bottom) salinity effect. Colors as in Figure 3.

during the 21st century the density gradient does not show a trend. In the 22nd century the density gradient decreases for both scenarios and differs significantly between A1B and B1 at 2200. While the thermosteric contribution further increases the density gradient, the halosteric effect becomes dominant resulting in a decreasing density gradient. Both effects are stronger in the A1B than in the B1 stabilization period. Since the differences between the scenarios are larger for the halosteric contribution, the density gradient is significantly reduced for the A1B stabilization period. Because the density gradient affects the AMOC, the AMOC weakens, although GHG concentrations are stabilized.

4. Discussion

[14] The fully coupled ocean-troposphere-stratosphere-GCM EGMAM is employed to analyze steric sea level change in the North Atlantic and its connection to the AMOC in climate change scenarios and stabilization thereafter. In contrast to *Meehl et al.* [2005] but in agreement with some other AOGCMs for example IPSL-CM4 [e.g., *Schmittner et al.*, 2005] the AMOC does not show a recovery in EGMAM in the stabilization period. Moreover, the differences between the scenarios are only significant during the stabilization period resulting from at least century scale adjustment processes.

[15] The stronger North Atlantic sea level change of the A1B scenario and stabilization period displays the larger response of the AMOC compared to B1. In line with the stronger circulation change a tongue of lower sea level rise extending north eastwards towards central North Atlantic is more prominent in A1B. These results are in line with *Levermann et al.* [2005], who used an Earth system model of intermediate complexity. However, in contrast to *Levermann et al.* [2005] wind stress induced sea level change is included in our simulations. In addition, we employed GHG scenarios leading to weakening of the AMOC instead of applying negative salt fluxes. Therefore, decomposition of thermosteric and halosteric contributions is possible.

[16] As shown by *Antonov et al.* [2002], salinity does play a prominent role when analyzing regional sea level change. Decomposition reveals the dominance of the saline contribution once the AMOC has weakened. While the simulated thermosteric sea level change increases the meridional density gradient and thus strengthens the AMOC, the halosteric effect counteracts the thermosteric effect in the subtropics and exceeds the thermosteric effect in the 22nd century, thereby reducing the meridional density gradient. This favors weakening of the AMOC. The effect is more prominent in the A1B scenario reflecting the reduced meridional salinity transport from the subtropics to the subpolar and polar regions with a weaker AMOC. The meridional heat and freshwater transports by the oceanic circulation lead to changes in temperature and salinity and are about one magnitude larger than heat and freshwater fluxes at the surface.

[17] Instead of analyzing the pattern of only one scenario as in the work by *Landerer et al.* [2007] we show here that the difference between two scenarios also gives valuable information on the connection between regional sea level change and the AMOC. Moreover, this study points out that due to long adjustment processes and large internal variability stabilization is useful to detect significant differences between the scenarios. In order to explain model differences in sea level change [*Gregory et al.*, 2001] the fingerprint of AMOC change in spatial sea level seems to hold potential for further understanding.

[18] **Acknowledgments.** We thank the DKRZ for computing time and I. Fast and F. Niehörster for technical support. We thank an anonymous reviewer for his helpful comments on an earlier version of this paper. The research was partially funded by the EU-project ENSEMBLES (contract 505539) and the DFG-project ProSECCO.

References

Antonov, J. I., S. Levitus, and T. P. Boyer (2002), Steric sea level variations during 1957–1994: Importance of salinity, *J. Geophys. Res.*, *107*(C12), 8013, doi:10.1029/2001JC000964.

Gregory, J. M., et al. (2001), Comparison of results from several AOGCMs for global and regional sea-level change 1900–2100, *Clim. Dyn.*, *18*, 225–240, doi:10.1007/s003820100180.

Huebener, H., U. Cubasch, U. Langematz, T. Spangehl, F. Niehörster, I. Fast, and M. Kunze (2007), Ensemble climate simulations using a fully coupled ocean-troposphere stratosphere GCM, *Philos. Trans. R. Soc., Ser. A*, *365*, 2089–2101, doi:10.1098/rsta.2007.2078.

Landerer, F. W., J. H. Jungclaus, and J. Marotzke (2007), Regional dynamic and steric sea level change in response to the IPCC-A1B scenario, *J. Phys. Oceanogr.*, *37*, 296–312, doi:10.1175/JPO3013.1.

Legutke, S., and R. Voss (1999), The Hamburg atmosphere-ocean coupled circulation model ECHO-G, *Tech. Rep. 18*, German Clim. Comput. Cent., Hamburg, Germany.

Levermann, A., A. Griesel, M. Hofmann, M. Montoya, and S. Rahmstorf (2005), Dynamic sea level changes following changes in the thermohaline circulation, *Clim. Dyn.*, *24*, 347–354, doi:10.1007/s00382-004-0505-y.

Manabe, S., and R. Stouffer (1993), Century-scale effects of increased atmospheric CO2 on the ocean-atmosphere system, *Nature*, *364*, 215–218, doi:10.1038/364215a0.

Manzini, E., and N. A. McFarlane (1998), The effect of varying the source spectrum of a gravity wave parameterization in a middle atmosphere general circulation model, *J. Geophys. Res.*, *103*, 31,523–31,539, doi:10.1029/98JD02274.

Meehl, G. A., W. M. Washington, W. D. Collins, J. M. Arblaster, A. Hu, L. E. Buja, W. G. Strand, and H. Teng (2005), How much more global warming and sea level rise?, *Science*, *307*, 1769–1772, doi:10.1126/science.1106663.

Meehl, G. A., W. M. Washington, B. D. Santer, W. D. Collins, J. M. Arblaster, A. Hu, D. M. Lawrence, H. Teng, L. E. Buja, and W. G. Strand (2006), Climate change projections for the 21st century and climate change commitment in the CCSM3, *J. Clim.*, *19*, 2597–2616.

Meehl, G. A., et al. (2007), Global climate projections, in *Climate Change 2007: The Physical Science Basis. Contribution of Working Group I to the Fourth Assessment Report on the Intergovernmental Panel on Climate Change*, edited by S. Solomon et al., pp. 747–845, Cambridge Univ. Press, Cambridge, U. K.

Min, S.-K., S. Legutke, A. Hense, and W.-T. Kwon (2005), Internal variability in a 1000-yr control simulation with the coupled climate model ECHO-G—I. Near-surface temperature, precipitation and mean sea level pressure, *Tellus, Ser. A*, *57*, 605–621, doi:10.1111/j.1600-0870.2005.00133.x.

Min, S.-K., S. Legutke, A. Hense, U. Cubasch, W.-T. Kwon, J.-H. Oh, and U. Schlese (2006), East Asian climate change in the 21st century as simulated by the coupled climate model ECHO-G under IPCC SRES scenarios, *J. Meteorol. Soc. Jpn.*, *84*, 1–26, doi:10.2151/jmsj.84.1.

Nakicenovic, N., et al. (2000), *Special Report on Emissions Scenarios: A Special Report of Working Group III of the Intergovernmental Panel on Climate Change*, 599 pp., Cambridge Univ. Press, Cambridge, U. K.

Rio, M.-H., and F. Hernandez (2004), A mean dynamic topography computed over the world ocean from altimetry, in situ measurements and a geoid model, *J. Geophys. Res.*, *109*, C12032, doi:10.1029/2003JC002226.

Schmittner, A., M. Latif, and B. Schneider (2005), Model projections of the North Atlantic thermohaline circulation for the 21st century assessed by observations, *Geophys. Res. Lett.*, *32*, L23710, doi:10.1029/2005GL024368.

Talley, L. D., J. L. Reid, and P. E. Robbins (2003), Data-based meridional overturning stream functions for the global ocean, *J. Clim.*, *16*, 3213–3226, doi:10.1175/1520-0442(2003)016<3213:DMOSFT>2.0.CO;2.

Wang, X., S. Dong, and E. Munoz (2009), Seawater density variations in North Atlantic and the Atlantic meridional overturning circulation, *Clim. Dyn.*, doi:10.1007/s00382-009-0560-5, in press.

Yin, J., M. E. Schlesinger, and R. J. Stouffer (2009), Model projections of rapid sea-level rise on the northeast coast of the United States, *Nat. Geosci.*, *2*, 262–266, doi:10.1038/ngeo462.

U. Cubasch, J. Körper, and T. Spangehl, Institute for Meteorology, Freie Universität Berlin, Carl-Heinrich-Becker-Weg 6-10, D-12165 Berlin, Germany. (janina.koerper@met.fu-berlin.de)

H. Huebener, Hessian Agency for Environment and Geology, Rheingaustraße 186, D-65203 Wiesbaden, Germany.

A.3 Johns et al. (2011)

This article has been published (Johns TC, Royer J-F, Höschel I, Hue bener H, Roeckner E, Manzini E, May W, Dufresne J-L, Otterå OH, van Vuuren DP, Salas y Melia D, Giorgetta MA, Denvil S, Yang S, Fogli PG, Körper J, Tjip utra JF, Stehfest E, Hewitt CD (2011) Climate change under aggressive mitigatio n: The ENSEMBLES multi-model experiment, *Clim. Dyn.*,**37**). It is available at
`http://dx.doi.org/10.1007/s00382-011-1005-5`

A.4 Körper et al. (2013)

This article has been published (Körper J, Höschel I, Lowe JA, Hewitt CD, Salas y Melia D, Roeckner E, Huebener H, Royer J-F, Dufresne J-L, Pardaens A, Giorgetta MA, Sanderson MG , Otterå OH, Tjiputra JF, Denvil S (2013) The effects of aggressive mitigat ion on steric sea level rise and sea ice changes, *Clim. Dyn.*, **40**). It is available at
`http://dx.doi.org/10.1007/s00382-012-1612-9`

A.5 Huebener and Körper (2013)

Journal of Environmental Protection, 2013, 4, 16-26
http://dx.doi.org/10.4236/jep.2013.48A2003 Published Online August 2013 (http://www.scirp.org/journal/jep)

Changes in Regional Potential Vegetation in Response to an Ambitious Mitigation Scenario

Heike Huebener[1], Janina Körper[2]

[1]Hessian Agency for Environment and Geology, Wiesbaden, Germany; [2]Freie Universität Berlin, Institut für Meteorolgie, Berlin, Germany.
Email: heike.huebener@hlug.hessen.de

Received May 25th, 2013; revised June 3rd, 2013; accepted July 26th, 2013

ABSTRACT

Climate change impacts on the potential vegetation (biomes) are compared for an ambitious emissions-reduction scenario (E1) and a medium-high emissions scenario with no mitigation policy (A1B). The E1 scenario aims at limiting global mean warming to 2˚C or less above pre-industrial temperatures and is closely related to the RCP2.6 sued in the CMIP5. A multi-model ensemble of ten state-of-the-art coupled atmosphere-ocean general circulation models (GCMs) is analyzed. A simple biome model is used to assess the response of potential vegetation to the different forcing in the two scenarios. Changes in biomes in response to the simulated climate change are less pronounced in E1 than in the A1B scenario. Most biomes shift polewards, with biomes adapted to colder climates being replaced by biomes adapted to warmer climates. In some regions cold biomes (e.g. Tundra, Taiga) nearly disappear in the A1B scenario but are also significantly reduced under the E1 scenario.

Keywords: Climate Change; Mitigation Scenario; Potential Vegetation

1. Introduction

The new socio-economic scenarios used in the fifth assessment report of the Intergovernmental Panel on Climate Change (IPCC), the "Representative Concentration Pathway" (RCP)-Scenarios [1] now include explicit mitigation policies. Thus, for the preparation of adaptation actions, an assessment of anticipated changes under strong mitigation scenarios compared to scenarios without mitigation is necessary.

In the EU-funded project ENSEMBLES [2] a mitigation scenario was developed that aims at keeping the 2˚-target: the E1 scenario [3]. E1 starts from an emission path corresponding to the "Special Report on Emission Scenarios" (SRES) A1B scenario, projecting greenhouse gas (GHG) concentrations to stabilize at 450 ppmv CO_2-equivalent (CO_2-e) in the 22nd century after an overshoot to 530 ppmv in the mid 21st century ([3,4]).

Current aerosol trends indicate that the increasing aerosol levels in the SRES A1B scenario are overestimated (e.g. [5,6]). The E1 scenario generates a lower aerosol loading than A1B. This leads to a stronger temperature increase in the E1 scenario compared to the SRES A1B scenario in the first half of the 21st century, despite the reduced greenhouse gas forcing. [4] highlights a non-linear precipitation versus temperature response in some models, possibly related to the balance of surface net radiation induced by the aerosol forcing. Thus, the global mean precipitation increase per degree warming is stronger in the E1 scenario than in the A1B scenario. This effect was already noted in the comparison between the A1B and the "Commit" experiment of the CMIP3 simulations [7] but it is even stronger in E1 compared with A1B [4]. [8] underscores the stronger precipitation response per degree warming in the regional analyses in the E1 scenario compared to the A1B scenario.

Simulations using the A1B and E1 scenarios are analyzed. Model descriptions for the contributing coupled atmosphere-ocean general circulation models (GCMs) and global mean results for temperature, precipitation and carbon cycle fluxes are given in [4]. An analysis of regional precipitation, cloud cover and evapotranspiration is given in [8]. Sea ice and sea level changes are assessed in [9].

The terrestrial biosphere is especially vulnerable to climatic changes [10]. Since anthropogenic land-use change is expected to have the largest effect [11] it is explicitly used as an anthropogenic driver in both of the scenarios

analyzed here. Continental scale shifts of biomes, *i.e*. major regional ecosystems consisting of typical plants, are projected for a future climate in response to regional temperature and water availability changes (e.g. [10,12, 13]). Since biomes depend on distinct hydrological and thermal thresholds, their response to climate change is not a simple linear shift in response to changes in temperature and/or precipitation. Moreover, there are biomes that are more sensitive to temperature changes and other biomes that respond to hydrological changes such as water stress ([11,14]). By analyzing biome shifts simulated in the E1 and the SRES A1B scenarios, we examine whether exceeding these specific thresholds may be avoided by aggressive mitigation measures. Here, we use offline biome calculations to analyze the complete set of available simulations.

We focus on the changes in biomes derived from the climatological monthly means of temperature, precipitation and cloud cover employing the BIOME1 model [15]. The models, data, and methods are described in Section 2. Biome results for the 26 Giorgi-regions form Section 3. In Section 4 the results are summarized and discussed.

2. Data and Methods

The models contributing to this study are given in **Table 1** (see [4] for further details). Simulations for the historical time period 1860-2100 use observed GHG-forcings until the year 2000 (*i.e*. most simulations exclude solar and volcanic variations) and two future scenarios for the time period 2001-2100: The SRES A1B scenario, which does not include an explicit climate mitigation policy and the mitigation scenario E1 which aims at keeping the 2˚-target.

For some, but not all, of the contributing models several simulations were performed, using different initial conditions. In these cases, the simulation results were averaged over all simulations, thus weighting each model equally in the multi-model ensemble analysis.

In accordance with previous analyses (e.g. [8,16,17]) we use the so-called "Giorgi-regions" [18] and consider changes over land areas only. **Figure 1** shows the Giorgi-regions and **Table 2** gives the abbreviations used in the

Table 1. Contributing models, research institutes and references.

Model name	*Institution*	*Ref.*
HadGEM2-AO	Met-Office, UK	Johns *et al*. (2006), Collins *et al*. (2008)
HadCM3C	Met-Office, UK	Gordon *et al*. (2000); Pope *et al*. (2000); Cox *et al*. (2000)
IPSL-CM4	IPSL, France	Marti *et al*. (2010)
IPSL-CM4-LOOP	IPSL, France	Cadule *et al*. (2009)
ECHAM5-C	MPI-M, Germany	Roeckner *et al*. (2006); Marsland *et al*. (2003)
EGMAM+	FUB, Germany	Huebener *et al*. (2007)
INGVCE	CMCC, Italy	Fogli *et al*. (2009); Vichi *et al*. (2011)
CNRM-CM3.3	CNRM, France	Salas-Mélia *et al*. (2005)
BCM2	BCCR, Norway	Furevik *et al*. (2003)
BCM-C	BCCR, Norway	Tjiputra *et al*. (2010)

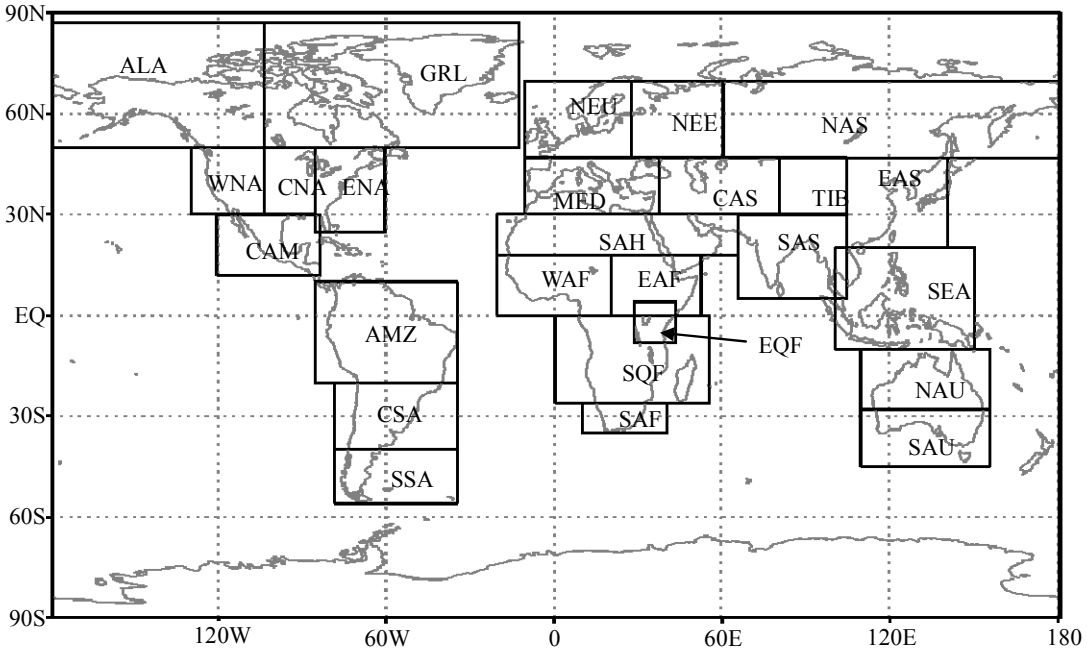

Figure 1. Giorgi-regions: outlines and abbreviations.

Table 2. Giorgi-regions: Abbreviations, region names and geographic borders.

Region abbreviation	*Region name*	*West*	*East*	*South*	*North*
NEU	Northern Europe	−10.5	27.5	47.0	70.0
MED	Mediterranean Basin	−10.5	37.5	30.0	47.0
NEE	North-Eastern Europe	27.5	60.5	47.0	70.0
NAS	North Asia	60.5	180.5	47.0	70.0
CAS	Central Asia	37.5	80.5	30.0	47.0
TIB	Tibet	80.5	104.5	30.0	47.0
EAS	East Asia	104.5	140.5	20.0	47.0
SAS	South Asia	65.5	104.5	5.0	30.0
SEA	Southeast Asia	100.5	150.5	−10.0	20.0
NAU	North Australia	109.5	155.5	−28.0	−10.0
SAU	South Australia	109.5	155.5	−45.0	−28.0
SAH	Sahara	−20.5	65.5	18.0	30.0
WAF	Western Africa	−20.5	20.5	0.0	18.0
EAF	Eastern Africa	20.5	52.5	0.0	18.0
EQF	Equatorial Africa	28.5	43.5	−8.0	4.0
SQF	Southern Equatorial Africa	0.5	55.5	−26.0	0.0
SAF	Southern Africa	10.0	40.5	−35.0	−26.0
ALA	Alaska	−179.5	−103.5	50.0	87.0
GRL	Greenland	−103.5	−12.5	50.0	87.0
WNA	Western North America	−129.5	−103.5	30.0	50.0
CNA	Central North America	−103.5	−85.5	30.0	50.0
ENA	Eastern North America	−85.5	−60.5	25.0	50.0
CAM	Central America	−120.5	−83.5	12.0	30.0
AMZ	Amazon Basin	−85.5	−34.5	−20.0	10.0
CSA	Central South America	−78.5	−34.5	−40.0	−20.0
SSA	Southern South America	−78.5	−34.5	−56.0	−40.0

following of this paper, the region full names and the geographic borders. We analyze the changes in the biomes distributions between the two periods 2080-2099 and 1980-1999, as used in [4].

For the analysis of the biomes, all model data were interpolated onto a common 2.5˚ × 2.5˚ latitude-longitude-grid for further analysis. We focus on the monthly mean changes over two 20 year periods (1980-1999 and 2080-2099) in temperature, precipitation and cloud cover as simulated by the models and the resulting impact on biome distributions. Interannual variability, even though important, is not analysed here.

Biomes current distributions and their projected changes are calculated using the BIOME1 model [15]. While newer versions of the model such as BIOME4 [19] include more than 25 biomes, we use BIOME1 with 17 biomes to assess the most prominent wide-spread changes. Using a limited number of biomes has the advantage of restricting the analyses to the most prominent biomes and avoiding an overinterpretation of the results in the light of the bandwidth of the simulated climate changes, particularly for precipitation and cloud cover.

To assess the models performance observed data are used to calculate biomes and the results are compared to the results obtained from the individual models (not shown) and for the ensemble mean for 1980-1999. To derive a biome map from observations, temperature data from the CRUTS2.1 dataset [20], precipitation data of

the Global Precipitation Climatology Project [21] and the cloud cover data set of the International Satellite Cloud Climatology Project are interpolated to a 2.5˚ × 2.5˚ grid. Additionally, biomes are also calculated from the National Center for Environmental Prediction (NCEP) Re-Analyses to assess the different biome distribution from using different observational data sets. The resulting present-day biome maps are compared to those calculated from the modeled present-day climate data to evaluate the model performance.

To assess the projected changes of the biomes we apply the delta-change method, which has previously been employed for the analysis for projected changes of the Köppen-Trewartha climate classification maps ([22,23]). For this approach the climate signals of temperature, precipitation and cloud cover (2080-2099 minus 1980-1999) from each model are calculated, as well as the ensemble mean signals. To derive the 2080-2099 biome maps, the change from each model is added to the observed 1980-1999 climatology. The delta-change method may produce negative precipitation or a cloud cover greater than 100%. These cases that make no physical sense are excluded.

3. Regional Change in Biomes

Biomes, or potential vegetation, do not necessarily represent the existing vegetation, particularly in regions where natural vegetation has been replaced by crops. Furthermore, changes in potential vegetation do not include direct anthropogenic disturbance (*i.e.* deforestation for cropland or pasture). In regions EAS and CNA, more than half of the area is used for crops and pasture. This fraction is between 33% and 50% in the regions NEU, NEE, SAS, SAF, CAM, and CSA, while in TIB, NAU, EAF and ALA the respective fraction is <10%, and in SAH and GRL <5% (percentages taken from the cropland and pasture fraction per grid cell land-use data in ENSEMBLES project, cf. [4]). However, for some natural ecosystems, such as large parts of the African rainforests or the Siberian tundra, potential vegetation is a reasonable approximation of current actual vegetation. Additionally, changes in climate might make some regions unsuitable for current land use, even under anthropogenic cultivation. This section aims to provide an insight into natural vegetation dynamics as driven by climate change, but will also briefly address the fraction of land used as either crop land or pasture versus natural vegetation.

To evaluate the agreement between the biome maps generated using observed and modelled climate data, we use kappa statistics [24] including their subjective scale for agreement from "No" to "Perfect" (**Table 3**). Since the degree of freedom varies for the different regions owing to the different numbers of grid boxes per Giorgi-region, kappa values estimate the significance of the difference for a given region only. Therefore, comparing kappa values calculated for regions with different sizes should be avoided. Kappa statistics are also used to assess the difference between the maps for the last two decades of the 21st century and the last two decades of the 20th century for the two scenarios.

Table 3. Scale for spatial agreement based on kappa statistics.

Kappa values	*Degree of Agreement*	*Kappa values*	*Degree of agreement*
<0.05	No	0.55 - 0.70	Good
0.05 - 0.20	Very poor	0.70 - 0.85	Very good
0.20 - 0.40	Poor	0.85 - 0.99	Excellent
0.40 - 0.55	Fair	0.99 - 1.00	Perfect

Figure 2 shows the calculated biomes for present-day climate for two different observational data-sets and the ensemble mean of the contributing models. The biomes calculated from the ensemble mean simulations shows in most regions biomes in the range of the biomes calculated from the two observational data-sets. In the following we will refer to the biome distribution calculated from CRU and ISCCP data (**Figure 2(a)**) as "observed" biome patterns.

The main characteristics of the spatial patterns of the present-day biomes are represented well using the ensemble mean climate (**Figure 2(c)**). The kappa values for the global maps, when compared to the map displayed in **Figure 2(a)**, vary between 0.49 and 0.60 for the different models. The Kappa value is highest for the ensemble mean biome map (0.65). It should be noted that the biome of a grid box generated using the ensemble mean climate data is not necessarily the same as the "mean" biome from the individual models.

In some regions the ensemble mean does not depict the observed patterns. For example, in South America all models tend to simulate savannah instead of tropical rain or tropical seasonal forests. The savannah area is largest in BCM-C and smallest in IPSL-CM4, which instead overestimates the extent of xerophytic woods. The largest extent of tropical forests for AMZ is simulated by HADGEM2-AO (largest extent of tropical rainforest) and INGV-CE (largest extent of tropical seasonal forest). Furthermore, in most models the extension of hot desert in CAS is overestimated combined with an underestimated extent of warm grassland. The largest extent of hot desert is found in ECHAM5C. EGMAM+ and HADGEM2-AO agree best with the observed patterns of hot desert and warm grassland (without figures). Globally averaged the ensemble mean overestimates the dry sub-

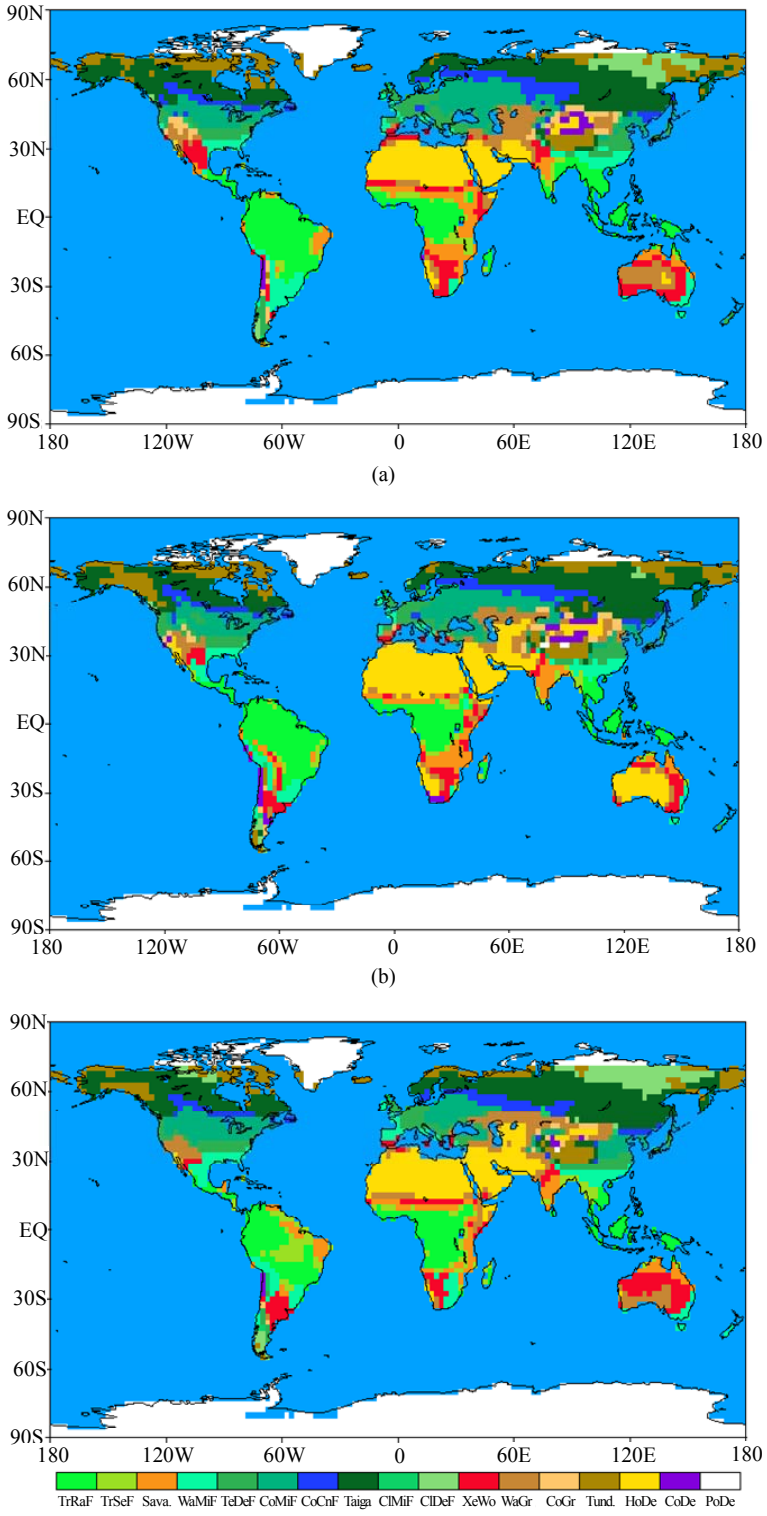

Figure 2. Calculated biomes using (a) observed 1980-1999 CRU (T), GPCP (P), and ISCCP (cloud cover) data, (b) NCEP Re-Analyses and (c) simulated ensemble mean data for 1980-1999. Biomes abbreviations: TrRaF = Tropical Rain Forest, TrSeF = Tropical Seasonal Forest, Sava = Savannah, WaMiF = Warm Mixed Forest, TeDeF = Temperate Deciduous Forest, CoMiF = Cool Mixed Forest, CoCnF = Cool Conifer Forest, Taiga = Taiga, ClMiF = Cold Mixed Forest, ClDeF = Cold Deciduous Forest, XeWo = Xerophytic Woods/Shrub, WaGr = Warm Grass/Shrub, CoGr = Cool Grass/Shrub, Tund. = Tundra, HoDe = Hot Desert, CoDe = Cool Desert, PoDe = Polar Desert/Ice.

tropical biomes hot desert, xerophytic woods and savannah and underestimates the extent of tropical forests. Largest ensemble spread is evident for hot desert and savannah, but also for taiga and tundra, for which the globally averaged ensemble mean is fairly close to observations (**Figure 3**).

Owing to the warming in the 21st century in both scenarios we find a poleward shift of the dominating biomes, leading to a retreat of northern hemispheric taiga and tundra in all models. Because of the drying in the subtropical land areas the extent of savannah, warm grassland and hot desert increases (without figures).

The changes in potential vegetation are analysed in detail using 24 Giorgi-regions (**Figure 4**). The regions SAH and SEA are excluded since the biomes there display only one type (SAH: hot desert, SEA: tropical rain forest) and no significant changes are simulated in either scenario. In the tropical regions consistent with the differences in the precipitation projections the models reveal large differences in biome projections.

In South Asia (SAS) there is a tendency for an increase of savannah replacing forest types. In Southern Equatorial Africa (SQF) and Western Africa (WAF) only small changes are simulated. Note that in these regions anthropogenic land use increases by more than ten percent of the area in the E1 scenario prescribed land use. In the Amazonas Basin (AMZ) the extent of tropical rainforests decreases from about 49% to about 38% in the SRES A1B scenario and to 44% in the E1 scenario. However, the differences between the models are large, consistent with the differences in precipitation, cloud cover and evapotranspiration in this region, as shown by [8]. For AMZ simulated biome changes range from very small (Kappa = 0.88 derived from the CNRM-CM3 model) to quite large (strongest decrease in tropical forest to about 11% - 16% of the total land area derived from HADGEM2-AO and HADCM3C). Rainforests are replaced by savannah, as a result of drying in this region.

In the northern hemispheric subtropics biome changes are relatively small (**Figure 4**). In the Mediterranean Basin (MED) temperate deciduous forests are replaced mainly by warm mixed forest and warm grassland. The latter effect is stronger in the SRES A1B scenario compared to E1 due to the stronger drying in this scenario. In Central America (CAM) the models agree that the dominant present-day biome xerophytic woods is diminished (in E1 significantly less than in A1B), but they disagree on whether it is replaced by warm grassland or savanna. In Central Asia (CAS) the models simulate an expansion of hot desert only in A1B. In the southern hemispheric

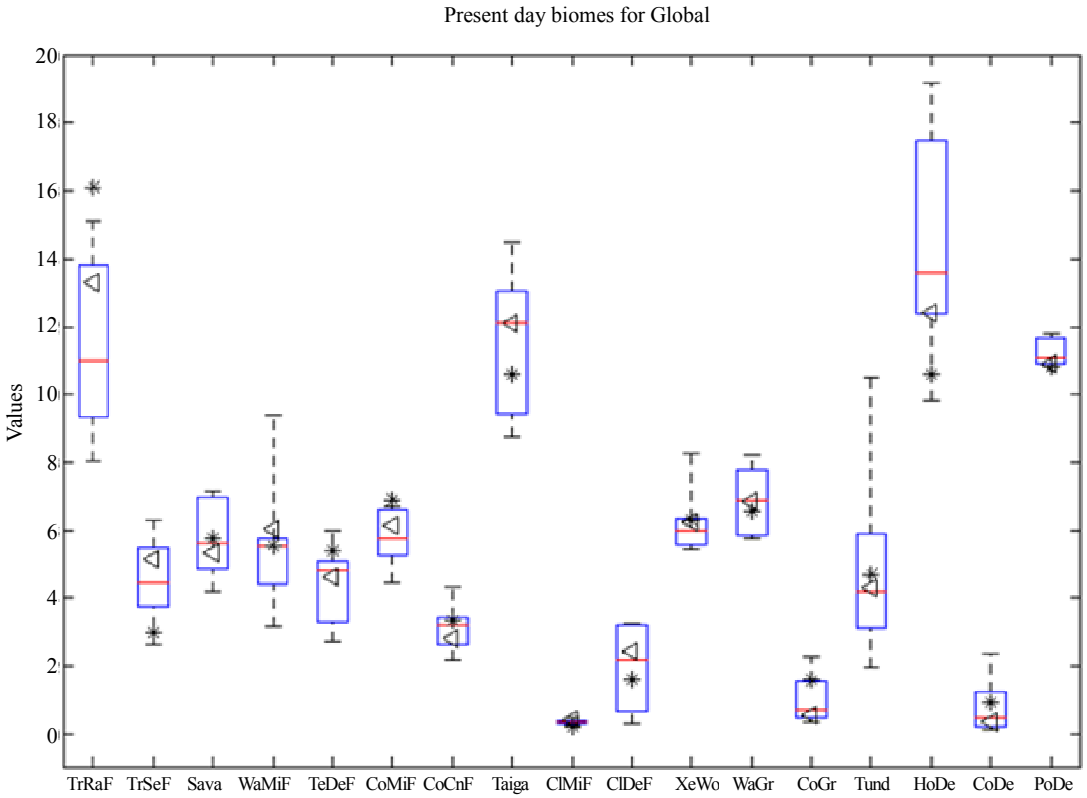

Figure 3. Global mean biome distribution, calculated from the "observed" climate (cf. Figure 5(a)) and from simulated climate by all models. Boxes: 25% - 75%, whiskers: min and max, horizontal line: mean of all simulated biome changes, triangle: biome change calculated from ensemble mean climate change. Asterisks: "observed" biome distribution.

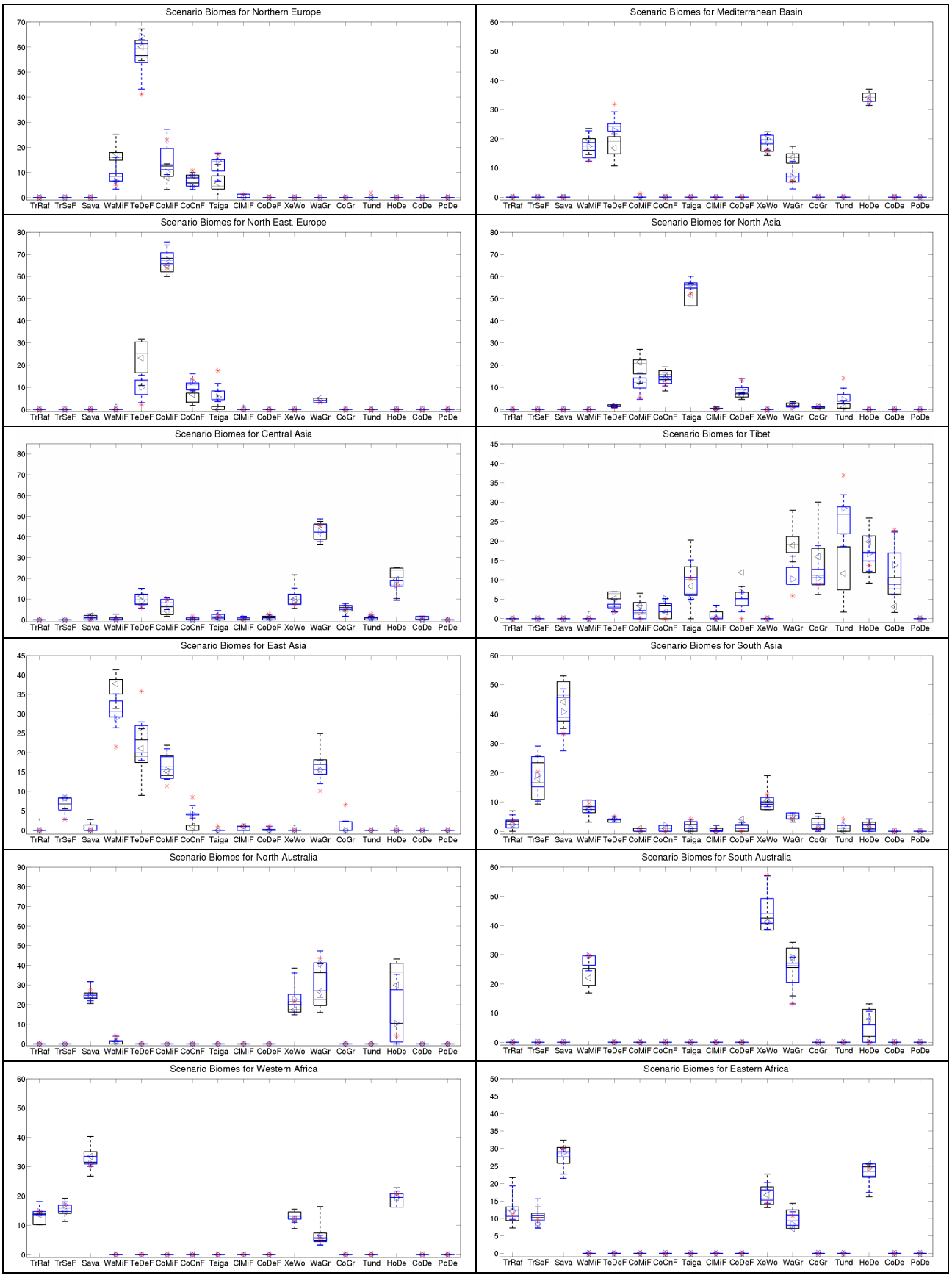

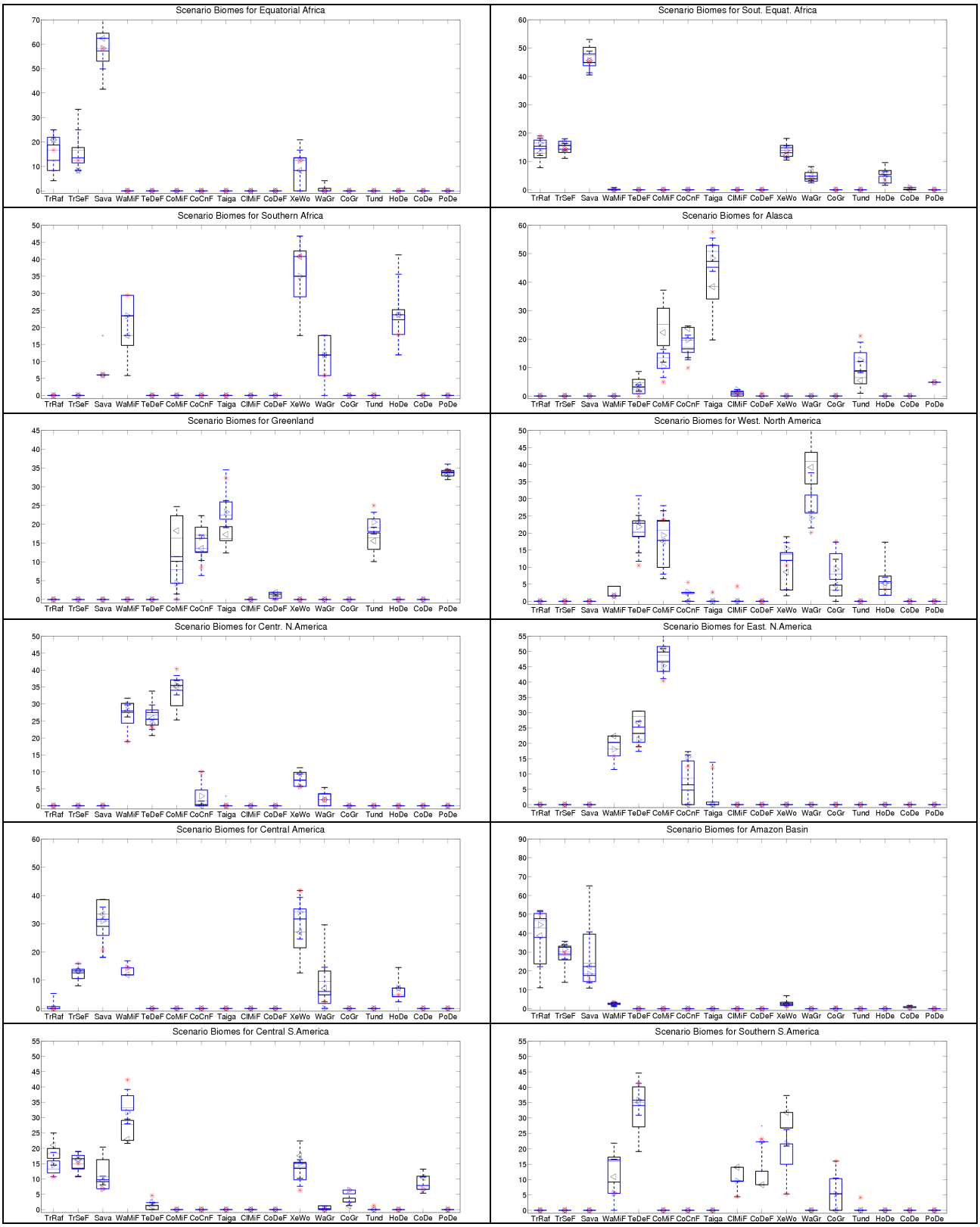

Figure 4. 2080-2099 biome distribution for Giorgi-regions for scenarios A1B (black) and E1 (blue), Boxes: 25% - 75%, whiskers: min and max, horizontal line: mean of all simulated biome changes, triangle: biome change calculated from ensemble mean climate change, cross: outlier (deviation > 2σ). Red asterisks: "observed" biome distribution. Note the differing y-axis for different regions.

subtropics an increase in drier climate biomes is projected in both scenarios. In Australia, consistent with the precipitation decrease [8], hot desert replaces warm grassland and xerophytic woods. This projected desertification is stronger in the A1B scenario than in the E1 scenario, even though the spread between the models is large (>30% for hot desert in North Australia, NAU, in A1B). In Southern Africa (SAF) the area of warm mixed forests decreases in all models in both scenarios, but is replaced by warm grassland in some models and by hot deserts in others.

In the mid-latitudes biomes with a higher cold tolerance are replaced by biomes that require longer growing periods (**Figure 4**). In both scenarios most models show an increased extent of warm mixed forests (ENA, EAS, CNA, NEU and SSA) and in some regions temperate deciduous forests (CNA, WNA, NEU) by the end of the 21st century. On the other hand, the extent of taiga (ENA, WNA, NEU) and cold coniferous forests (ENA, CNA, EAS) decreases according to most models. In Northern Europe (NEU) tundra disappears in all models by the end of the 21st century. In (WNA) taiga and cool mixed forest disappear in both scenarios. In addition, cold coniferous forests disappear in the SRES A1B scenario, while in the E1 scenario some remain. Considerably lower changes in biomes in E1 compared to A1B are evident in the mid-latitudes. For example, in WNA, the first quartile of the simulated fraction of warm and cold grasslands is higher than the third quartile in the E1 scenario under the A1B scenario. This is consistent with the stronger summer drying in this area in the SRES A1B scenario.

As a result of temperature changes there is amplification of biome changes in polar and subpolar latitudes (**Figure 4**). Taiga and tundra are replaced by temperate deciduous forests, cold mixed forests and cold coniferous forests (NEE, NAS, GRL, ALA). Although the main features of biome changes in the two scenarios are similar across these latitudes, the strength of biome changes differs significantly.

In Tibet (TIB) the area of tundra and cold deserts decreases in both scenarios, while the area of cold deciduous forest and warm grassland increases. Despite of the large inter-model spread the 25th and the 75th percentiles of changes in tundra and warm grassland for the two scenarios do not overlap.

4. Summary and Conclusions

We have assessed the difference in resulting biome shifts for different regions of the world when following an ambitious mitigation scenario (E1) as compared with a baseline scenario (SRES A1B) using multi-model results from 10 state-of-the-art coupled atmosphere-ocean general circulation models (GCMs).

Resulting biome changes in the mid-latitudes and sub-polar regions are larger than those in the tropics and subtropics. In the mid-latitudes and sub-polar regions, biomes with less freezing resistance and a higher demand for growing degree days replace the current vegetation consistent with previous studies (e.g. [19]). In the subtropics and tropics biome changes reflect precipitation decrease over land confirming previous results (e.g. [13, 25]). Considerable uncertainty in the likelihood of dieback of the Amazonian rainforest due to climate change and vegetation feedbacks remains [26]. The particularly strong potential vegetation change for the Amazonas region in HadCM3C and HadGEM2-AO compared to the other analyzed GCMs is consistent with the simulated strong forcing response in these regions for precipitation and cloud cover as shown by [8].

In 13 of the 26 regions, namely NEU, MED, NEE, NAS, CAS, TIB, EAS, SAU, ALA, GRL, WNA, CSA and SSA, differences at least for some of the projected biomes changes are much smaller in the E1 scenario than in the A1B scenarios. Thus, in these regions strong mitigation actions could significantly reduce changes in growing conditions when compared with a non-mitigation scenario. On the other hand, even under the E1 scenario, considerable changes in the biome distribution are projected in some regions, particularly in biomes tundra, taiga and cold grassland (e.g. Regions NAS, TIB, EAS, ALA, GRL) but also in the form of shifts from Cold Mixed Forest to Temperate Deciduous Forest and from this to Warm Mixed Forest (e.g. NEU, EAS, CNA, CSA). These regions seem to be particularly sensitive to climate change impacts on growing conditions and might suffer adverse impacts even under strong climate change mitigation action, indicating the need for adaptation measures.

While the vegetation patterns presented here are not the existing vegetation in large parts of the world but the potential vegetation calculated from climatic conditions, they nevertheless provide important insights into growing conditions in different parts of the world under present day conditions and under the two future scenarios considered. Instead of using the most sophisticated available biome models, we use a simple model to account for the coarse resolution of our data and to restrict the analysis to a limited number of biomes and dominant changes between them. Furthermore we did not use the vegetation patterns simulated by the embedded terrestrial carbon cycle components of some of the models but calculated biomes forced by all the models' physical output. The advantage is that we can provide a multi model analysis of 10 state-of-the-art global climate models and the response of terrestrial biomes to the climate change signals simulated by them for the two scenarios. Thus, we provide a consistent overview of potential vegetation

response to an ambitious mitigation scenario (E1) compared to a baseline scenario (A1B). Further research should focus on the regions with the largest sensitivity to climate change with respect to growing conditions. In these regions, both natural vegetation and anthropogenic land-use should be reviewed as to their resilience under projected climate change for different forcing scenarios.

5. Acknowledgements

The ENSEMBLES model-outputs used in this work were produced with the partial funding of the EU FP6 Integrated Project ENSEMBLES (Contract number 505539), whose support is gratefully acknowledged.

REFERENCES

[1] R. H. Moss, *et al*., "The Next Generation of Scenarios for Climate Change Research and Assessment," *Nature*, Vol. 463, 2010, pp. 747-756. doi:10.1038/nature08823

[2] P. van der Linden and J. F. B. Mitchell, "ENSEMBLES: Climate Change and Its Impacts: Summary of Research and Results from the ENSEMBLES Project," Met Office Hadley Centre, 2009, 160 p.

[3] J. A. Lowe, C. D. Hewitt, D. P. van Vuuren, T. C. Johns, E. Stehfest, J.-F. Royer and P. J. van der Linden, "New Study for Climate Modeling, Analyses, and Scenarios," *Eos*, *Transactions American Geophysical Union*, Vol. 90, No. 21, 2009, pp. 181-182. doi:10.1029/2009EO210001

[4] T. C. Johns, J.-F. Royer, I. Höschel, H. Huebener, E. Roeckner, E., Manzini, W. May, J.-L. Dufresne, O. H. Otterå, D. P. van Vuuren, D. Salas y Melia, M. Giorgetta, S. Denvil, S. Yang, P. G. Fogli, J. Körper and C. D. Hewitt, "Climate Change under Aggressive Mitigation: The ENSEMBLES Multi-Model Experiment," *Climate Dynamics*, Vol. 37, No. 9-10, 2011, pp. 1975-2003. doi:10.1007/s00382-011-1005-5

[5] D. G. Streets, *et al*., "Two-Decadal Aerosol Trends as a Likely Explanation of the Global Dimming/Brightening Transition," *Geophysical Research Letters*, Vol. 33, No. 15, 2006, p. L15806. doi:10.1029/2006GL026471

[6] M. I. Mischchenko, *et al*., "Long-Term Satellite Record Reveals Likely Recent Aerosol Trend," *Science*, Vol. 315, No. 5851, 2007, p. 1543. doi:10.1126/science.1136709

[7] G. A. Meehl, T. F. Stocker, *et al*., "Global Climate Projections," In: S. Solomon, *et al*., Eds., *Climate Change* 2007: *The Physical Science Basis*, Cambridge University Press, Cambridge, New York, 2007, pp. 747-846.

[8] H. Huebener, M. G. Sanderson, I. Höschel, J. Körper, T. C. Johns, J.-F. Royer, E. Roeckner, E. Manzini, J.-L. Dufresne, O. H. Otterå, J. Tjiputra, D. S. Y Melia, M. Giorgetta, S. Denvil and P. G. Fogli, "Regional Hydrological Cycle Changes in Response to an Ambitious Mitigation Scenario," *Climatic Change*, 2013. doi:10.1007/s10584-013-0829-x

[9] J. Körper, I. Höschel, J. A. Lowe, C. D. Hewitt, D. Salas y Melia, E. Roeckner, H. Huebener, J.-F. Royer, J.-L. Dufresne, A. Pardaens, M. A. Giorgetta, M. G. Sanderson, O. H. Otterå, J. Tjiputra and S. Denvil, "The Effects of Aggressive Mitigation on Steric Sea Level Rise and Sea Ice Changes," *Climate Dynamics*, Vol. 40, No. 3-4, 2013, pp. 531-550. doi:10.1007/s00382-012-1612-9

[10] A. Fischlin, G. F. Midgley, J. T. Price, R. Leemans, B. Gopal, C. Turley, M. D. A. Rounsevell, O. P. Dube, J. Tarazona and A. A. Velichko, "Ecosystems, Their Properties, Goods, and Services," In: M. L. Parry, O. F. Canziani, J. P. Palutikof, P. J. van der Linden and C. E. Hanson, Eds., *Climate Change* 2007: *Impacts*, *Adaptation and Vulnerability*, Cambridge University Press, Cambridge, 2007, pp. 211-272.

[11] O. E. Sala, F. S. Chapin, J. J. Armesto, E. Berlow, J. Bloomfield, R. Dirzo, E. Huber-Sanwald, L. F. Huenneke, R. B. Jackson, A. Kinzig, R. Leemans, D. M. Lodge, H. A. Mooney, M. Oesterheld, A. L. Poff, M. T. Sykes, B. H. Walker, M. Walker and D. H. Wall, "Global Biodiversity Scenarios for the Year 2100," *Science*, Vol. 287, No. 5459, 2000, pp. 1770-1774.

[12] A. D. Hansen, R. P. Neilson, V. H. Dale, C. H. Flather, L. R. Iverson, D. J. Currie, S. Shaver, R. Cook and P. J. Bartlein, "Global Change in Forests: Responses of Species, Communities and Biomes," *BioScience*, Vol. 51, No. 9, 2001, pp. 765-779. doi:10.1641/0006-3568(2001)051[0765:GCIFRO]2.0.CO;2

[13] S. Sitch, C. Huntingford, N. Gedney, P. E. Levy, M. Lomas, S. L. Piao, R. Betts, P. Ciais, P. Cox, P. Friedlingstein, C. D. Jones, I. C. Prentice and F. I. Woodward, "Evaluation of the Terrestrial Carbon Cycle, Future Plant Geography and Climate-Carbon Cycle Feedbacks Using Five Dynamic Global Vegetation Models (DGVMs)," *Global Change Biology*, Vol. 14, No. 9, 2008, pp. 2015-2039. doi:10.1111/j.1365-2486.2008.01626.x

[14] M. Kirschbaum and A. Fischlin, "Climate Change Impacts on Forests," In: R. Watson, M. C. Zinyowera and R. H. Moss, Eds., *Climate Change* 1995: *Impacts*; *Adaptations and Mitigation of Climate Change*. *Scientific-Technical Analysis*, Cambridge University Press, Cambridge, 1996, pp. 95-129.

[15] I. C. Prentice, W. Cramer, S. P. Harrison, R. Leemans, R. A. Monserud and M. A. Solomon, "A Global Biome Model Based on Plant Physiology and Dominance, Soil Properties and Climate" *Journal of Biogeography*, Vol. 19, No. 2, 1992, pp. 117-134. doi:10.2307/2845499

[16] W. May, "Climatic Changes Associated with a Global '2˚C-Stabilization' Scenario Simulated by the ECHAM5/MPI-OM Coupled Climate Model," *Climate Dynamics*, Vol. 31, No. 2-3, 2008, pp. 283-313. doi:10.1007/s00382-007-0352-8

[17] J. H. Christensen, B. Hewitson, *et al*., "Regional Climate Projections," In: S. Solomon, *et al*., Eds., *Climate Change* 2007: *The Physical Science Basis*, Cambridge University Press, Cambridge, New York, 2007, Chapter 11.

[18] F. Giorgi and X. Bi, "Updated Regional Precipitation and Temperature Changes for the 21st Century from Ensembles of Recent AOGCM Simulations," *Geophysical Research Letters*, Vol. 32, No. 21, 2005, p. L21715. doi:10.1029/2005GL024288

[19] J. O. Kaplan, *et al*., "Climate Change and Arctic Ecosystems: 2. Modeling, Paleodata-Model Comparisons, and Future Projections," *Journal of Geophysical Research*: *Atmospheres*, Vol. 108, No. D19, 2003, p. 8171. doi:10.1029/2002JD002559

[20] T. D. Mitchell and P. D. Jones, "An Improved Method of Constructing a Database of Monthly Climate Observations and Associated High-Resolution Grids," *Journal of Geophysical Research*: *Atmospheres*, Vol. 25, No. 6, 2005, pp. 693-712. doi:10.1002/joc.1181

[21] G. J. Huffman, R. F. Adler, M. Morrissey, D. T. Bolvin, S. Curtis, R. Joyce, B. McGavock and J. Susskind, "Global Precipitation at One-Degree Daily Resolution from Multi-Satellite Observations," *Journal of Hydrometeorology*, Vol. 2, No. 1, 2001, pp. 36-50. doi:10.1175/1525-7541(2001)002<0036:GPAODD>2.0.CO;2

[22] M. de Castro, C. Gallardo, K. Jylha and K. Tuomenvirta, "The Use of a Climate-Type Classification for Assessing Climate Change Effects in Europe from Ensemble of Nine Regional Climate Models," *Climatic Change*, Vol. 81, No. 1, 2007, pp. 329-342. doi:10.1007/s10584-006-9224-1

[23] F. Hanf, J. Körper, T. Spangehl and U. Cubasch, "Shifts of Climate Zones in Multi-Model Climate Change Experiments Using the Koppen Climate Classification," *Meteorologische Zeitschrift*, Vol. 21, No. 2, 2012, pp. 111-123. doi:10.1127/0941-2948/2012/0344

[24] R. A. Monserud and R. Leemans, "Comparing Global Vegetation Maps with the Kappa Statistic," *Ecological Modelling*, Vol. 62, No. 4, 1992, pp. 275-293. doi:10.1016/0304-3800(92)90003-W

[25] C. A. Alo and G. Wang, "Potential Future Changes of the Terrestrial Ecosystem Based on Climate Projections by Eight General Circulation Models," *Journal of Geophysical Research*, Vol. 113, No. G1, 2008, p. G01004. doi:10.1029/2007JG000528

[26] Y. Malhi, *et al*., "Exploring the Likelihood and Mechanism of a Climate-Change Induced Dieback of the Amazon Rainforest," *Proceedings of the National Academy of Sciences*, Vol. 106, No. 49, 2009, pp. 20610-20615. doi:10.1073/pnas.0804619106

Curriculum Vitae

Der Lebenslauf ist in der Online-Version aus Gründen des Datenschutzes nicht enthalten.

List of Peer-reviewed Publications

Berking, J., J. Körper, S. Wagner, U. Cubasch and B. Schütt (2013): Heavy rainfalls in a desert(ed) city – a climate-archaeologial case study from sudan. *AGU Monograph Climates, Landscapes and Civilizations*, **1**, doi:10.1029/2012BM001208.

Hanf, F., J. Körper, T. Spangehl and U. Cubasch (2012): Shifts of climate zones in multi-model climate change experiments using the köppen climate classification. *Meteorologische Zeitschrift*, **21**, doi:10.1127/0941-2948/2012/0344.

Huebener, H. and J. Körper (2013): Changes in regional potential vegetation in response to an ambitious mitigation scenario. *Journal of Environmental Protection*, **4**, 16–26, doi:10.4236/jep.2013.48A2003.

Huebener, H., M. Sanderson, I. Höschel, J. Körper, T. Johns, J.-F. Royer, E. Roeckner, E. Manzini, J.-L. Dufresne, O. H. Otterå, J. Tjiputra, D. Salas y Melia, M. Giorgetta, S. Denvil and P. Fogli (2013): Regional hydrological cycle changes in response to an ambitious mitigation scenario. *Climatic Change*, **120**, 389–403, doi:10.1007/s10584-013-0829-x.

Johns, T. C., J.-F. Royer, I. Höschel, H. Huebener, E. Roeckner, E. Manzini, W. May, J.-L. Dufresne, O. H. Otterå, D. Van Vuuren, D. Salas y Melia, M. A. Giorgetta, S. Denvil, S. Yang, P. G. Fogli, J. Körper, J. F. Tjiputra, E. Stehfest and C. D. Hewitt (2011): Climate change under agressive mitigation: The ENSEMBLES multi-model experiment. *Climate Dynamics*, **37**, doi:10.1007/s00382-011-1005-5.

Körper, J., I. Höschel, J. A. Lowe, C. D. Hewitt, D. Salas y Melia, E. Roeckner, H. Huebener, J.-F. Royer, J.-L. Dufresne, A. Pardaens, M. A. Giorgetta, M. G. Sanderson, O. H. Otterå, J. Tjiputra and S. Denvil (2013): The effects of aggressive mitigation on steric sea level rise and sea ice changes. *Climate Dynamics*, **40**, 531–550, doi:10.1007/s00382-012-1612-9.

Körper, J., T. Spangehl, U. Cubasch and H. Huebener (2009): Decomposition of projected regional sea level rise in the North Atlantic and its relation to the AMOC. *Geophysical Research Letters*, **39**, L199714, doi:10.1029/2009GL039757.

Schimanke, S., J. Körper, T. Spangehl and U. Cubasch (2011): Multi-decadal variability of sudden stratospheric warmings in an AOGCM. *Geophysical Research Letters*, **38**, L01801, doi:10.1029/2010GL045856.

Spangehl, T., U. Cubasch, C. Raible, S. Schimanke, J. Körper and D. Hofer (2009): Transient climate simulations from the Maunder Minimum to present day: the role of the stratosphere. *Journal of Geophysical Research*, **115**, D00l10, doi:10.1029/2009JD012358.